ESD ACCESSION LIST
TRI Call No. 73099
Copy No. 1 of 1 cys.

ESD-TR 71-297

ESD RECORD COPY
RETURN TO
SCIENTIFIC & TECHNICAL INFORMATION DIVISION
(TRI), Building 1210

UIAL-71-14
September 1971

INVESTIGATION OF SOME ELECTRICALLY SMALL CONICAL LOG-SPIRAL ANTENNAS

Prepared by

Antenna Laboratory

Department of Electrical Engineering

University of Illinois

Urbana, Illinois 61801

for

Massachusetts Institute of Technology

Lincoln Laboratory

RECEIVED
JAN 10 1972
DISTRIBUTION
AD736500

Approved for public release; distribution unlimited.

UIAL-71-14
September 1971

Annual Report

INVESTIGATION OF SOME ELECTRICALLY SMALL CONICAL LOG-SPIRAL ANTENNAS

John D. Dyson
University of Illinois

Prepared for

Massachusetts Institute of Technology
Lincoln Laboratory

Under
Purchase Order No. CC-401
Prime Contract No. F19628-70-C-0230

This Report Covers Period

1 October 1970 - 31 August 1971

Approved for public release; distribution unlimited.

UILU-ENG-71-2550

ABSTRACT

This report is concerned with the experimental evaluation of the radiation pattern, power gain, and voltage standing wave ratio of balanced and unbalanced conical spiral antennas when operated at wavelengths much longer than would normally be considered for a given size structure.

The unbalanced antenna investigated was a bifilar logarithmic spiral constructed on a dielectric cone with an inner metal core to house electronic equipment. At the base, one arm is bonded to the core. The antenna is an essentially end-fire (in the direction of the apex of the cone) radiator for base diameters greater than 0.14 wavelength and heights greater than 0.43 wavelength. For longer wavelengths a marked transition in the mode of radiation occurs, and the antenna radiates a maximum of energy broadside to the cone axis.

Although the direction of the maximum of radiation changes with frequency the maximum power gain of the antenna (without impedance matching techniques being employed) remains greater than -3.5 db over at least an octave range of frequencies such that the maximum dimension of the antenna is greater than or equal to 0.33 wavelength.

It has been determined that broadside radiation occurs because the antenna arms act as a transmission line for current flowing away from the apex. At the base one arm excites the inner cone. The current on the other arm is reflected, and this reflected current is radiated by successive turns of the antenna which are approximately in phase. The antenna is thus equivalent to normal-mode monofilar conical helix, fed at the base against an inner metal core.

Accepted for the Air Force
Joseph R. Waterman, Lt. Col., USAF
Chief, Lincoln Laboratory Project Office

TABLE OF CONTENTS

I. INTRODUCTION

This report summarizes most of the work performed under the subject contract during the period 1 October 1970 to 31 August 1971. [Under this contract the University of Illinois has furnished support to Lincoln Laboratory for research in the general area associated with broadband near-isotropic antennas.] This work has centered around the evaluation of conical log-spiral antennas, and similar type structures, when operated at wavelengths 2 to 3 times longer than those that would normally be considered for the specified physical size of the structure.

The original effort was directed toward the study of an antenna designed and constructed by the Space and Re-Entry Systems Division, Philco-Ford Corporation. It was intended that this be a relatively short time-scale investigation but because of the characteristics of the antenna, the range of frequencies of operation that were specified, severe local r.f. interference near these frequencies, and other problems, the first phase of the study stretched into an investigation over the greater part of 6 months.

Initial results of the investigation were covered in a progress report submitted on April 7, 1971[1]. The present report supersedes that report and also covers work performed on this and related antennas since that time.

In addition, another type of unbalanced spiral antenna has been investigated. This work is continuing and will be reported in a Technical Report at a later date.

For those readers who have read the earlier preliminary report, only pages 43 through 51 in sections II through VII (pages 2 through 62) contain new information. Sections following VII cover work that was not covered in reference No. 1.

II. The Antenna

The antenna is shown in Figure 1. It is a two arm conical logarithmic spiral constructed by wrapping thin copper arms onto a fiberglass dielectric cone. The antenna is excited at the apex of the cone by carrying the coaxial feed line along (and bonded to) one arm. At the apex the center conductor of this feed cable is bonded to the opposite arm, upon which an inactive coaxial cable has been placed to maintain symmetry of construction. This is an accepted method of feeding the balanced spiral antennas and has been termed an "infinite balun" feed, because in conventional operation, the antenna itself acts as a balun to decouple the antenna currents from the feed cable[3]. The coaxial connector on this feed cable may be seen at the base of the antenna. The physical dimensions and measured antenna parameters of the antenna are given in Appendix B attached here-to.

Figure 2 is a view of the base end of the cone. The antenna arms, the feed cable connector, and the hollow dielectric cone may be seen. Inside this dielectric cone is a coaxially placed hollow metal cone. Soft foam rubber spacers, such as that visible in the upper part of the photograph held this metal cone in place. The metal cone is bonded to one of the arms of the antenna by a wide copper strap that covers an arc of approximately 125.5° in a plane perpendicular to the axis of the cones. This strap can be seen in the lower left of Figure 2.

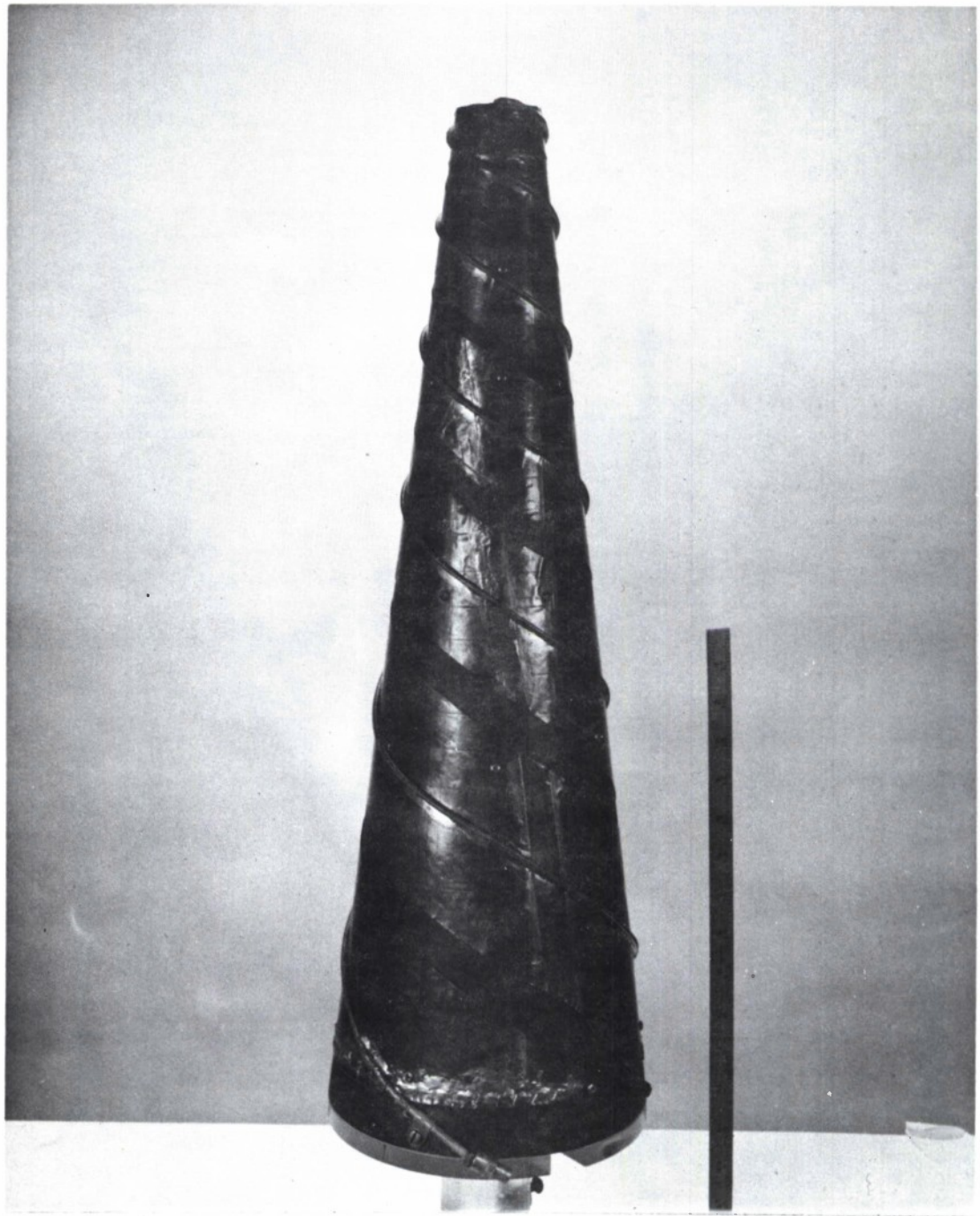

Figure 1. Two arm conical log-spiral antenna with infinite balun feed.

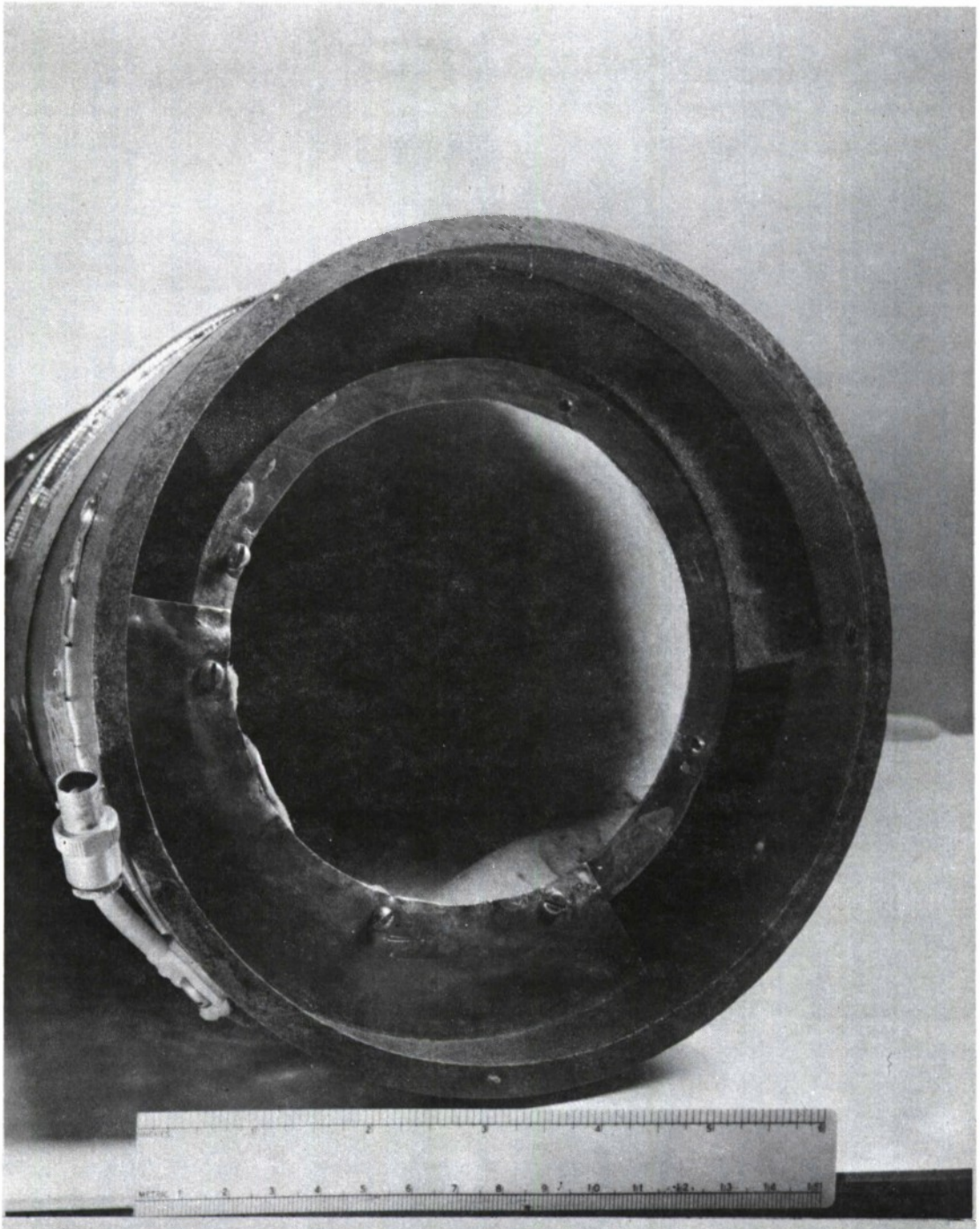

Figure 2. End view of the conical antenna showing internal metal cone and bonding strap between this metal cone and the end of one arm.

The antenna was designed so that all of the electronic equipment required for excitation could be housed inside this metal cone. The base plate, made for the metal cone, has a hole of approximately 5/8 inch in diameter through which a coaxial cable could be placed to connect the enclosed r.f. source to the antenna feed cable.

In the range of frequencies for which the characteristics of the antenna scale with frequency in a normal manner, the fact that the inner cone is bonded to one arm might be expected to have little effect upon the radiation characteristics. At the frequencies of interest here, the connection of the metal cone to one of the antenna arms causes the antenna to be extremely unbalanced, and any cables carrying r.f. signals to or from the antenna for testing purposes would tend to support antenna currents and become a part of the radiating structure. For that reason it was considered necessary to test the antenna as an "isolated" structure.

Although a study of the radiation characteristics was of prime importance, it was considered desirable to be able to measure the input reflection coefficient, or VSWR of the antenna. Such information could be correlated with the radiation measurements for a better understanding of the operation of the antenna. For such measurements, information would have to be brought from the antenna to indicating instruments on the ground by electrical cables, unless some sort of r.f. or optical telemetering system was used. These latter options were ruled out for practical reasons.

For measuring the relative gain of the antenna when it was isolated on the antenna test tower, it was also considered desirable to be able to control the frequency of operation from the ground for possible sweep

frequency testing. Since the output of the usable source oscillators was not constant with frequency, it was also necessary to monitor the power incident to the antenna when it was used as a radiating structure. To carry frequency control signals to the oscillator, and information on the relative output power level of the oscillator, and on the reflection coefficient of the antenna back to indicating instruments, "non-metallic" cables were used. This type cable consisted of a rubber covered nylon center conductor, or core, which was impregnated with graphite. The resistance of these conductors was approximately 5000 ohms per foot. The cable can be used to carry small audio or d-c currents, with a suitable allowance for the resistive dissipation. Induced r.f. currents are quickly damped, and the antenna is effectively isolated in the r.f. electromagnetic field. This type cable has been used here and at other laboratories for far-field[4] and near-field[5] antenna pattern measurements, and for field strength measurements[6].

The antenna, with such "non-metallic" cables extending from the hole in the base plate, can be seen in Figure 3. The RG 58/U cable which connects the oscillator to the antenna feed cable can also be seen.

To support the antenna structure, two mounts were designed. The first of these, and the one used for most of the measurements, was of polystyrene. It is shown in Figures 3, 4, and 5. For all measurements, the antenna was mounted on a 35 foot high dielectric antenna test tower which was spaced approximately 30 feet from a log-periodic dipole array receiving antenna.

Figure 3. End view of the conical antenna with the internal cone capped with a base plate. The polystyrene support designed to fit the base of the dielectric cone is shown nearby.

Figure 4. The polystyrene support mounted on the antenna.

Figure 5. Conical antenna mounted on antenna test tower. Tower, tower head, antenna mount, and all cables shown in back of the antenna are of non-metallic or dielectric material.

The log-periodic dipole array, LPDA, was also mounted on a tower so that it was 35 feet above the roof of the building. A rotating mount was available for this LPDA so that it could be continually rotated about its axis while patterns of the antenna under test were being recorded. All patterns which were recorded thus indicate directly the axial ratio of the radiated fields at all angles included in the plane of the pattern. To identify the radiation pattern cuts the polar coordinate system shown in Figure 6 will be used.

Because of the very high resistance of the non-metal cable it was necessary to parallel several strands of the cable to carry the control voltage. This kept the required maximum control voltage at the equipment room at a reasonable level and yet supplied up to 28 volts at the oscillator. These cables carried only 2 or 3 milliamperes of direct current and tests with, and without, the cables present will be described in a later section.

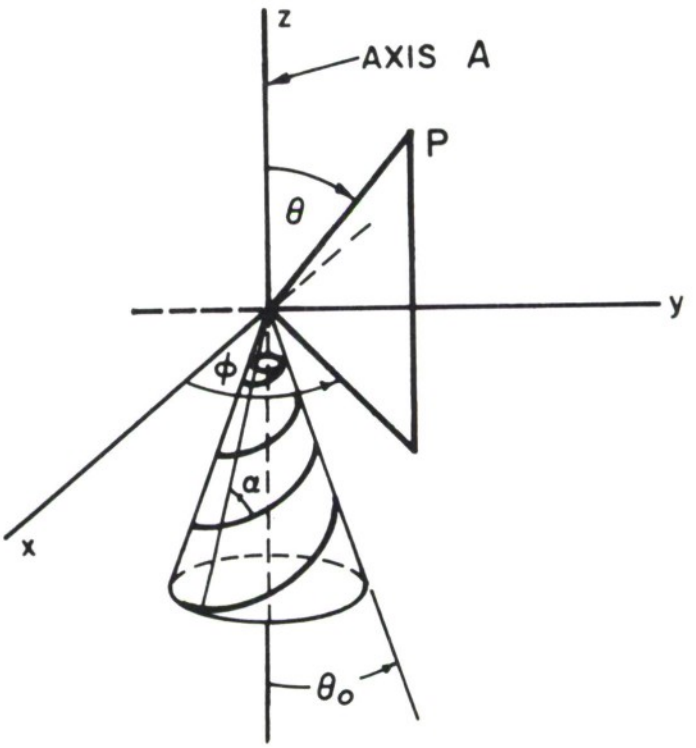

Figure 6. The log-spiral antenna in an associated coordinate system.

III. Equipment Used for Radiation Measurements

Small battery powered oscillators, which supplied approximately 100 milliwatts of power, had been shipped with the antenna for convenience in making the desired measurements. After the antenna mount had been constructed, initial attempts were made to measure radiation patterns. It became immediately clear that any meaningful measurements were impossible over the desired frequency range (at and above 150 MHz), with the receiving equipment that was available at this laboratory. The general level of interfering signals was so high that the desired signals from the small oscillator in the conical antenna were at best 1 to 2 db above the background interference, and in most cases buried in this background.

To overcome this condition several steps were taken. An r.f. filter with a passband from 125 to 400 MHz, an r.f. amplifier with 23 db gain from 50 to 500 MHz, and a voltage controlled miniature battery-powered oscillator supplying up to 200 milliwatts from 130 to 280 MHz were ordered. It required over two months to obtain all three of these items.

Even with these improvements, operation was still marginal when the oscillator was operated as a CW source. To provide increased sensitivity and selectivity, an available small solid state DPDT switch was used as a modulator This necessitated designing and building a small battery-powered 1000 Hz square-wave driver for the switch. Figure 7 is a block diagram of the equipment in its final form.

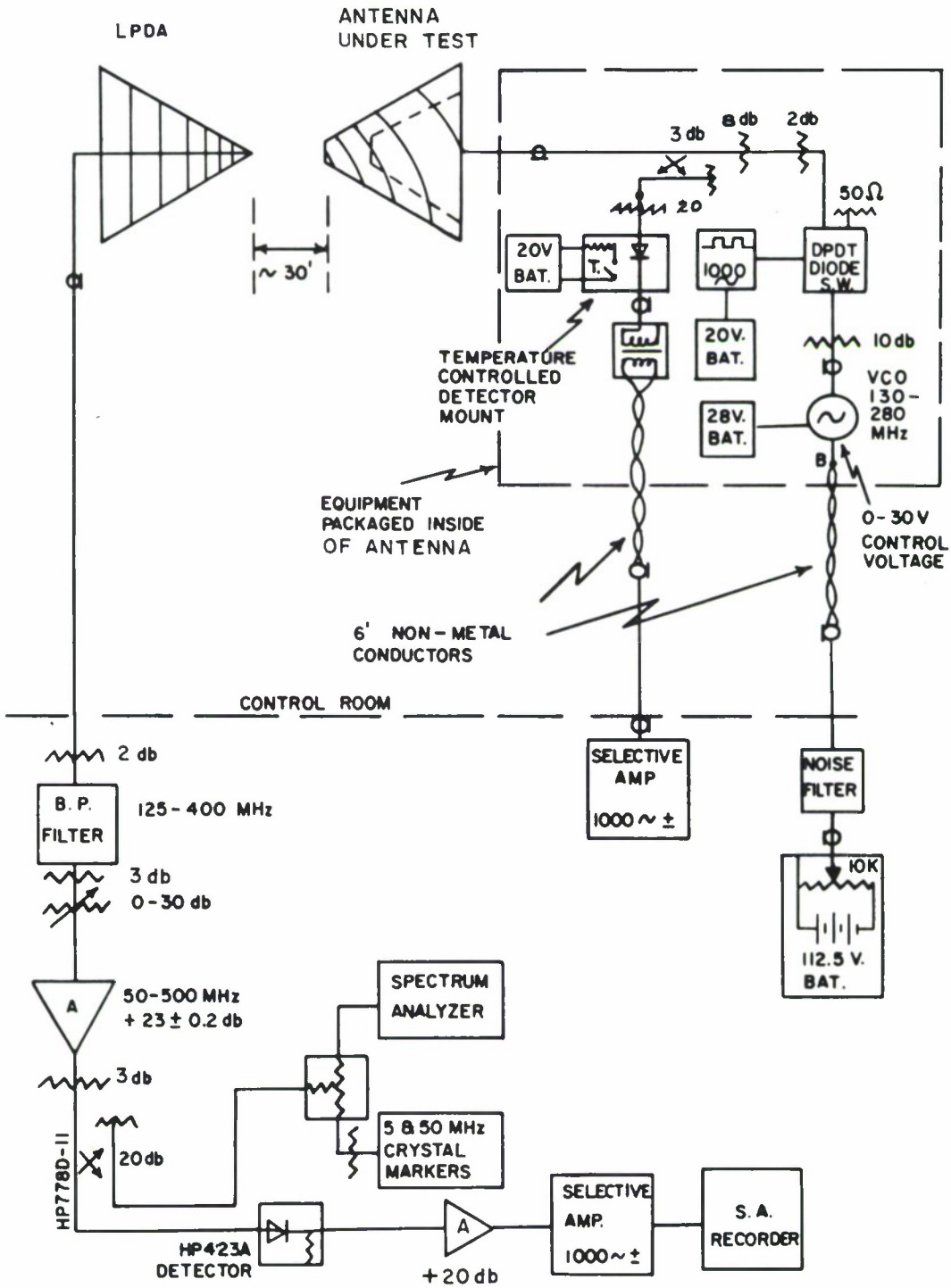

Figure 7. Block diagram of the equipment used to measure the radiation patterns and relative gain.

The VCO and solid state modulator with their battery packs are indicated. Since gain measurements were to be made, 20 db of dissipative isolation was inserted after the oscillator. In addition, the power level incident upon the antenna feed line terminal was monitored with a small power splitter that had greater than 30 db of isolation between the output ports. This item is essentially a hybrid, with one port internally terminated. One of the output ports was connected to a well-matched broadband crystal detector (HP423A). From this detector, audio information was brought back to a 1000 Hz selective amplifier.

The severe winter weather, that was present when most of these measurements were made, forced several refinements in the equipment. It became obvious that the repetition rate of the switch driver, which was nominally 1000 Hz, was temperature sensitive. It thus became necessary, for monitoring and for recording purposes, to utilize selective amplifiers that had tunable pass-bands.

It was also observed, by a selective elimination process, that the crystal detector used for monitoring the incident power was also temperature sensitive, when the difference between indoor and outdoor temperatures was in the neighborhood of 50 to 70 degrees F. To stabilize this detector, it was bound together with a thermostatic switch, covered with absbestos paper, then wrapped with high resistance heating wire and covered with insulation. This "oven" worked very well and held the temperature of the detector mount to less than 1 degree change.

The r.f. signal was brought down from the LPDA receiving antenna through, isolating attenuators, the filter, and the r.f. amplifier, to a crystal detector that is identical to that used in the conical antenna for incident power monitoring, then to audio amplifiers and a rectangular pattern recorder. The horizontal drive for this recorder was selsyn controlled from the rotation of the antenna test tower.

The frequency of operation was determined and continuously monitored, by sampling some of the received signal and displaying it, and a crystal controlled frequency comb presentation, on a spectrum analyzer.

The equipment set-up represents several months of evolution. In its final form, it provided very convenient and reliable operation, with all controls necessary to detect any change in the frequency or power output of the r.f. signal fed to the antenna, and to change this frequency for sweep operation.

A photograph of the equipment that was placed inside the antenna is shown as Figure 8. Reading from left to right, we see the non-metallic cable for carrying monitoring information, the audio transformer inserted between this cable and the detector, the battery pack for temperature control of the detector mount, and the insulated detector mount. Next, there is a 20 db attenuator, then the hybrid power splitter with an 8 db attenuator attached. The coaxial cable at the top center leads to the antenna.

Continuing in the picture, we see the solid state modulator with a 2 db attenuator on one output terminal and a 10 db attenuator and the VCO connected to the input. To the right of this assembly is the 28 volt battery pack for the VCO, and above that the non-metallic cable for the d.c. control voltage. On the extreme right, in the picture, the 1000 Hz modulator driver and its battery pack are evident. The scale that is visible at the bottom of the picture is 18 inches in length.

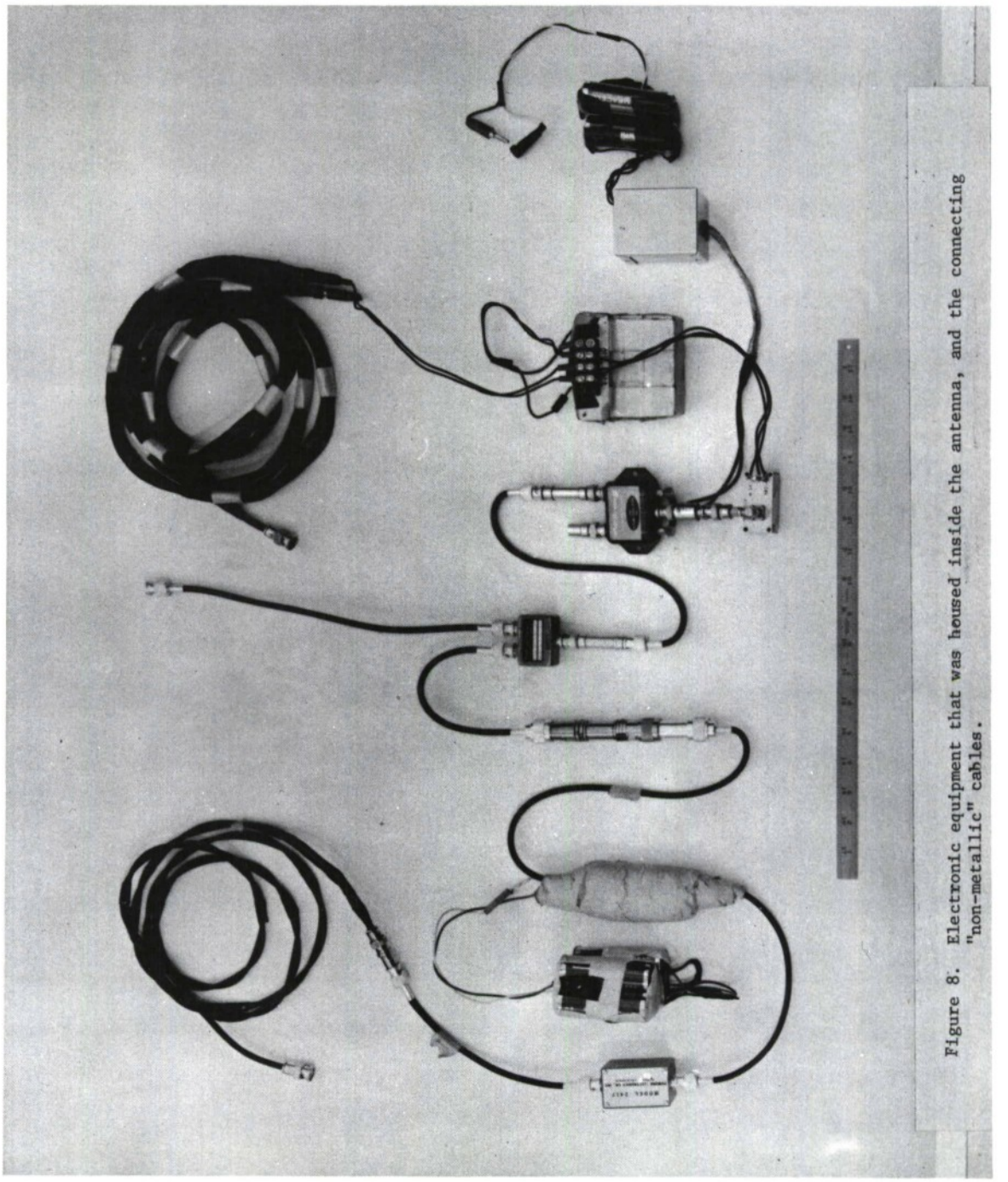

Figure 8. Electronic equipment that was housed inside the antenna, and the connecting "non-metallic" cables.

IV. Radiation Pattern Measurements

Using the system described in the previous section, it became possible to measure radiation patterns over a dynamic range of approximately 20 to 22 db, and over a frequency range from 150 to 280 MHz. Radiation measurements were not attempted below 150 MHz because of the limitations of the antenna pattern range.

Before making extensive measurements, the possible effect of the presence of the non-metallic cables was investigated. Patterns were recorded with the control voltage supplied by a small battery inside the antenna cone. The monitor cable was also removed so that there were no electrical connections to the structure. The frequency of the received signal was monitored as indicated in Figure 7. The antenna tower was then lowered, the control voltage battery was disconnected, and the non-metal control and monitoring cables connected. The control voltage was adjusted to bring the operating frequency to that measured previously, and a new pattern was recorded without changing the control settings of any receiving or recording equipment.

Two patterns, so recorded, are shown in Figure 9. The vertical scale is one db per division, and the horizontal scale the angle θ about the axis of the cone. All patterns were recorded with the LPDA, a linearily polarized receiving antenna, continually rotating. Thus, the envelope of the pattern, i.e., the difference between the maximum and minimum of the pattern at any given angle θ, is the "measurable axial ratio" of the received field in decibels.

It is indicated as a measurable axial ratio because the minimum of the pattern is, in these patterns at least, determined by the noise or background interference level. The changing character of this background

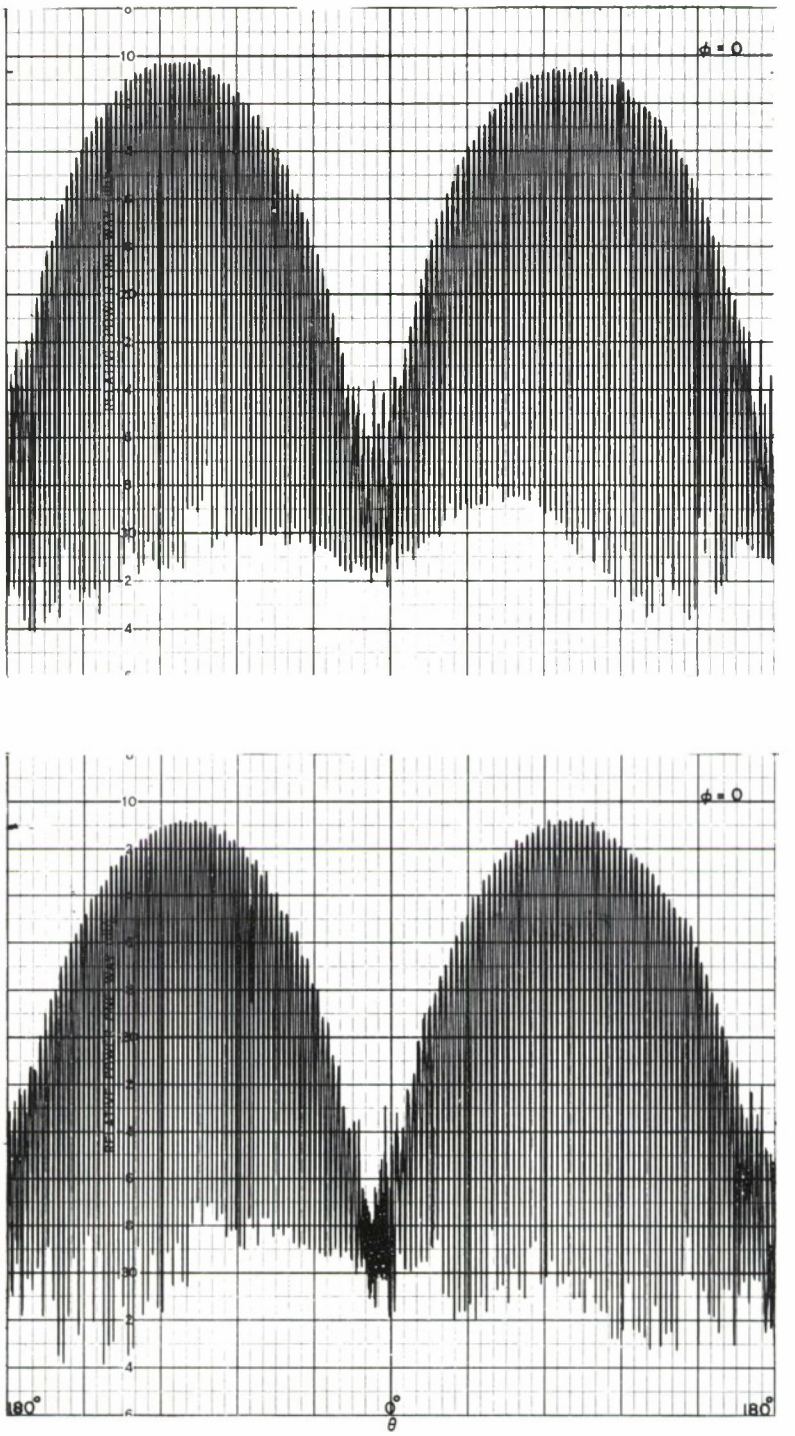

Figura 9. Radiation Pattern of Conical Antenna with control voltage carried to the antenna and monitoring signal carried from the antenna with non-metallic cables (top pattern) and control voltage supplied by an internal battery and antenna completely isolated (bottom pattern). Frequency 150 MHz.

is evident in patterns repeated one after another without change in the measurement system. Thus the indicated axial ratio in db is a lower bound on the possible true axial ratio.

In comparing these two patterns, a difference of approximately 0.3 db is evident in the pattern maxima and a greater difference at the indicated minima of the pattern. This latter difference was not considered significant, since the primary interest was in the maximum radiated gain of the antenna, and because of the above noted effects of the background radiation level. Differences of a fraction of a db were noted at other frequencies, but there was considered to be no significant change in pattern shape, indicating little effect of the presence of the non-metal cables. Based upon these tests all further measurements were made with the monitoring and control voltage cables in use.

Radiation patterns were recorded at 150, 160, 170, 180, 200, 208, 220, 230, 250, 270, 279 MHz. One pattern cut at each of these frequencies is shown in Figures 10 through 20. All patterns are recorded on a linear db scale with one db per division. On these patterns the angle $\theta = 0°$ indicates a directed line extending away from the apex of the cone, along the cone axis.

The patterns indicate that from 150 to approximately 200 MHz the structure is radiating a broadside, essentially linearily polarized, field. The field gradually changes from broadside radiation to one of no particular character from approximately 200 to 250 MHz, and then at higher frequencies into essentially end-fire radiation. Characteristics could be measured only to 280 MHz. At still higher frequencies the radiated field could be expected to become essentially circularly polarized, and unidirectional, directed off the apex of the cone.

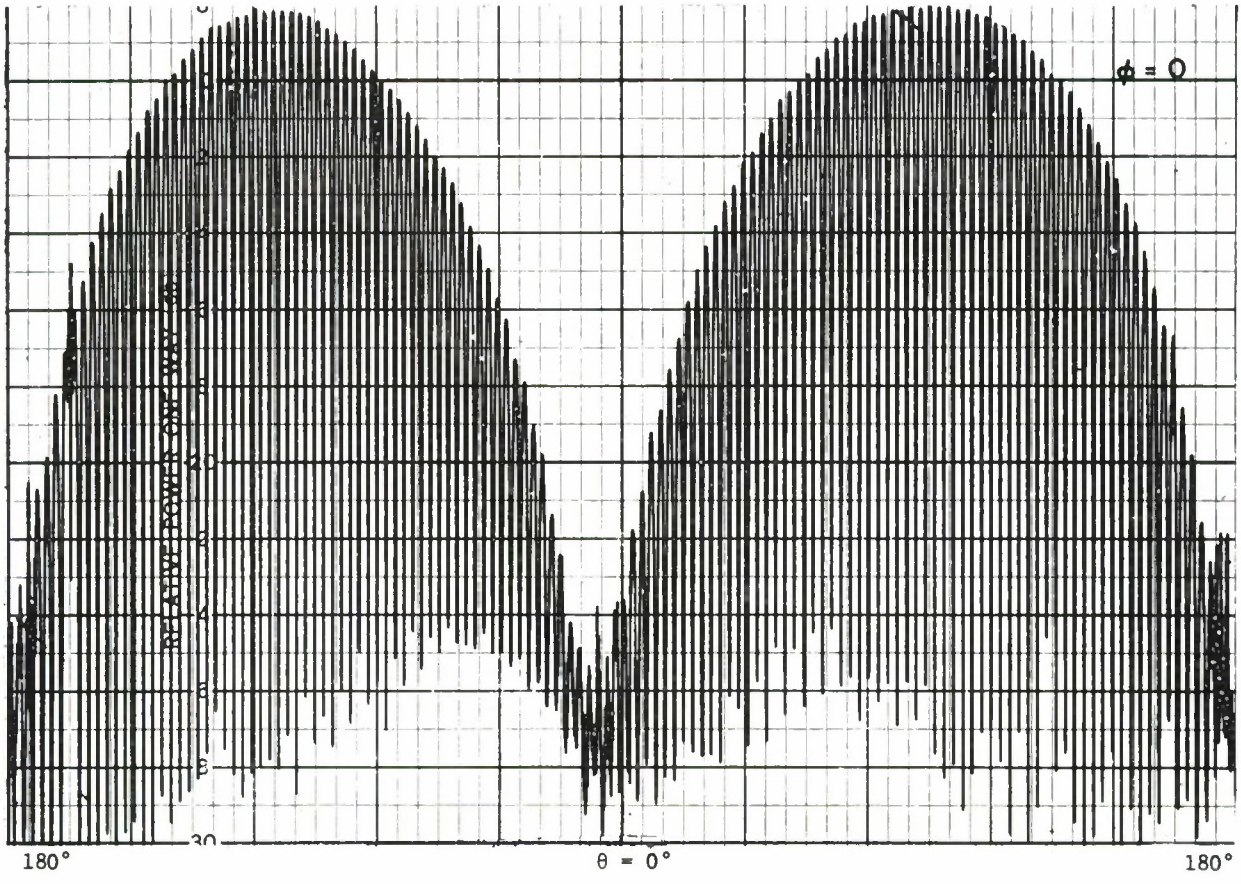

Figure 10 Radiation Pattern of Unbalanced Conical Antenna. 2π variation in θ, $\phi = 0$. Frequency 150 MHz.

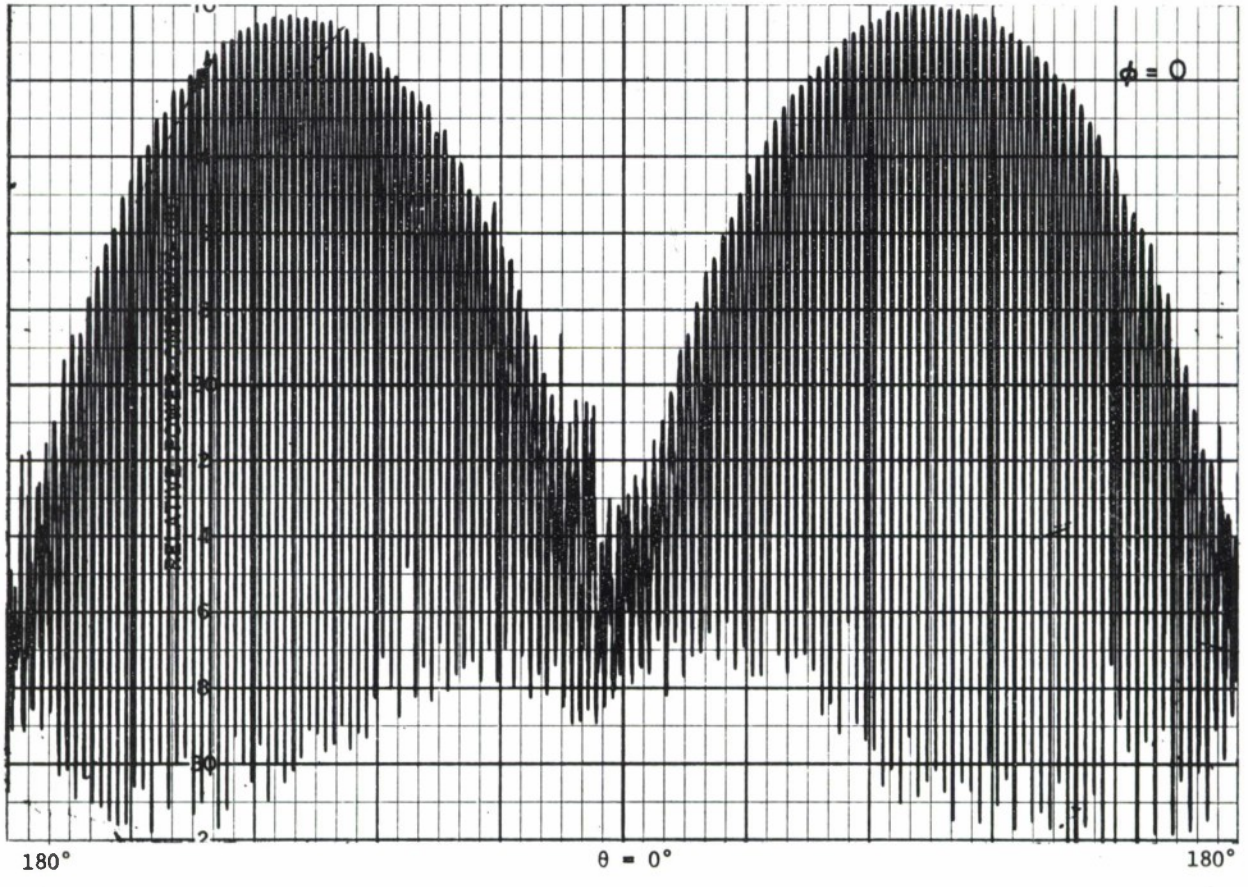

Figure 11 Radiation Pattern of Unbalanced Conical Antenna. 2π variation in θ, $\phi = 0$. Frequency 160 MHz.

Figure 12 Radiation Pattern of Unbalanced Conical Antenna. 2π variation in θ, $\phi = 0$. Frequency 170 MHz.

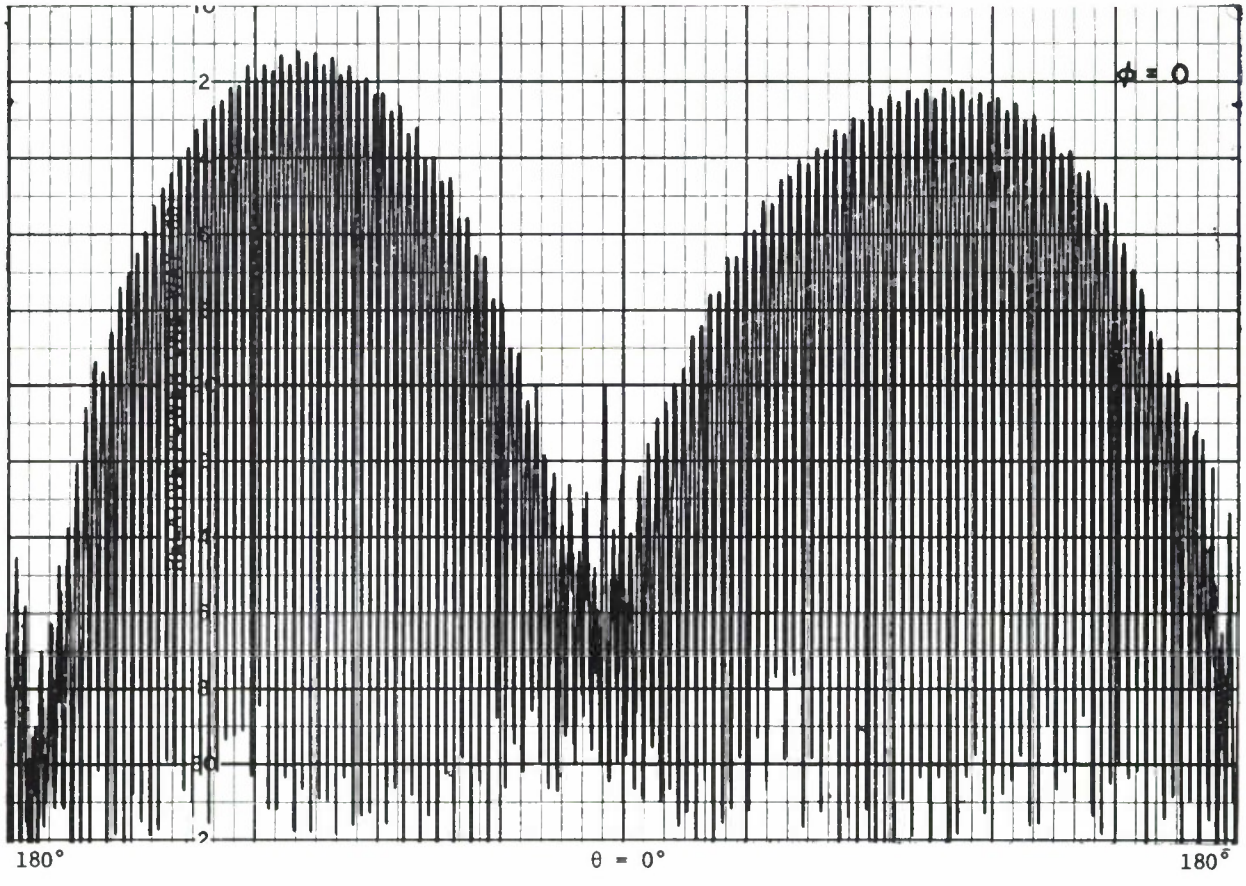

Figure 13 Radiation Pattern of Unbalanced Conical Antenna. 2π variation in θ, $\phi = 0$. Frequency 180 MHz.

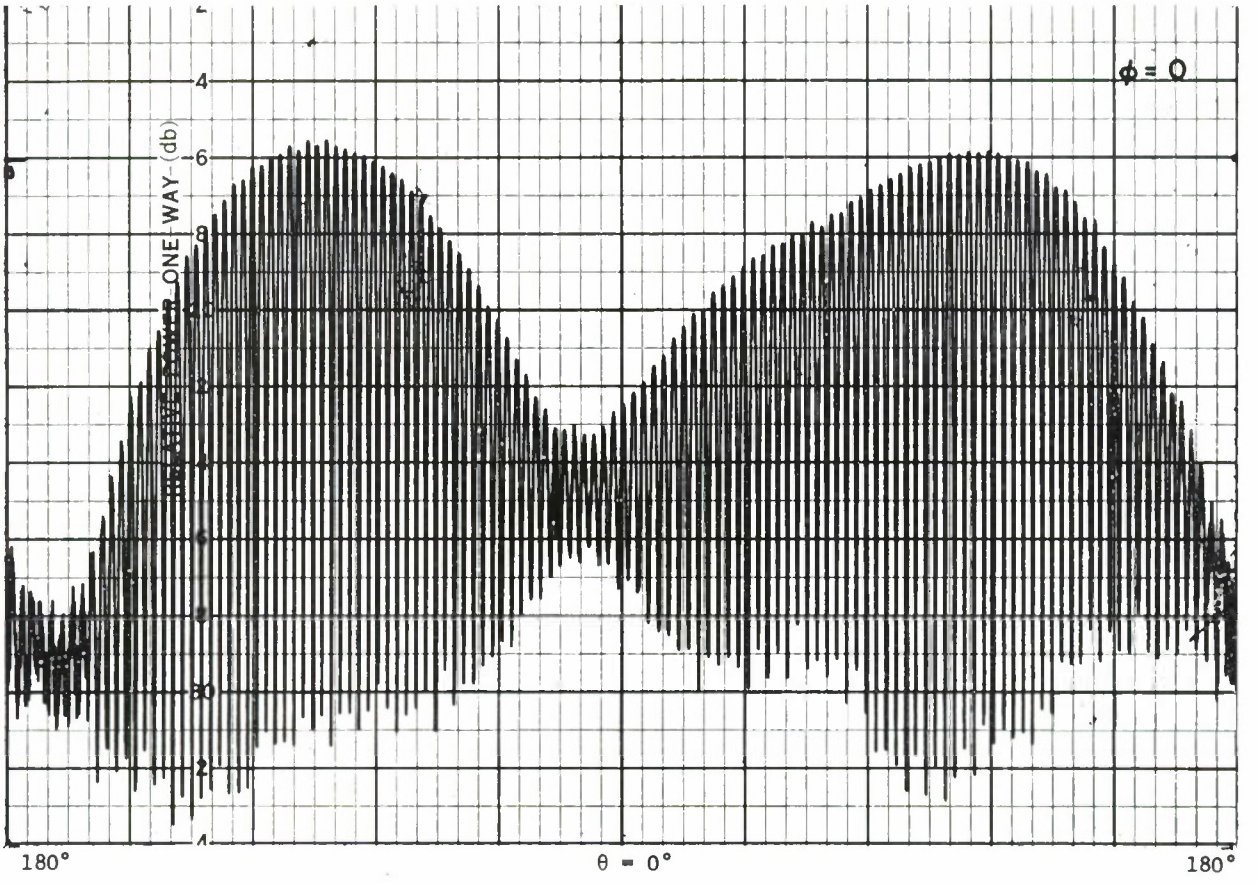

Figure 14 Radiation Pattern of Unbalanced Conical Antenna. 2π variation in θ, $\phi = 0$. Frequency 200 MHz.

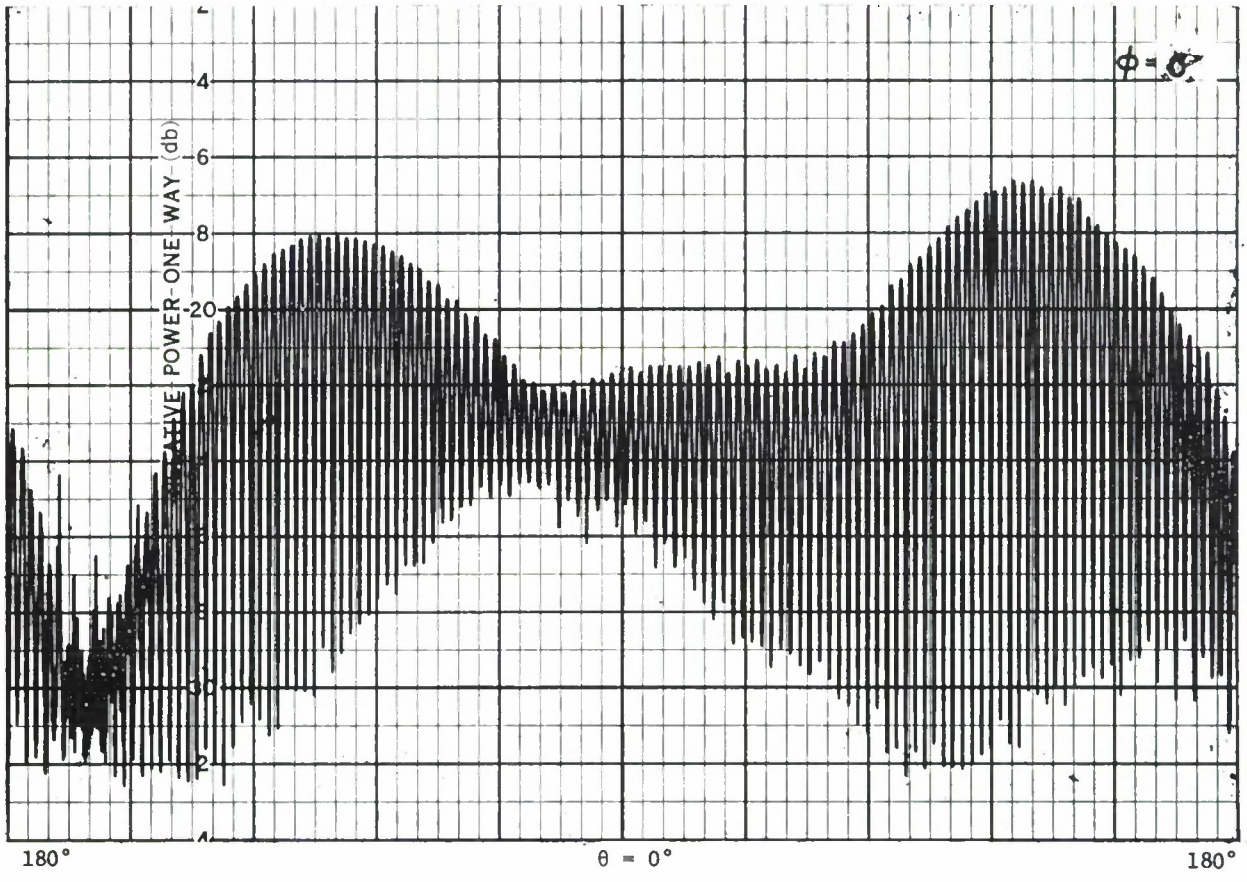

Figure 15 Radiation Pattern of Unbalanced Conical Antenna. 2π variation in θ, $\phi = 0$. Frequency 208 MHz.

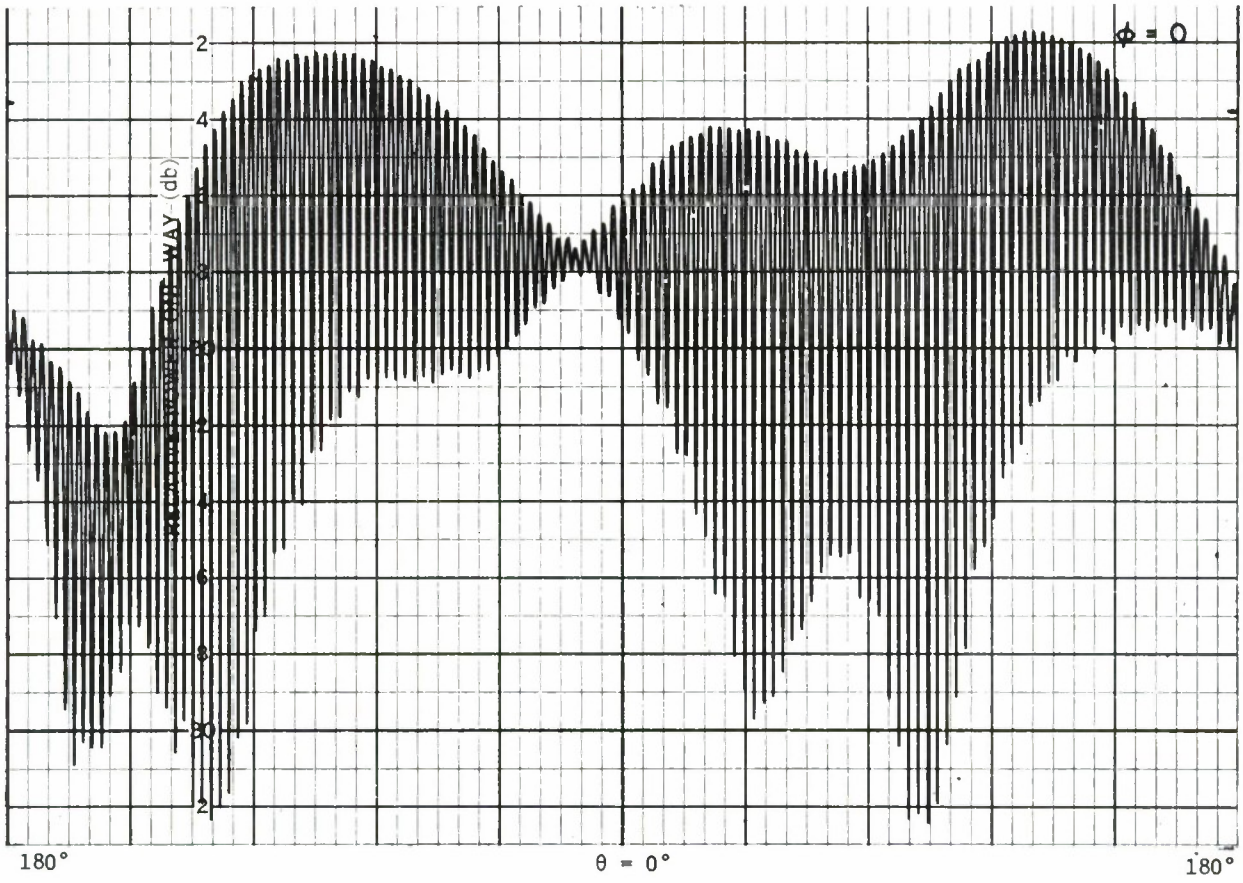

Figure 16 Radiation Pattern of Unbalanced Conical Antenna. 2π variation in θ, $\phi = 0$. Frequency 220 MHz.

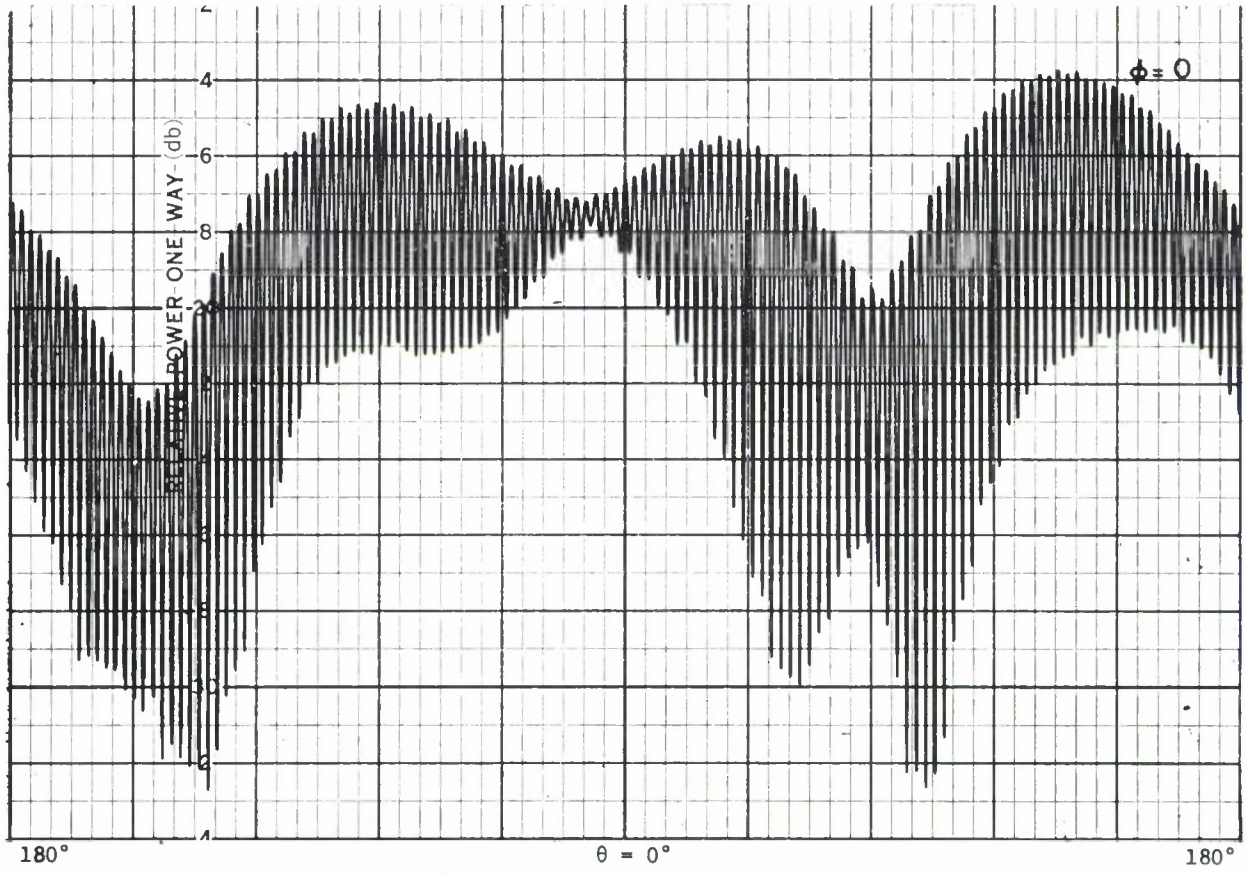

Figure 17 Radiation Pattern of Unbalanced Conical Antenna. 2π variation in θ, $\phi = 0$. Frequency 230 MHz.

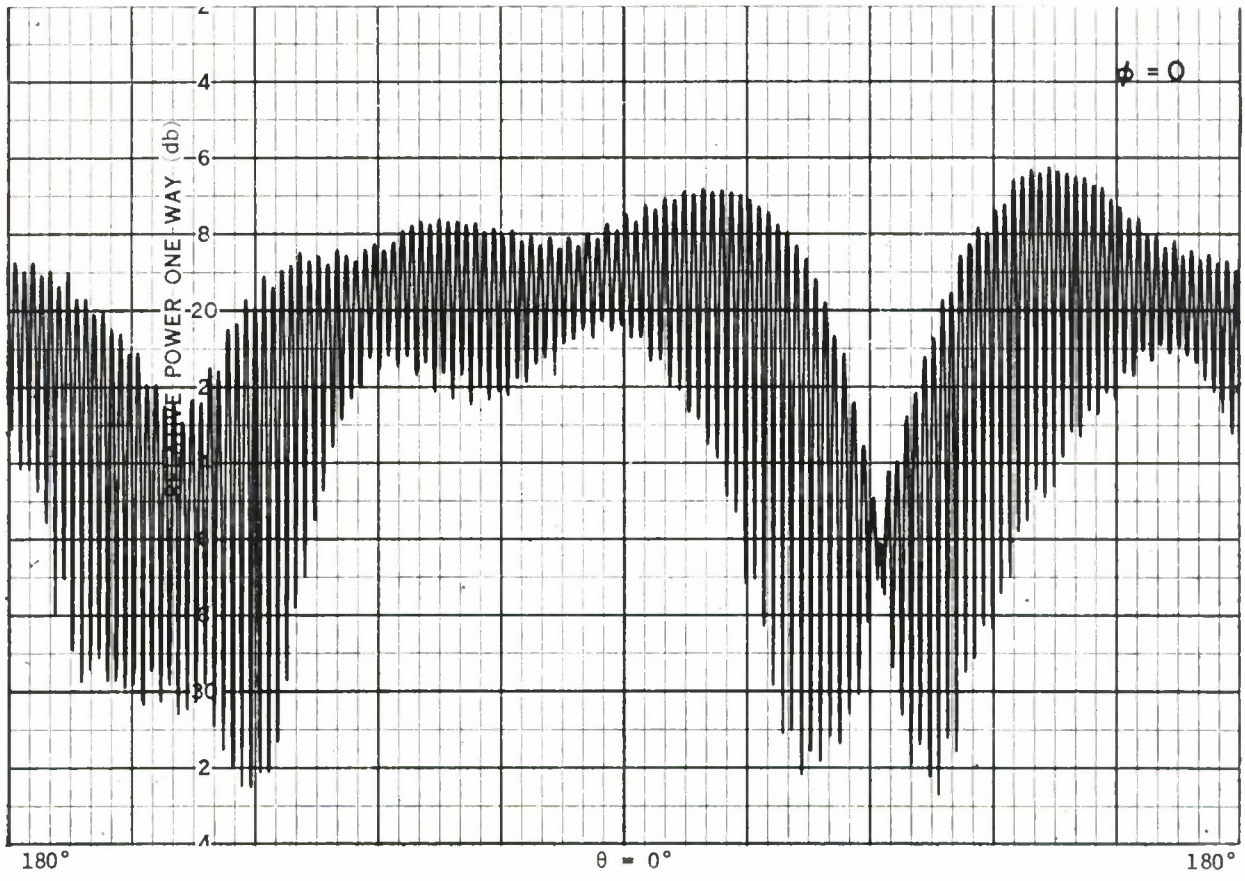

Figure 18 Radiation Pattern of Unbalanced Conical Antenna. 2π variation in θ, $\phi = 0$. Frequency 250 MHz.

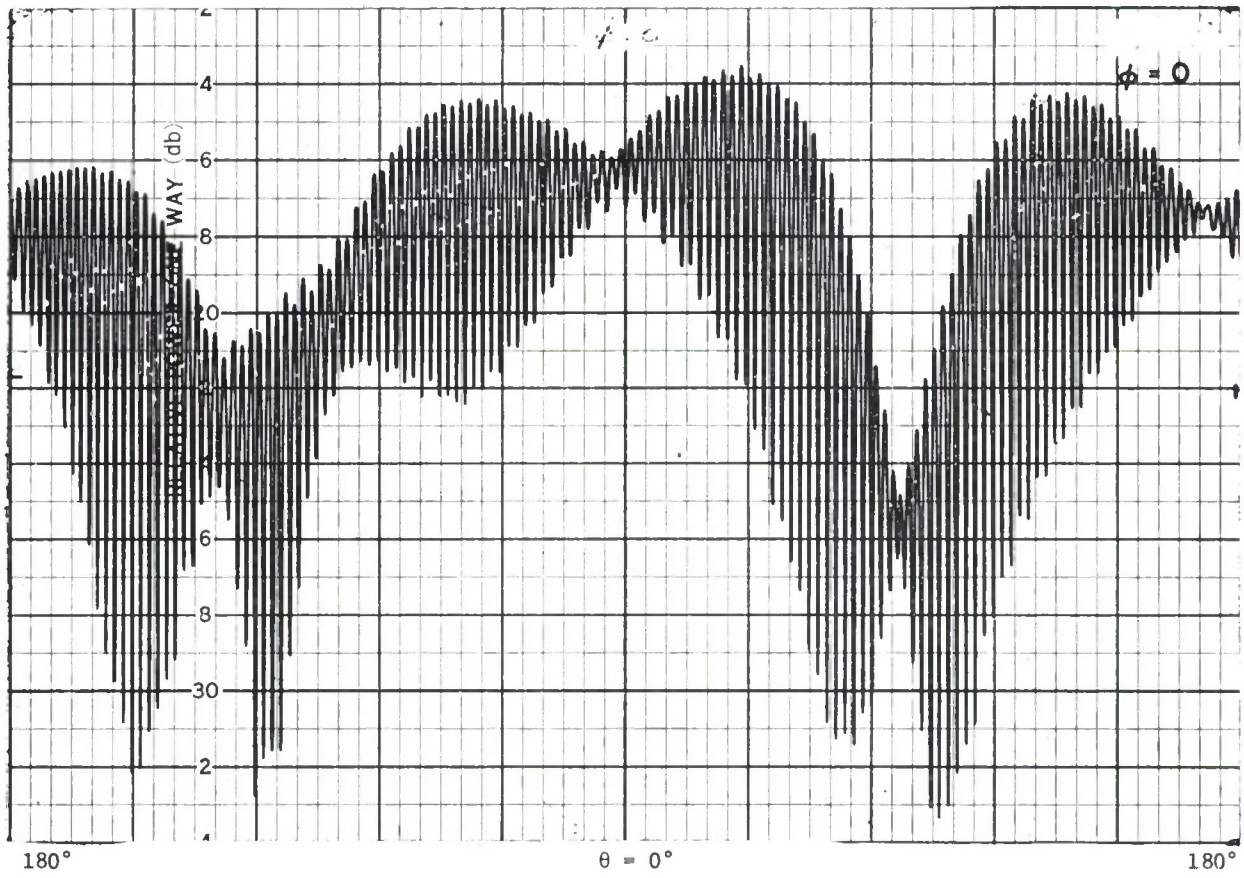

Figure 19 Radiation Pattern of Unbalanced Conical Antenna. 2π variation in θ, $\phi = 0$. Frequency 270 MHz.

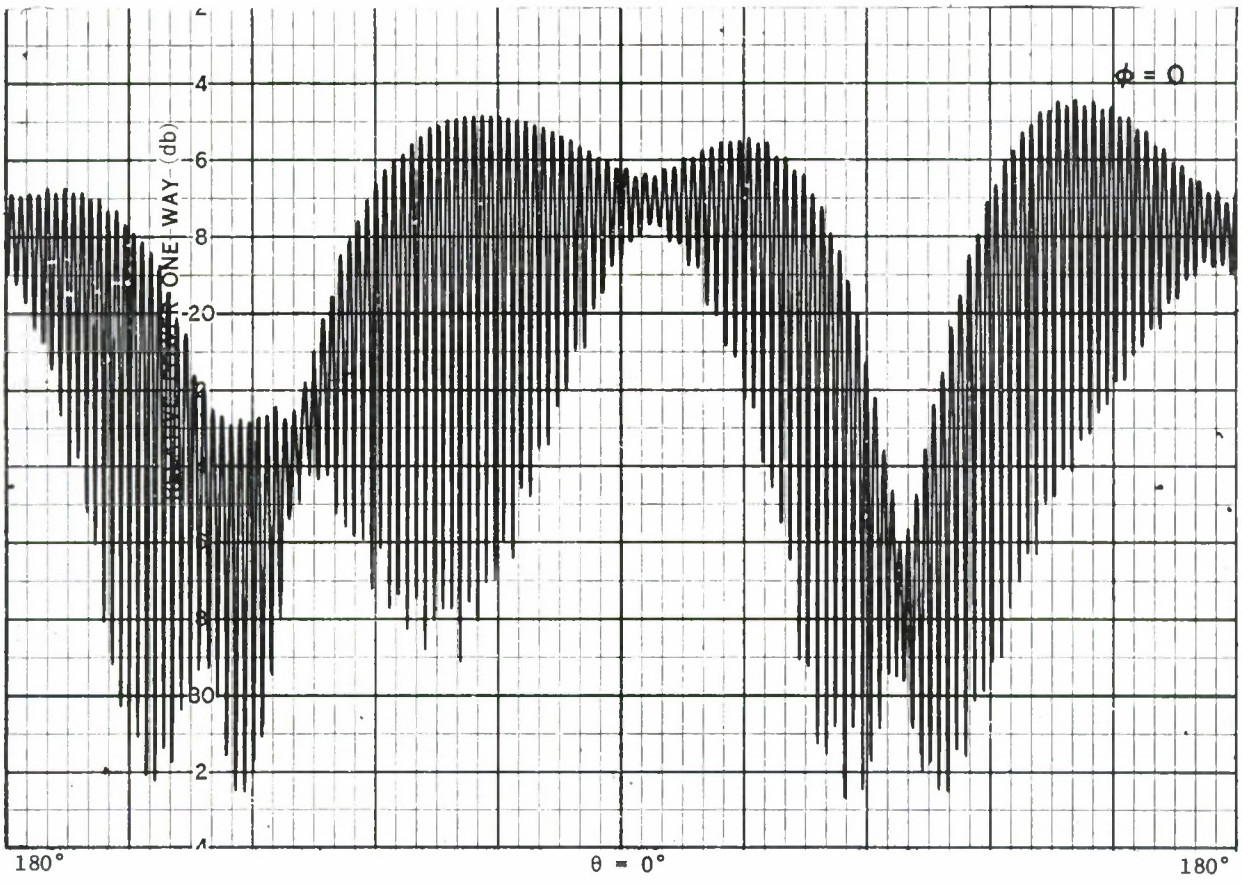

Figure 20 Radiation Pattern of Unbalanced Conical Antenna. 2π variation in θ, $\phi = 0$. Frequency 279 MHz.

Radiation patterns for three different ϕ cuts are shown for many of these frequencies in Appendix A hereto.

It was mentioned earlier that a second type antenna mount was constructed and tried. This is shown in Figure 21. It is a cradle support of polyfoam. The antenna was bound to this support with 2 strips of thin fiberglass tape. Patterns were recorded with this mount and compared to those taken with the polystrene base-mount. Figures 22 and 23 show two such patterns. The major difference is a slight change in axial ratio along the cone axis. Whether this is due to the presence of the polystyrene mount at the base of the antenna or the polyfoam block covering one-half the antenna is undetermined. This author believes that one source is as likely the cause of the difference as the other, and that the difference is not of significant proportions in the present study.

Figure 21. Polyfoam cradle designed to support the conical antenna.

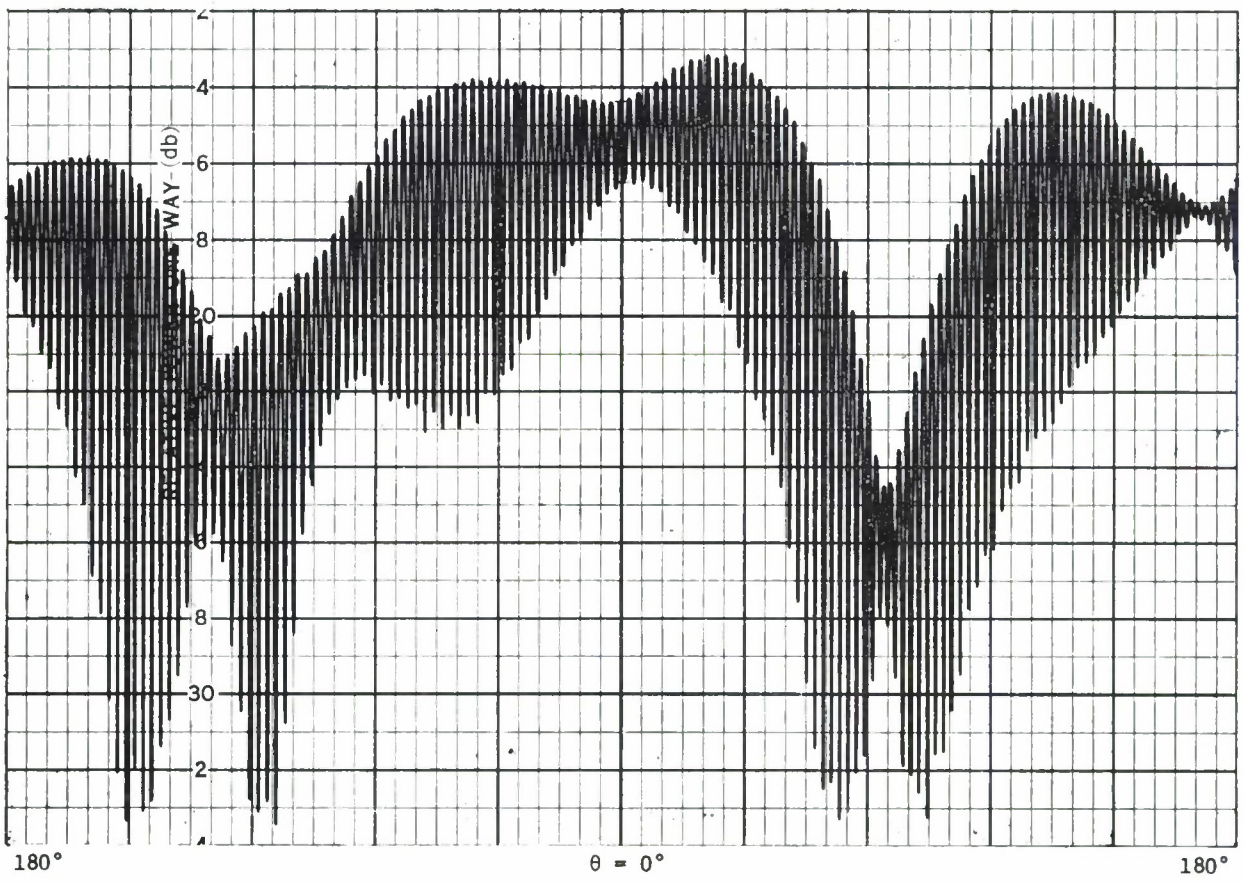

Figure 22 Radiation Pattern of Unbalanced Conical Antenna supported in polyfoam cradle mount shown in Figure 21. Pattern covers 2π variation in θ with $\phi = 0$. Frequency 270 MHz.

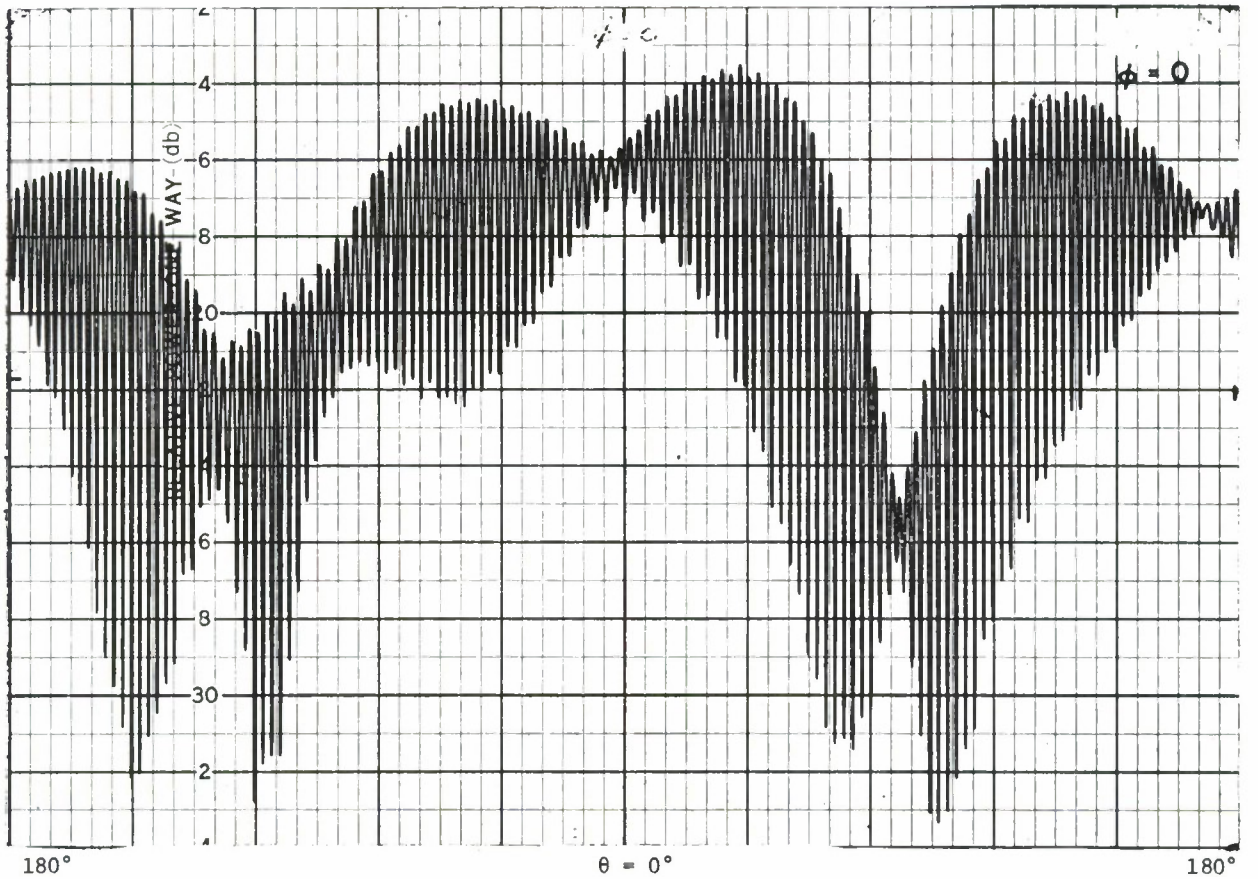

Figure 23 Radiation Pattern of Unbalanced Conical Antenna. 2π variation in θ, $\phi = 0$. Frequency 270 MHz.

V. The Measured Power Gain

The power gain of the antenna was of primary consideration. Before considering measurements on the conical antenna, it will be helpful to define some terms that will be used. Using the current IEEE Standard[7] "the power gain of an antenna in a specified direction is 4π times the ratio of the power radiated per unit solid angle in that direction to the net power accepted by the antenna from its generator. This term is an inherent property of the antenna, and does not involve system losses arising from mismatch of impedance or of polarization."

In this definition the standard for gain comparison is a hypothetical radiator called the isotropic radiator, which radiates equally in all directions, is lossless, and has a gain of unity. Again quoting from reference (7): "the gain of an antenna is usually measured in the direction of its maximum value. Knowledge of the radiation pattern amplitude then permits determination of the gain in any other direction. In the direction of the maximum value, power gain is termed maximum power gain."

In the present case it is convenient to use the antenna without tuning or matching circuits. Thus the measured "gain" involves some mismatch loss. Strictly speaking then, what we have measured and will describe does not fulfill the exact criteria for "power-gain" as defined above. To identify it we will define it to be the "broadband power gain."

In practice, the maximum power gain of an antenna is almost always determined from a measurement of relative gain involving a standard-gain antenna. The power received by the antenna under test is compared with the power received by the standard-gain antenna when both antennas are placed in a uniform plane-wave field and oriented for maximum received power.

This method of measurement was used, and the "standard-gain" half wave dipole antenna, to which the conical antenna was compared, is shown in Figure 24. The dipole antenna is constructed of brass, with a split drum (or split coax) balun with a movable shorting ring. It also has removable arms. At each frequency of measurement, a set of half-wavelength arms was attached to the antenna, and the effective length of the balun was adjusted to one fourth wavelength.

In Figure 25 the antenna is shown mounted on the antenna test tower. For measurement of the radiated fields of the dipole, the electronic equipment that had been enclosed inside the metal cone was put in an insulated bag and positioned in back of the tower head.

It is recognized that the oscillator package and tower head are in the dipole field. However, absorbing material was used as shown, and the relative strength of the radiated field was recorded in both the front (the direction away from the tower head) and in the back (the direction toward the tower head) of the dipole. The "back" radiation was approximately 1 db less than that in "front" due partly to the absorber. It is felt that the maximum error due to the use of the dipole in this way is approximately 0.5 db or less.

With the padding and isolation of the oscillator that is shown in Figure 7, the incident power levels delivered to the antenna feed cable terminals of the conical and the dipole antennas differed typically by 0.2 db or less. In any case, it was monitored and the recorded data corrected accordingly.

No attempt was made to tune or match the dipole antenna, but instead a high directivity, 20 db, 4 port directional coupler (Hewlett-Packard 778D-11) was inserted between the dipole feed cable terminal and the oscillator

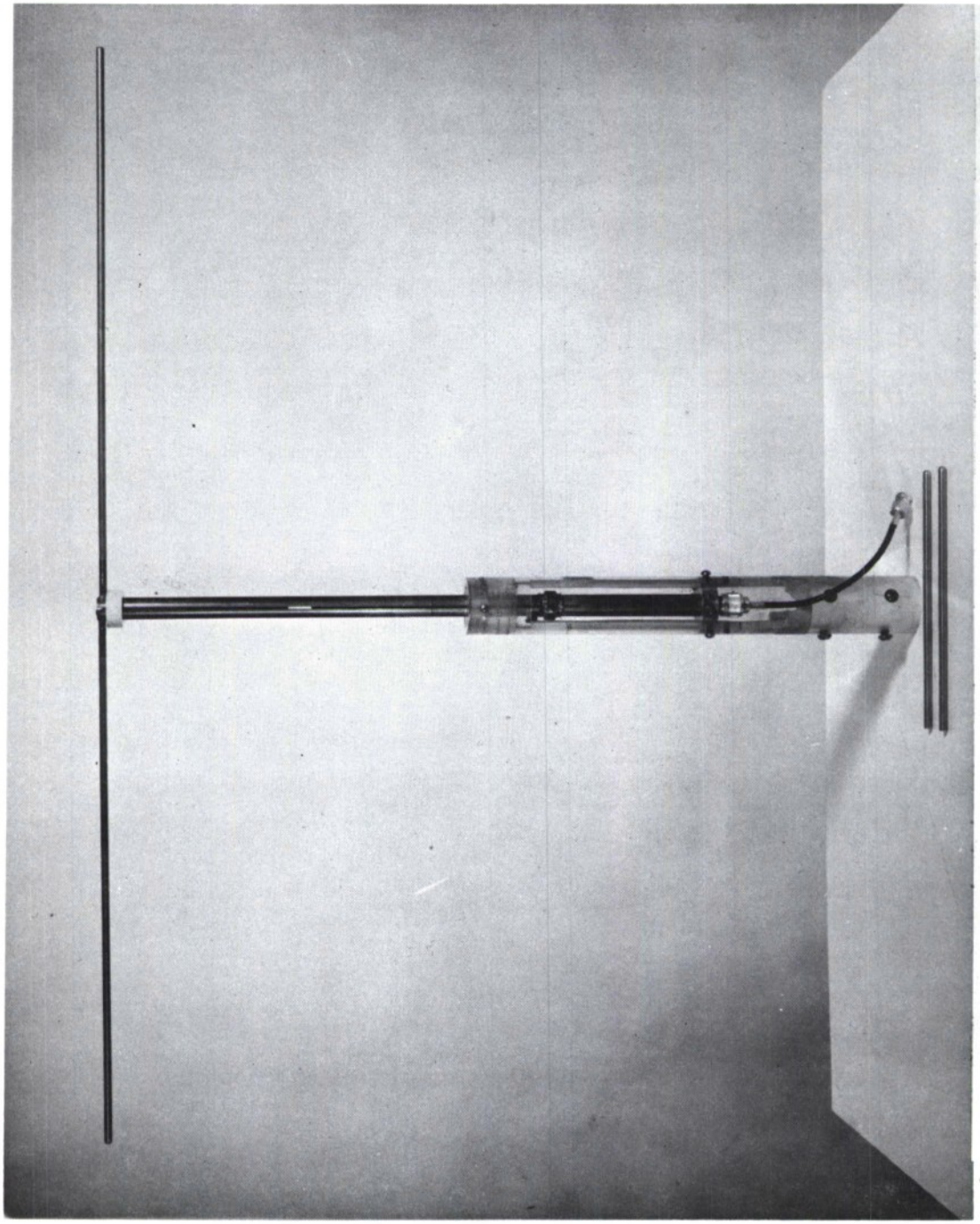

Figure 24. Dipole antenna used as a standard. Split drum balun with movable shorting ring is visible and one pair of alternate removable arms is shown.

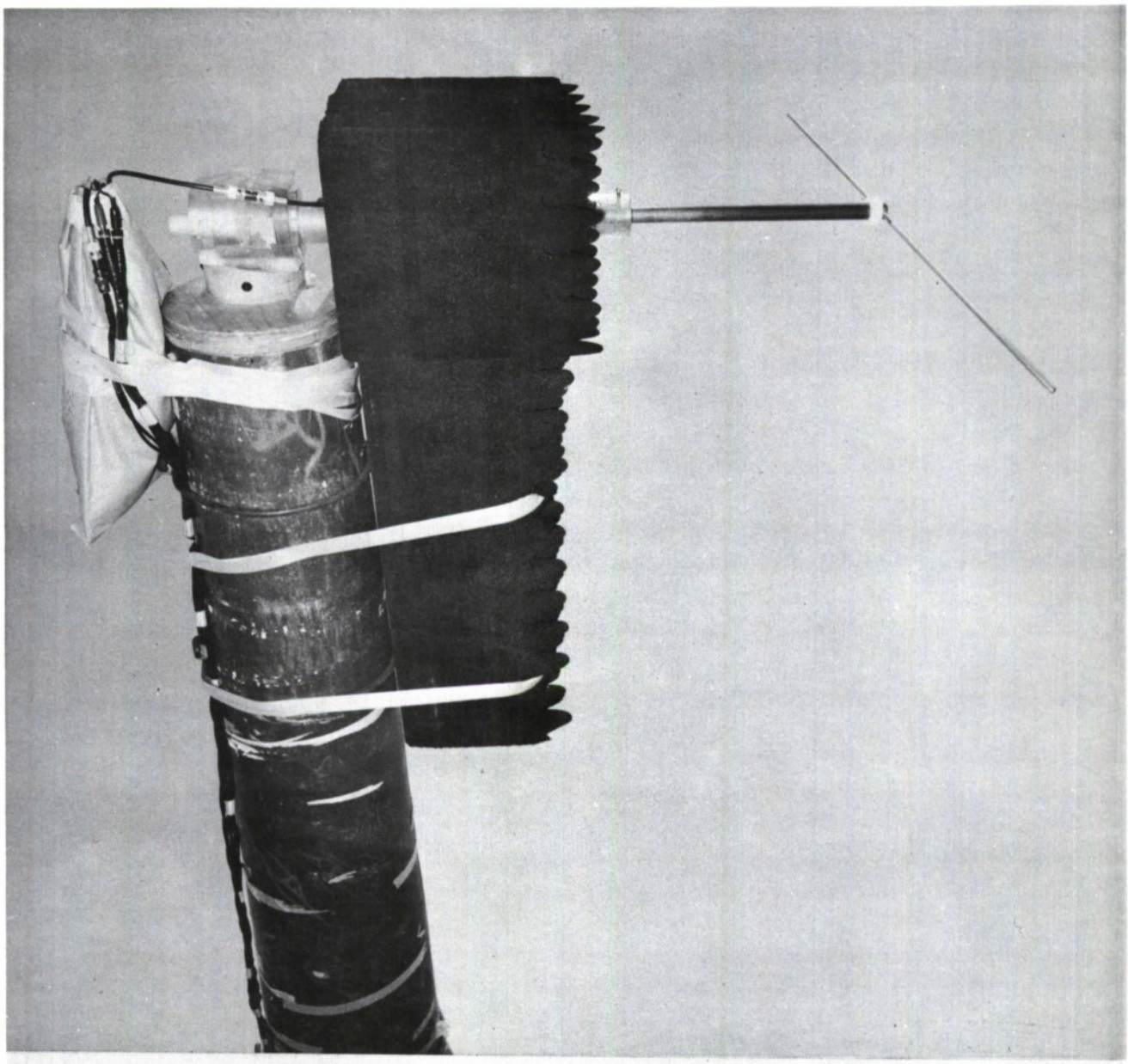

Figure 25. Dipole and oscillator package mounted on antenna test tower.

package for calibration purposes. The difference between the incident power to the antenna, and the reflected power from the antenna, was measured at each frequency of interest. This difference in db is, by definition, the return loss of the dipole-balun combination. The return loss varied from 4.6 to 5.8 db. From this, an equivalent input VSWR of this antenna could be determined, with values varying from 3.9 to 3.3:1. Since the type of balun that was used provides a 4 to 1 impedance transformation, the output terminals of the ideal balun are at approximately a 208 ohm level. At resonance, a 70 ohm dipole would cause a VSWR of approximately 3:1 on a 208 ohm line. The VSWR determined from the measured return loss of the practical antenna, was considered close enough to this 3:1 level to be satisfactory.

From the measured return loss, a transmission loss was determined. This varied from 1.3 to 1.8 db. The value of this transmission loss in db, determined for each particular frequency, was added to the measured radiated power of the "standard dipole", expressed in db, to get an equivalent power that would have been radiated by a reflectionless, resonant, half-wave dipole.

The dipole was considered to be lossless. If it is not, this loss would cause the "standard" to radiate less energy than a lossless unit, and the measured gain of conical antenna to be high. The losses of such a dipole should be low. However, if desired, the final data could be easily corrected for any assumed efficiency of the dipole.

At each of 11 frequencies from 150 to 280 MHz the recorded patterns of the conical antenna were scanned to find an angle of observation for which there was a maximum signal level. At this particular angle of observation, the power in the two orthogonal components of the field was added to find the maximum power radiated by the antenna at that given frequency of operation.

If P_1 and P_2 are the powers radiated in these two orthogonal components, the axial ratio in db is

$$R_{db} = 10 \log \left(\frac{P_1}{P_2}\right) \tag{1}$$

This axial ratio was read from the radiation pattern as the width of the envelope of the recorded pattern which had been made with a constantly rotating plane of polarization of the linearily polarized receiving antenna. The maximum of the envelope corresponds to the P_1 and the minimum to the P_2 above.

The total power radiated, at the chosen angle of observation and frequency of operation is then P_1 plus a correction C, in db, where

$$C_{db} = 10 \log \left(\frac{P_1 + P_2}{P_1}\right) \tag{2}$$

This correction may conveniently be expressed in the form

$$C_{db} = 10 \left[\log\left[1 + \text{antilog } \left(\frac{R}{10}\right)\right] - \frac{R}{10}\right] \tag{3}$$

and a table of values of C_{db} for various values of R_{db} is included as Table No. 1 which follows.

Table No. 1. Relationship between a given axial ratio in db (R), and the relative power in db in the smaller of the two orthogonal circularly polarized field components (C).

R db	C db	R db	C db	R db	C db	R db	C db	R db	C db	R db	C db	R db	C db
0.00	3.01	1.00	2.54	2.00	2.12	3.00	1.76	4.10	1.43	6.75	0.83	10.7	0.35
0.02	3.00	1.02	2.53	2.02	2.12	3.02	1.76	4.15	1.41	6.80	0.82	10.8	0.35
0.04	2.99	1.04	2.52	2.04	2.11	3.04	1.75	4.20	1.40	6.85	0.82	10.9	0.34
0.06	2.98	1.06	2.51	2.06	2.10	3.06	1.74	4.25	1.39	6.90	0.81	11.0	0.33
0.08	2.97	1.08	2.50	2.08	2.09	3.08	1.74	4.30	1.37	6.95	0.80	11.1	0.32
0.10	2.96	1.10	2.50	2.10	2.09	3.10	1.73	4.35	1.36	7.00	0.79	11.2	0.32
0.12	2.95	1.12	2.49	2.12	2.08	3.12	1.72	4.40	1.35	7.05	0.78	11.3	0.31
0.14	2.94	1.14	2.48	2.14	2.07	3.14	1.72	4.45	1.33	7.10	0.77	11.4	0.30
0.16	2.93	1.16	2.47	2.16	2.06	3.16	1.71	4.50	1.32	7.15	0.77	11.5	0.30
0.18	2.92	1.18	2.46	2.18	2.06	3.18	1.71	4.55	1.31	7.20	0.76	11.6	0.29
0.20	2.91	1.20	2.45	2.20	2.05	3.20	1.70	4.60	1.29	7.25	0.75	11.7	0.28
0.22	2.90	1.22	2.44	2.22	2.04	3.22	1.69	4.65	1.28	7.30	0.74	11.8	0.28
0.24	2.89	1.24	2.43	2.24	2.03	3.24	1.69	4.70	1.27	7.35	0.73	11.9	0.27
0.26	2.88	1.26	2.43	2.26	2.03	3.26	1.68	4.75	1.25	7.40	0.73	12.0	0.27
0.28	2.87	1.28	2.42	2.28	2.02	3.28	1.67	4.80	1.24	7.45	0.72	12.2	0.25
0.30	2.86	1.30	2.41	2.30	2.01	3.30	1.67	4.85	1.23	7.50	0.71	12.4	0.24
0.32	2.85	1.32	2.40	2.32	2.00	3.32	1.66	4.90	1.22	7.55	0.70	12.6	0.23
0.34	2.84	1.34	2.39	2.34	2.00	3.34	1.65	4.95	1.21	7.60	0.70	12.8	0.22
0.36	2.83	1.36	2.38	2.36	1.99	3.36	1.65	5.00	1.19	7.65	0.69	13.0	0.21
0.38	2.82	1.38	2.37	2.38	1.98	3.38	1.64	5.05	1.18	7.70	0.68	13.2	0.20
0.40	2.81	1.40	2.37	2.40	1.97	3.40	1.63	5.10	1.17	7.75	0.67	13.4	0.19
0.42	2.81	1.42	2.36	2.42	1.97	3.42	1.63	5.15	1.16	7.80	0.67	13.6	0.19
0.44	2.80	1.44	2.35	2.44	1.96	3.44	1.62	5.20	1.15	7.85	0.66	13.8	0.18
0.46	2.79	1.46	2.34	2.46	1.95	3.46	1.62	5.25	1.13	7.90	0.65	14.0	0.17
0.48	2.78	1.48	2.33	2.48	1.94	3.48	1.61	5.30	1.12	7.95	0.65	14.2	0.16
0.50	2.77	1.50	2.32	2.50	1.94	3.50	1.60	5.35	1.11			14.4	0.16
0.52	2.76	1.52	2.32	2.52	1.93	3.52	1.60	5.40	1.10	8.00	0.64	14.6	0.15
0.54	2.75	1.54	2.31	2.54	1.92	3.54	1.59	5.45	1.09	8.10	0.63	14.8	0.14
0.56	2.74	1.56	2.30	2.56	1.92	3.56	1.59	5.50	1.08	8.20	0.61	15.0	0.14
0.58	2.73	1.58	2.29	2.58	1.91	3.58	1.58	5.55	1.07	8.30	0.60	15.2	0.13
0.60	2.72	1.60	2.28	2.60	1.90	3.60	1.57	5.60	1.06	8.40	0.59	15.4	0.12
0.62	2.71	1.62	2.28	2.62	1.89	3.62	1.57	5.65	1.05	8.50	0.57	15.6	0.12
0.64	2.70	1.64	2.27	2.64	1.89	3.64	1.56	5.70	1.04	8.60	0.56	15.8	0.11
0.66	2.69	1.66	2.26	2.66	1.88	3.66	1.56	5.75	1.02	8.70	0.55	16.0	0.11
0.68	2.68	1.68	2.25	2.68	1.87	3.68	1.55	5.80	1.01	8.80	0.54	16.5	0.10
0.70	2.67	1.70	2.24	2.70	1.87	3.70	1.54	5.85	1.00	8.90	0.53	17.0	0.09
0.72	2.66	1.72	2.24	2.72	1.86	3.72	1.54	5.90	0.99	9.00	0.52	17.5	0.08
0.74	2.66	1.74	2.23	2.74	1.85	3.74	1.53	5.95	0.98	9.10	0.50	18.0	0.07
0.76	2.65	1.76	2.22	2.76	1.85	3.76	1.53	6.00	0.97	9.20	0.49	18.5	0.06
0.78	2.64	1.78	2.21	2.78	1.84	3.78	1.52	6.05	0.96	9.30	0.48	19.0	0.05
0.80	2.63	1.80	2.20	2.80	1.83	3.80	1.51	6.10	0.95	9.40	0.47	19.5	0.05
0.82	2.62	1.82	2.20	2.82	1.82	3.82	1.51	6.15	0.94	9.50	0.46	20.0	0.04
0.84	2.61	1.84	2.19	2.84	1.82	3.84	1.50	6.20	0.93	9.60	0.45	21.0	0.03
0.86	2.60	1.86	2.18	2.86	1.81	3.86	1.50	6.25	0.92	9.70	0.44	22.0	0.03
0.88	2.59	1.88	2.17	2.88	1.81	3.88	1.49	6.30	0.91	9.80	0.43	23.0	0.02
0.90	2.58	1.90	2.16	2.90	1.80	3.90	1.48	6.35	0.91	9.90	0.42	24.0	0.02
0.92	2.57	1.92	2.16	2.92	1.79	3.92	1.48	6.40	0.90	10.00	0.41	25.0	0.01
0.94	2.57	1.94	2.15	2.94	1.78	3.94	1.47	6.45	0.89	10.1	0.40	26.0	0.01
0.96	2.56	1.96	2.14	2.96	1.78	3.96	1.47	6.50	0.88	10.2	0.40	27.0	0.01
0.98	2.55	1.98	2.13	2.98	1.77	3.98	1.46	6.55	0.87	10.3	0.39	28.0	0.01
						4.00	1.46	6.60	0.86	10.4	0.38	29.0	0.01
						4.05	1.44	6.65	0.85	10.5	0.37	30.0	0.00
								6.70	0.84	10.6	0.36		

Thus to determine the maximum gain of the antenna at a particular frequency, the pattern was searched for a maximum level. The axial ratio in db, at this chosen angle of observation was read from the antenna pattern. Table No. 1 was entered at this axial ratio and C_{db} determined. This value of C_{db} was then added to $P_{1_{db}}$ to get the total power radiated in this particular direction.

After recording the conical antenna pattern, this antenna was removed from the tower, the dipole was mounted, and its radiated field recorded. The recorded data for the dipole were corrected for any change in incident power level to the antenna, and for the dipole mismatch. These corrected data were then compared to those recorded for the conical antenna. The difference in db between these data was considered to be the "maximum broad-band gain", of the conical antenna relative to that of a matched half-wave dipole. To convert to gain relative to an isotropic source, it was assumed that the standard dipole in use, had the 2.15 db free-space gain of a lossless half-wave dipole.

The "maximum broadband power gain" of the unbalanced conical antenna is plotted in Figure 26 as the top curve. Because the conical antenna changes from a endfire to a broadside radiator, the angular coordinates corresponding to the maximum gain, are a function of frequency. To more adequately describe the character of the radiated fields, three other "broadband power gains" were plotted. That along the antenna axis ($\theta = 0°$), that broadside to the cone axis ($\theta = 90°$), and the minimum gain that was observed. These curves reinforce what is observed in the patterns. By definition, all plotted power gain curves are referred to an <u>isotropic level</u>.

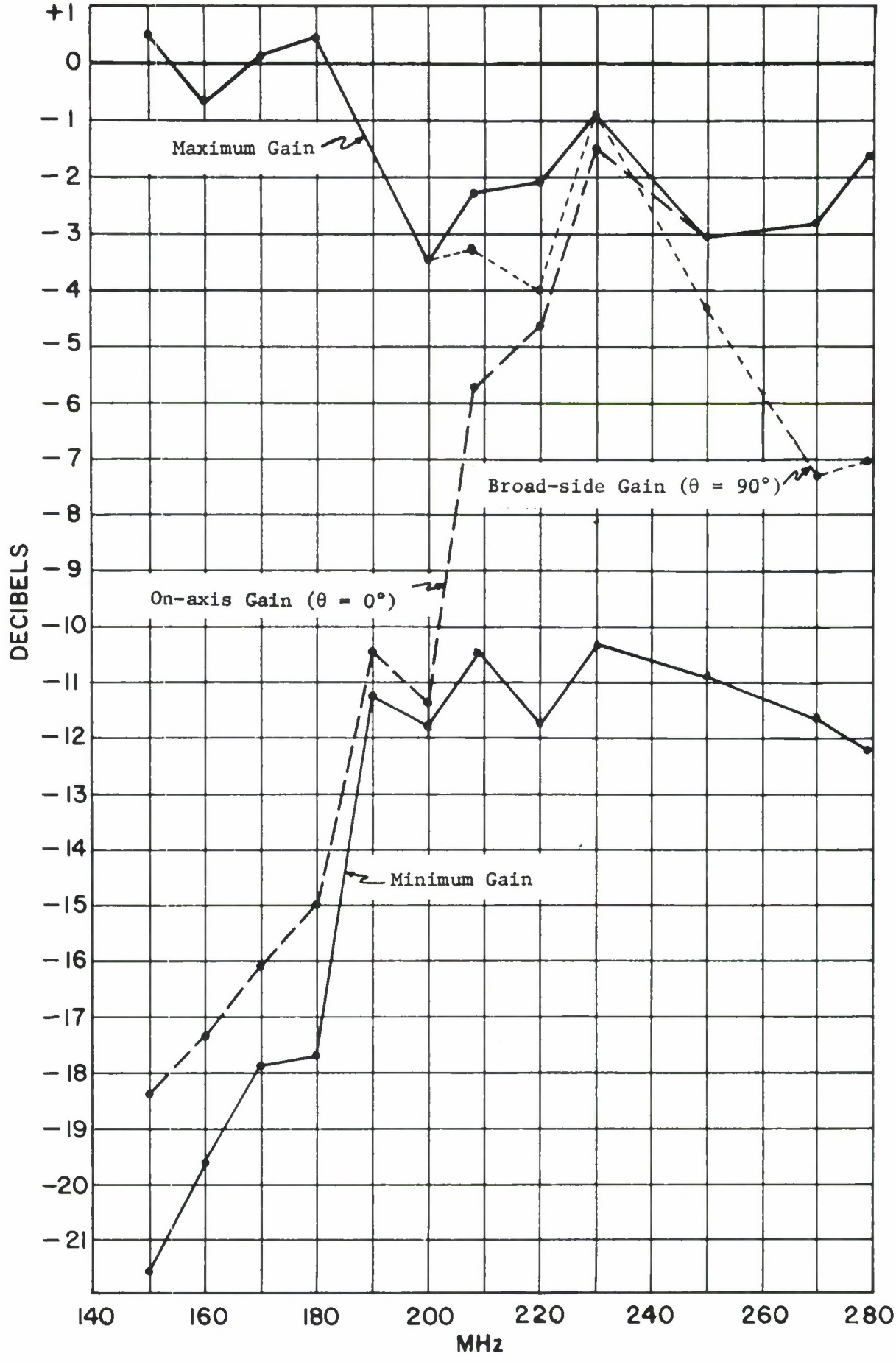

Figure 26. The measured "broadband power gain" of the unbalanced conical antenna.

The reader who is familiar with reference No. 1 will note that the on-axis and minimum gain, below 200 MHz in Figure 26 are both somewhat lower than that shown in the earlier report. In the earlier measurements, values of gain more than 10 to 12 db below isotropic were biased slightly upward because of the local noise and background level. The use of a very selective cavity filter improved the patterns and gain measurements. The sort of improvement that was obtained in the recorded radiation patterns is shown in Figure C-1 in the appendix hereto.

From 280 down to 250 MHz the antenna is an end-fire device with maximum power gain on axis. Below 250 MHz the axial gain drops off at a rate of roughly 30 db per octave. Between 200 and 250 MHz there is the transition from end-fire to broadside radiation. Below 200 MHz broadside radiation is predominant, while above 200 MHz the broadside radiation drops off at roughly 20 db per octave. At the lower frequencies the "minimum broadband power gain" differs from the axial gain only because the unbalance in the antenna causes the pattern minima to be slightly off axis. These characteristics can be related to the size of this particular antenna as shown below.

Diameter of Cone Base in Wavelengths d	Slant Surface of Cone in Wavelengths ρ	Character of Radiated fields
$d \leq .14$	$\rho \leq .43$	Broadside
$.14 < d < .175$	$.43 < \rho < .54$	Undefined
$d \geq .175$	$\rho \geq .54$	End-fire

The antenna was not tested for d less than $.11\lambda$ or greater than $.32\lambda$ or for ρ less than $.198\lambda$ or greater than $.61\lambda$.

To gain a general idea of the relative gain of these type antennas in a short period of time a technique for recording a plot of this gain (or a quantity directly related to it) while sweeping over a wide range of frequencies was developed.

To do this the potentiometer shown in Figure 7 , which determined the VCO control voltage, was motor driven. This motor was also geared to a selsyn transmitter which drove a conventional rectangular pattern recorder. The horizontal axis of a rectangular plot, so obtained, could now be calibrated in frequency. If the pen, and hence the vertical deflection of the plot, is driven by the signal received by the LPDA receiving antenna as it continuously rotates, the maximum radiated power, and axial ratio, of the antenna under test, in a particular direction, is recorded as a function of frequency. This data is, of course, subject to the proper calibration of the system and proper interpretation. This technique was used in an earlier study[6], but in that report the gain can only be determined at a few spot frequencies where the received power from a resonant dipole was recorded.

To make the recorded data more meaningful, an attempt was made to determine the level of power that would have been radiated by an isotropic antenna connected to the r.f. source in use, as <u>received and recorded</u> by the given receiving system, on the antenna pattern range in use, as this source was swept over a wide band of frequencies. This was done by using twelve dipoles resonant within the range of 170 to 280 MHz. This sweep technique, which required a "wide open" receiving system could not be used

below 180 or 190 MHz because of severe local r.f. interference. It was necessary to use a 200 MHz high pass filter in the receiving line and terminate the sweep at 180 MHz. For all "spot frequency" measurements of gain, a tunable r.f. amplifier, or a very selective cavity filter, was used in the receiving system. An ideal system would have a tunable receiver that tracked the sweeping source.

The power radiated by these dipoles was recorded as they were swept over a band of frequencies near resonance. If enough dipoles are available the bands overlap and hence the response of one could be normalized to that of the next until the desired range of frequencies is covered. This normalization was necessary because the output of the source, and the characteristic of the antenna range and those of the LPDA receiving antenna and the receiving system, were not necessarily constant with frequency.

After normalizing and cross-checking these swept responses as much as possible, the combined, or "constructed" level was corrected for dipole mismatch, and then reduced to an equivalent isotropic level.

Immediately before and after a swept response was recorded for an antenna under test, the response of the receiving system was recorded for that same source driving a resonant 250 MHz dipole. Thus drift in the source or system, with time, could be detected. Also, since the response of the system to that same dipole had been included in the data used to construct the "isotropic" power level curve, this provided a check point for use in normalizing this curve to the recorded antenna data. Thus day to day variations in the source or receiving systems could be normalized out.

This technique cannot provide data of high accuracy because of the assumptions made when the swept response curves of the dipoles were used. Further, any one swept response curve records the radiated power in one direction only. If the direction of maximum radiated power changes, as it does for many of this type of antenna, several sweeps are necessary, and it would be necessary to use the envelope of the recorded responses in some fashion.

None-the-less, in a short period of time, the technique permits recording a considerable amount of data of sufficient accuracy to determine the general characteristics of these antennas. To supplement this data, conventional direct substitution measurements can be made at any desired frequency.

The swept response of the CUSP antenna is shown in Figures 27 through 29. It is possible to determine the approximate broadband power gain at any frequency at the given direction, by adding the power in the two orthogonal components of the received signal, and then taking the difference between this combined level and the isotropic level curve. Thus at any given frequency, the relative power radiated in the major component of the field in db, in the given direction can be noted. To this is added the correction determined from Table No. 1 and the difference between this corrected value and the isotropic curve is then determined.

The approximate broadband gain of the original CUSP antenna is indicated in Figures 27, 28, and 29 at $\theta = 0$ (on axis), at $\theta = 30°$, and at $\theta = 90°$ (broadside to the antenna axis). Since the dynamic response of the receiving system was only about 24 db, the system (and interference) noise level prevents a determination of the true axial ratio in Figure 29. It is only possible to say that it is equal to, or greater than, the value shown.

The decrease in axial gain and build-up in the broadside gain is clearly evident. Similarly we can note the change in the axial ratio of the radiated fields. The field is nearly circularly polarized on axis, but it has a higher ellipticity ratio at 30° off axis, and is essentially linear polarized at broadside.

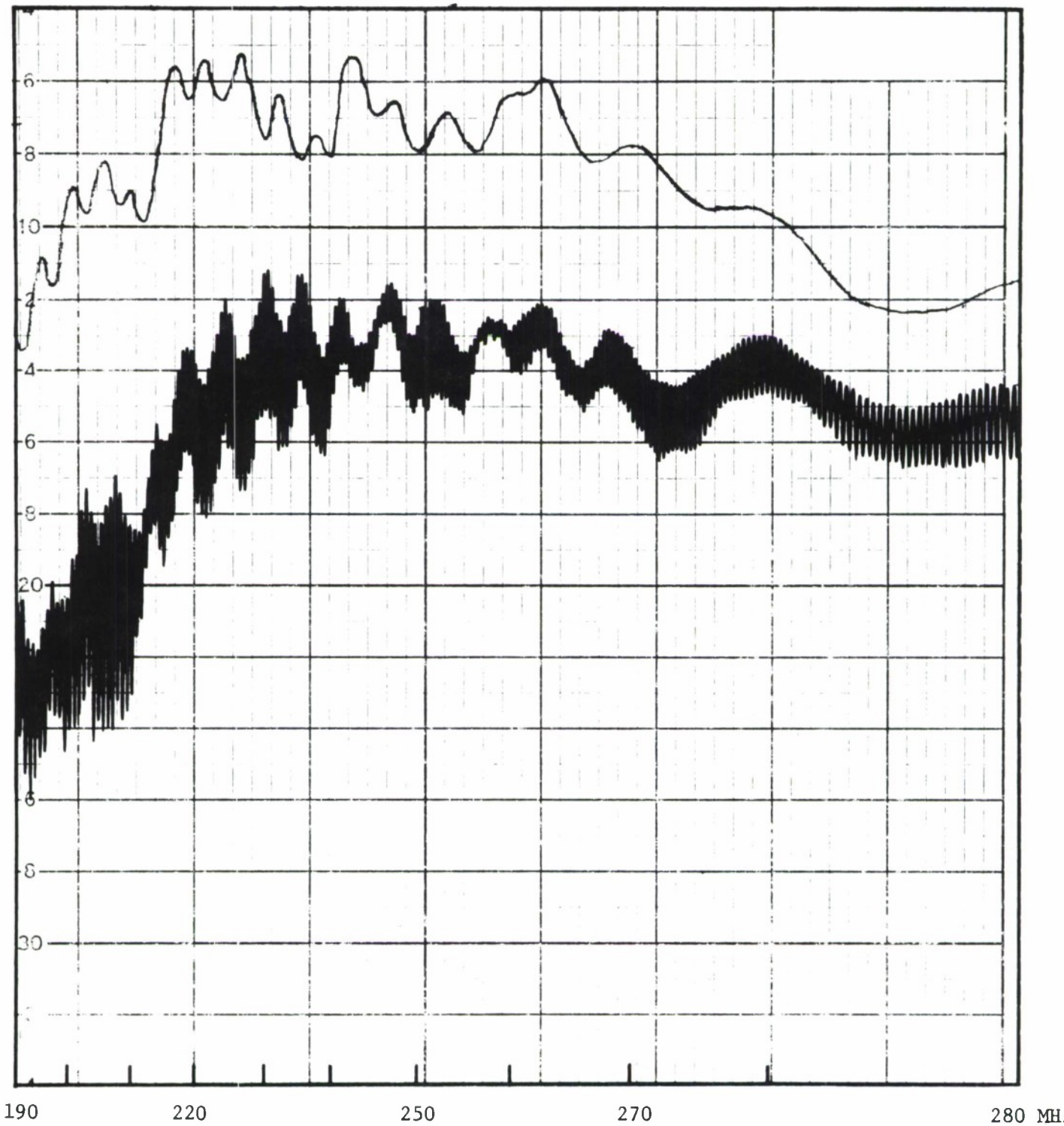

Figure 27 . Relative radiated power of Philco CUSP antenna at $\theta = 0°$, recorded with a rotating linearly polarized receiving antenna. For reference an approximate level that would have been radiated by a matched isotropic antenna is shown.

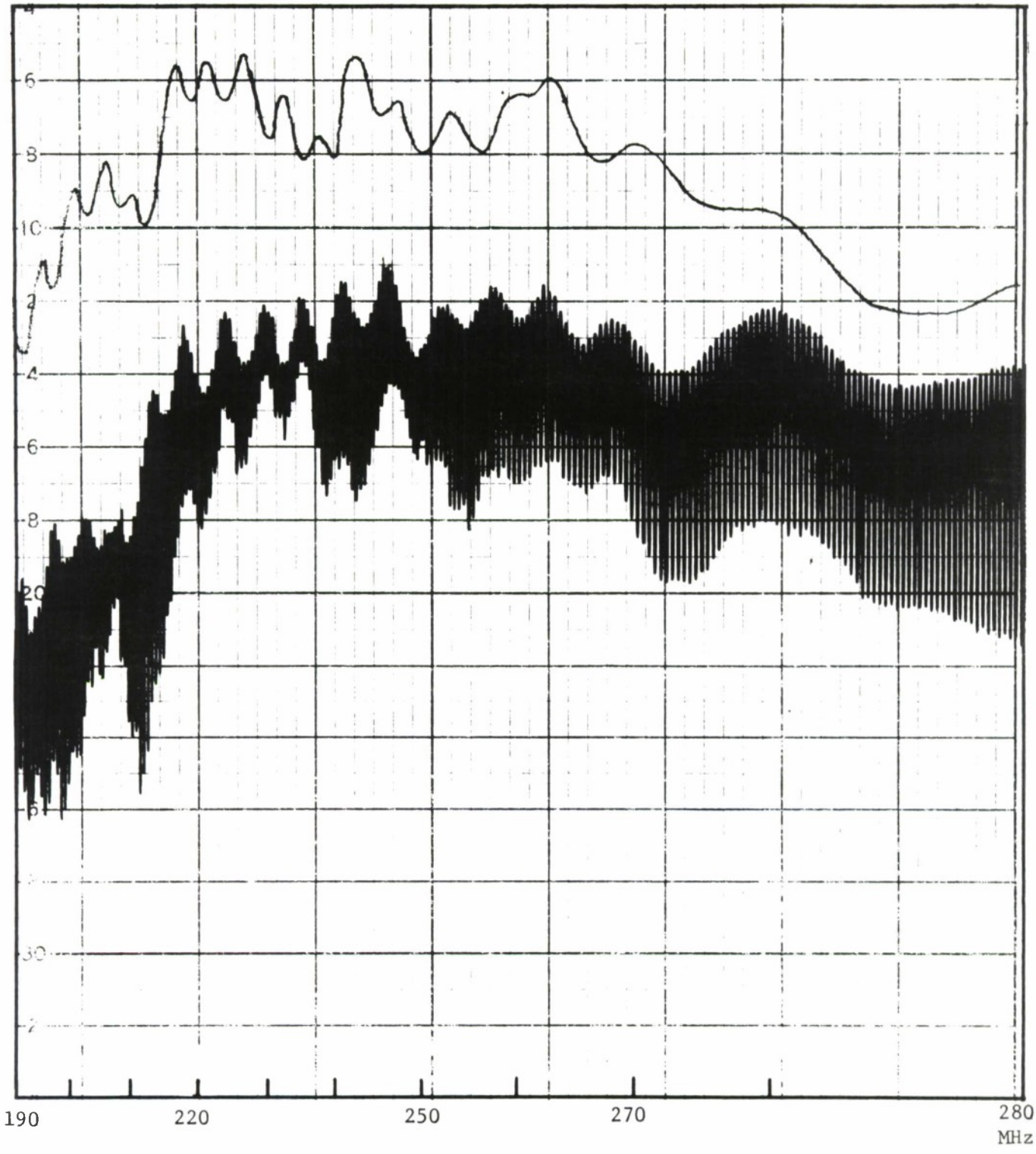

Figure 28. Relative radiated power of Philco CUSP antenna at $\theta = 30°$, recorded with a rotating linearly polarized receiving antenna. For reference an approximate level that would have been radiated by a matched isotropic antenna is shown.

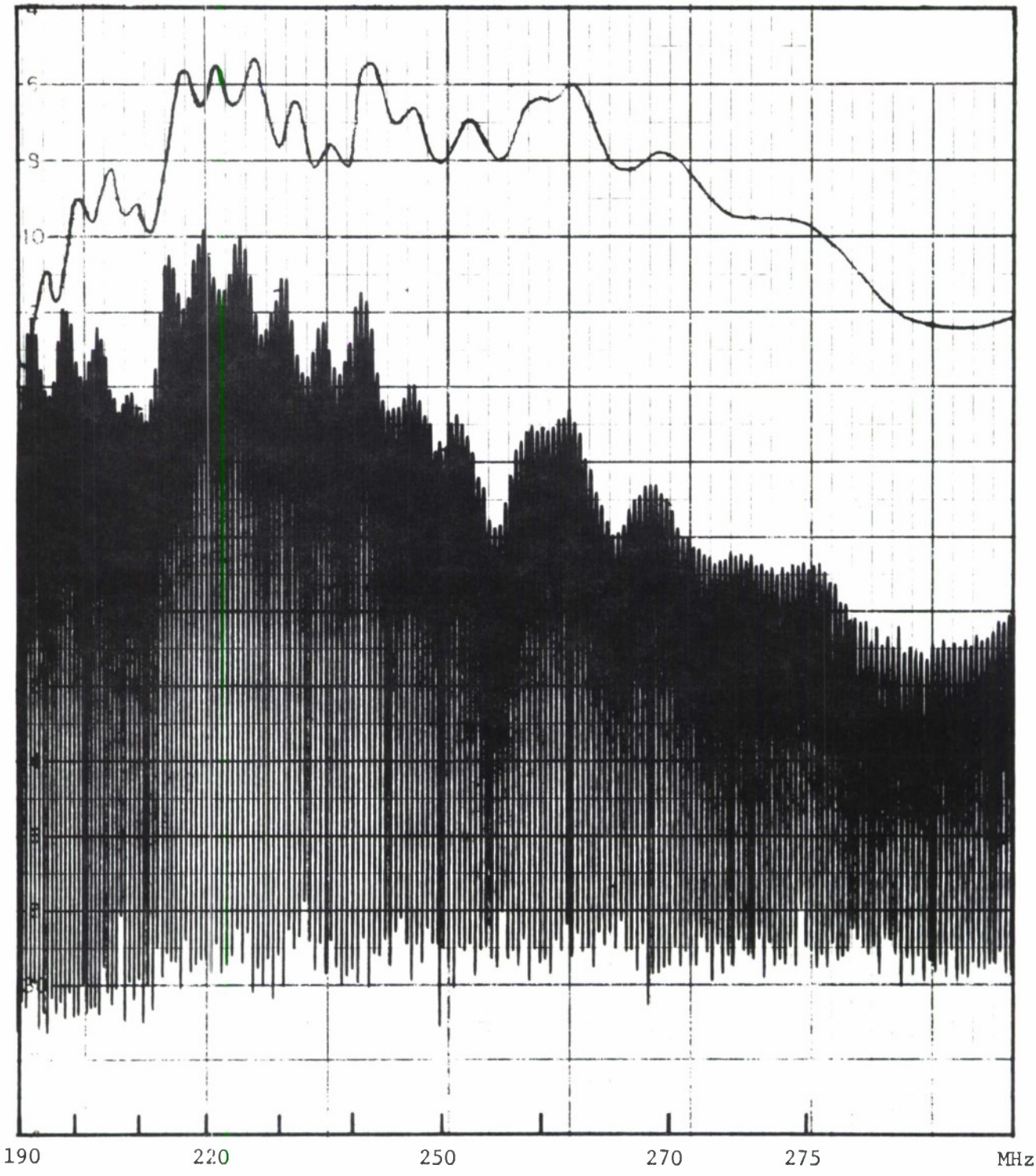

Figure 29 . Relative radiated power of Philco CUSP antenna at $\theta = 270°$ recorded with a rotating linearly polarized receiving antenna. For reference an approximate level that would have been radiated by a matched isotropic antenna is shown.

VI. THE MEASURED VSWR

The voltage standing wave ratio that the conical spiral antenna causes on a 50 ohm coaxial line was measured with set-up of Figure 30. In this case the power reflected from the antenna was sampled with a directional coupler. A signal proportional to this reflected power was recorded as the frequency was swept from 130 to 280 MHz. One such recorded curve is shown in Figure 31.

To provide a VSWR calibration, commercial mismatch loads with a known reflection coefficient were connected at point A in the system in place of the antenna. The frequency was then swept over the above range. In this manner a grid of known VSWR values was obtained. Measurements were made down to 130 MHz because the characteristics of the pattern range were not involved.

It will be observed that the antenna is well matched to a 50 ohm system at 150 MHz. The VSWR, and hence the reflection coefficient, rises as operation departs in each direction from 150 MHz.

Similar measurements, as shown in Figure 32, were made when the antenna was mounted in the polyfoam cradle. There is some difference between the two curves. The antenna, on the polystyrene base-mount has the lowest reflection coefficient between 200 and 250 MHz, while the antenna in the foam cradle has the lowest reflection coefficient from 250 to 280 MHz. Again it is difficult to judge the merits of the mounts, so the base-mount was selected for further study.

The attenuation of the feed cable which had been bonded to the antenna arm was measured by open circuiting this cable at the apex of the antenna, and then measuring its return loss. As can be seen in Figure 33, this

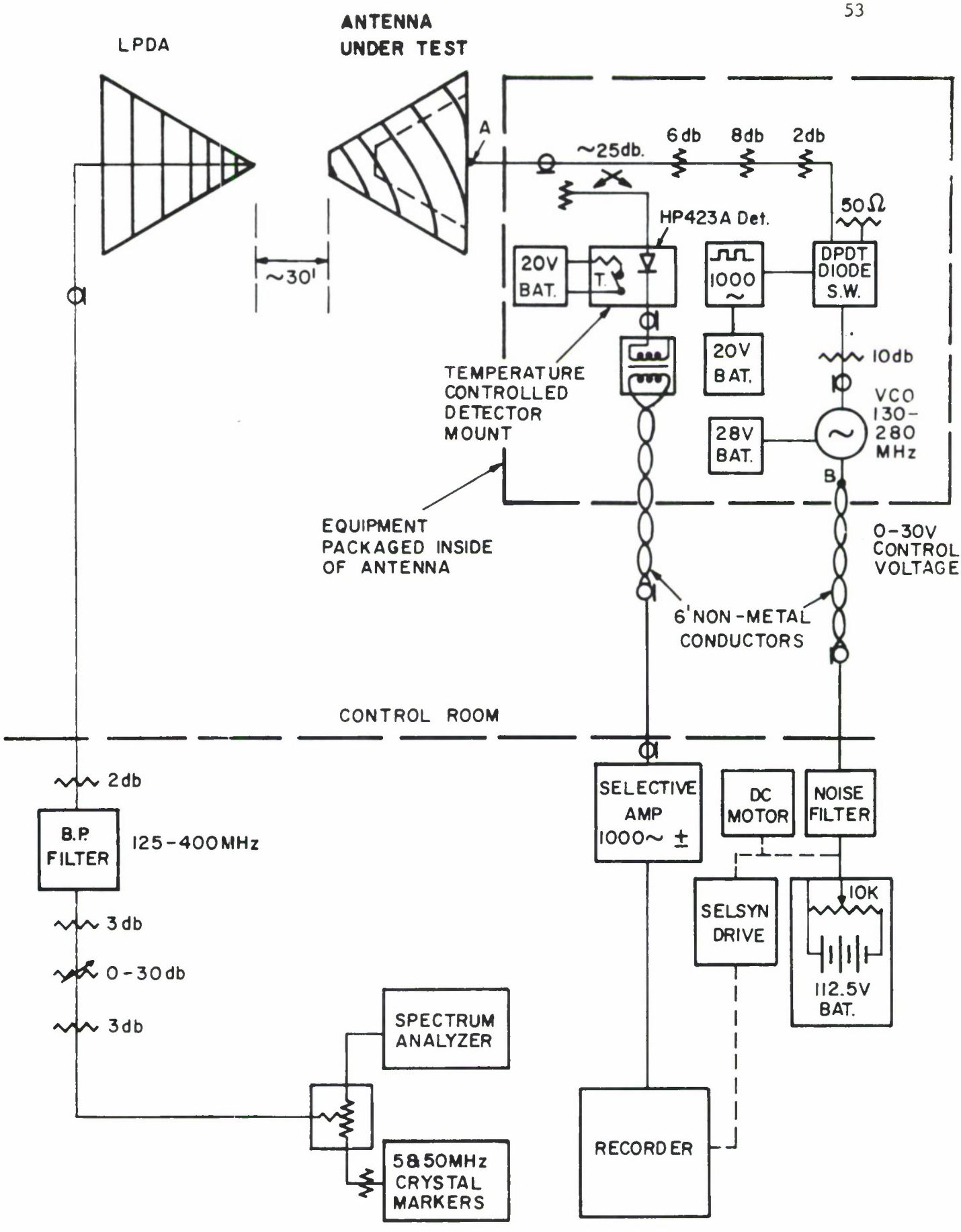

Figure 30 Block diagram of the system used to measure the VSWR.

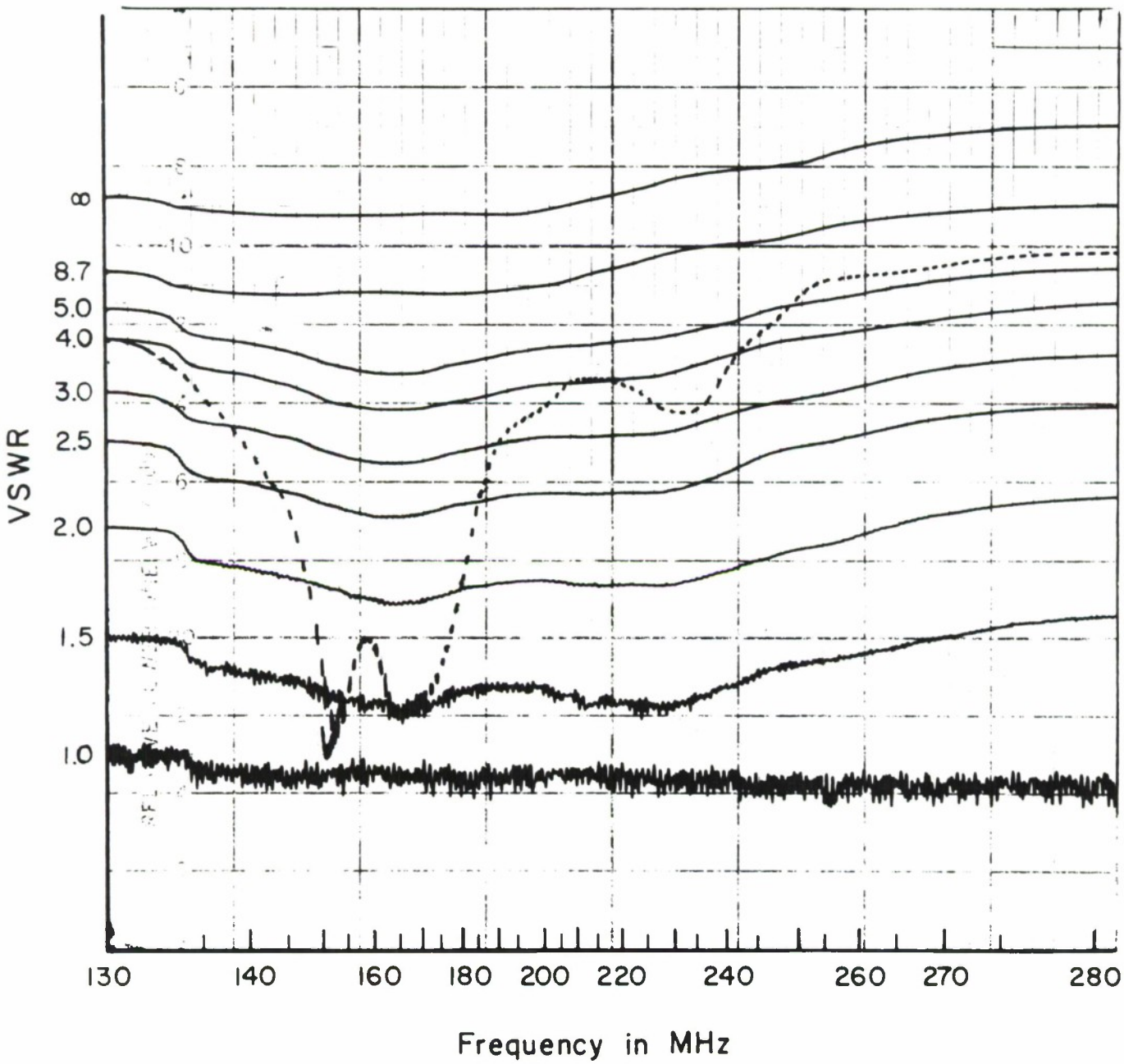

Figure 31 Measured VSWR of the unbalanced conical spiral antenna, referred to 50 ohms. Antenna mounted on the polystyrene mount and antenna tower.

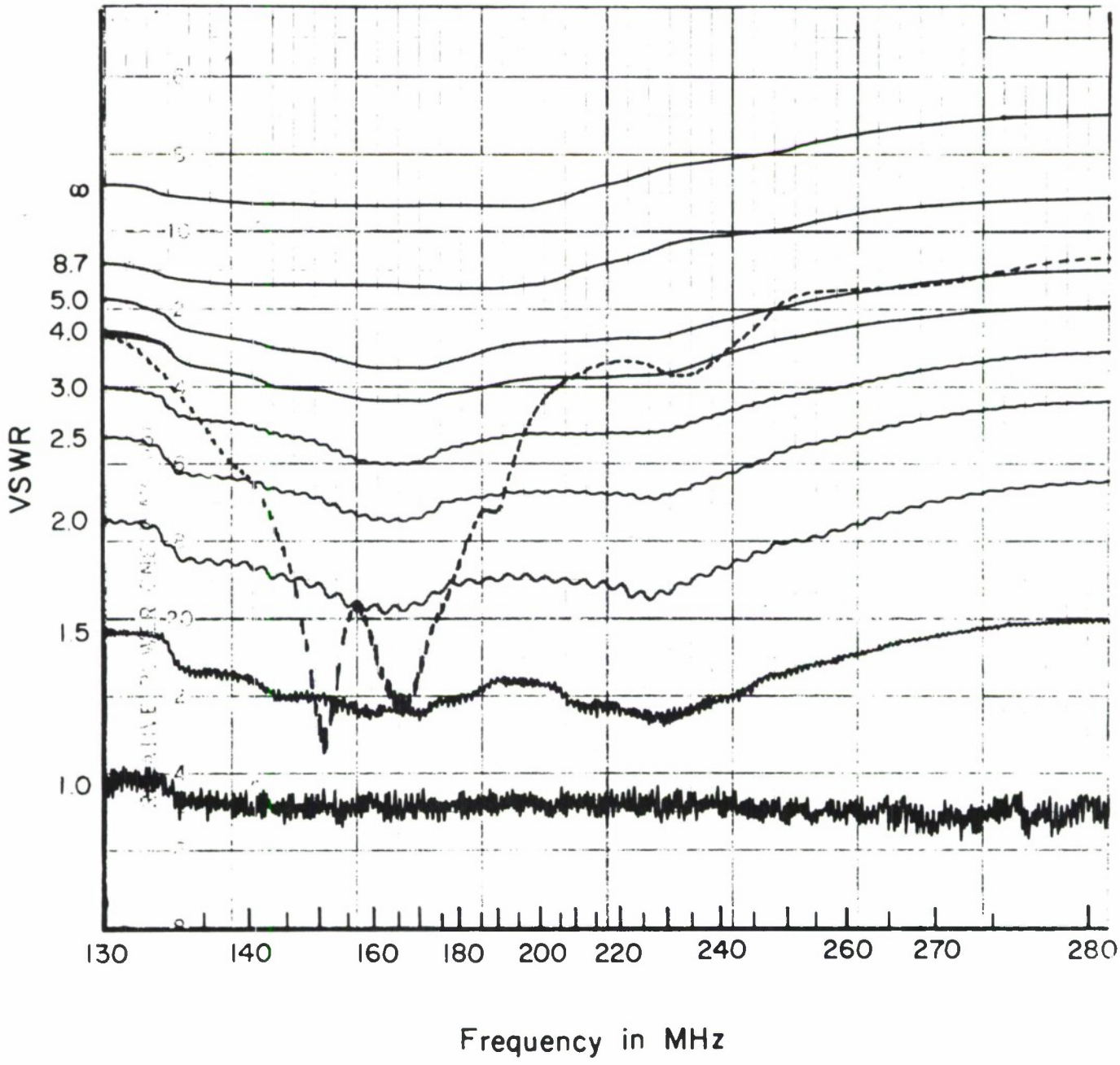

Figure 32 Measured VSWR of the unbalanced conical spiral antenna, referred to 50 ohms. Antenna mounted in the polyfoam cradle on the antenna test tower.

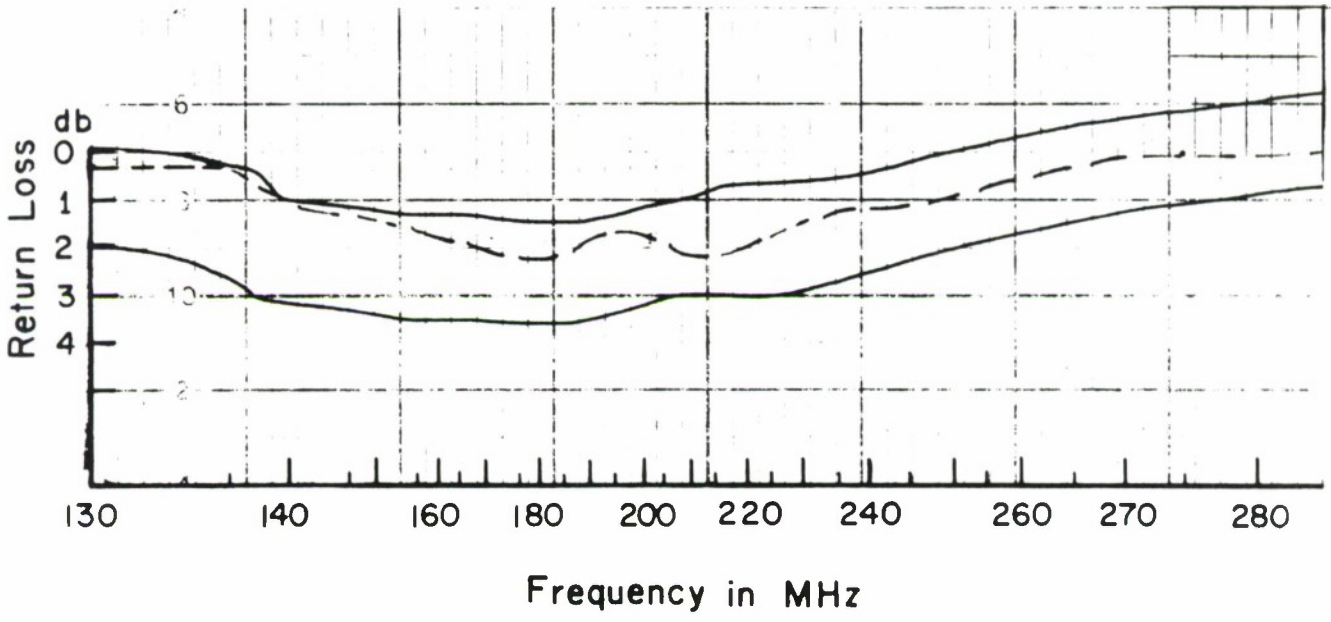

Figure 33 Measured return loss of the open-circuited feed cable used as the infinite-balun feed for the unbalanced conical antenna.

return loss varied from about 0.4 db at 130 MHz, to 1.1 db at 280 MHz. This corresponds to a one-way attenuation of 0.2 to 0.55 db. The small variations in the return loss curve are undoubtedly caused by discontinuities at the connector and along the cable.

Using this data, the measured VSWR referred to the input terminal of the feed cable was modified to correspond to that which would have been observed at the apex terminals of the antenna. This modified curve is plotted in Figure 34.

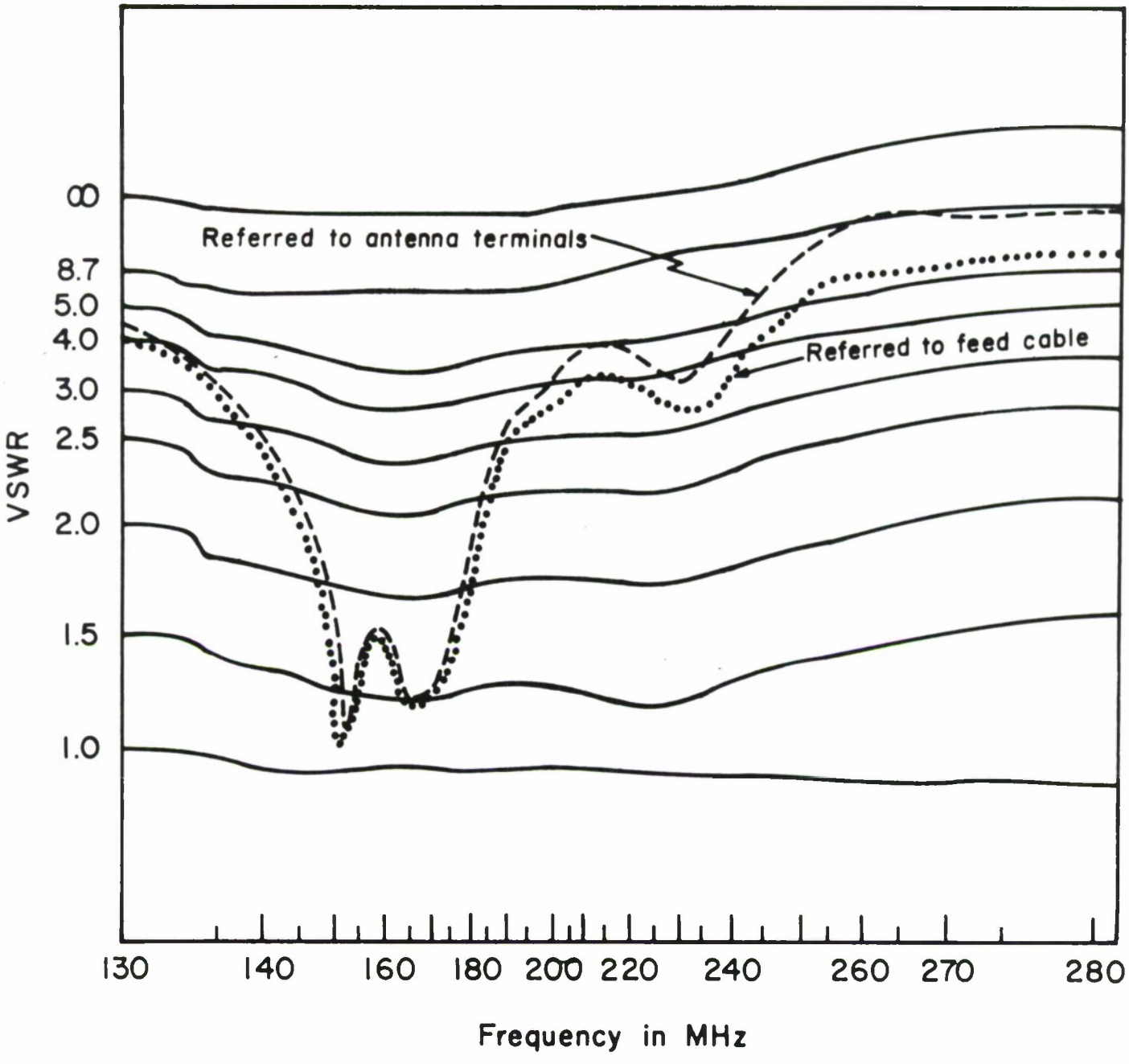

Figure 34. Measured VSWR referred to 50 ohms at the input of the antenna feed cable, and this VSWR translated to the input terminals of the antenna at the apex of the cone.

VII. Correlation of the Measured Gain with the Measured VSWR of the CUSP Antenna

The measured maximum broadband power gain is plotted in Figure 35 on the same frequency scale as the measured VSWR. There is a definite inverse correlation indicated.

To see how good this correlation really was, a transmission loss corresponding to the measured VSWR was calculated. This involves converting the VSWR to a reflection coefficient and calculating the reflected power.

This transmission loss, which represents power rejected by the antenna and therefore not available to be radiated, is plotted in Figure 36.

This transmission loss curve was then normalized to the maximum broadband power gain measured at 150 MHz and plotted with this gain curve in Figure 37. It should be recalled that the transmission loss curve takes into account only reflected power, while the gain curve takes into account reflected power and changes in pattern shape. In this light, the agreement between the curves is quite acceptable. This agreement says nothing, of course, about the absolute level of the gain curve, only something about its change with frequency.

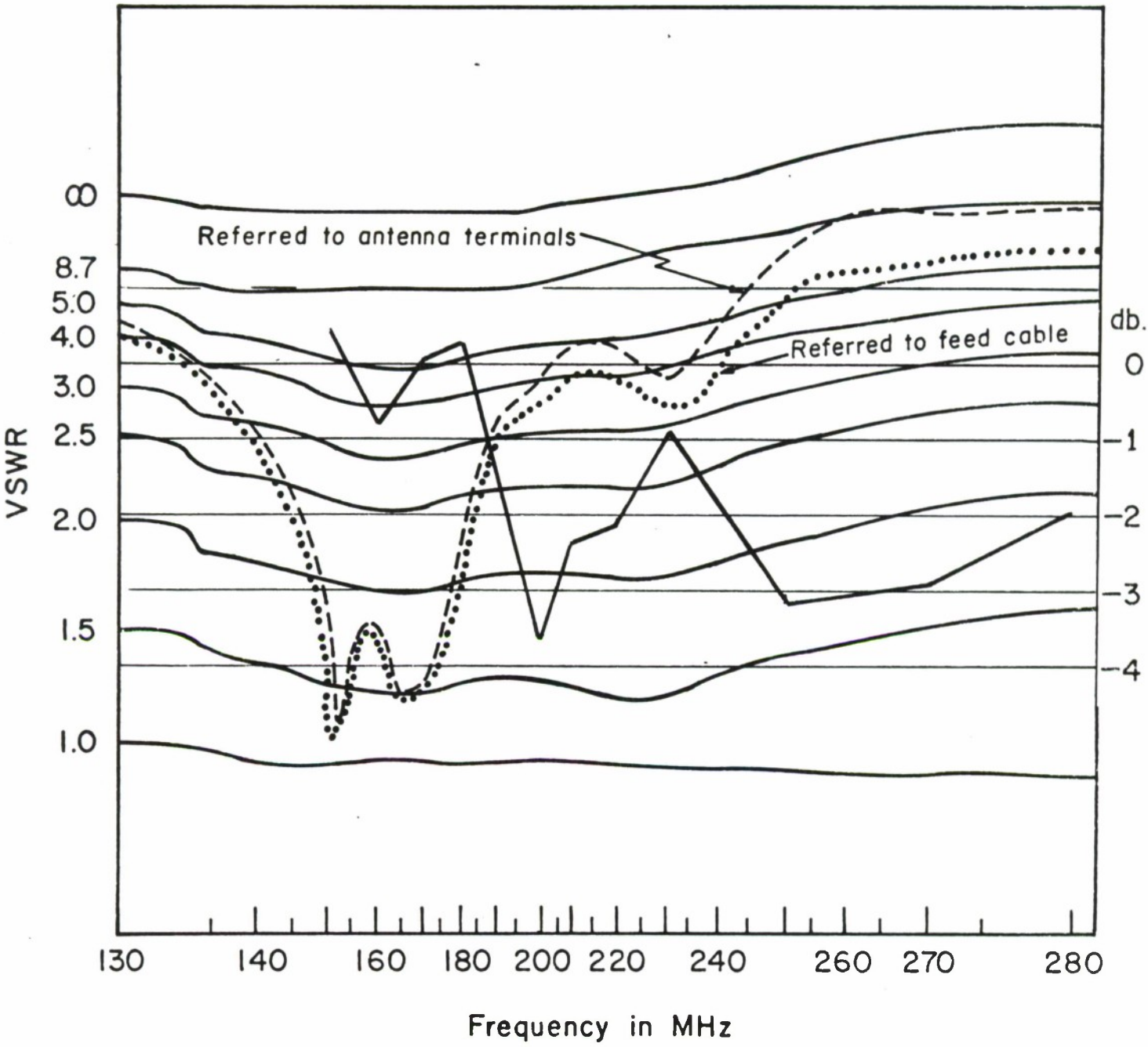

Figure 35. The relationship between the measured broadband power gain (solid curve) and the measured VSWR (dashed curves). Use the scale on the left and the variable grid lines for VSWR. Use the scale on the right and parallel grid lines for the measured gain. The two VSWR curves are as defined in Figure 31.

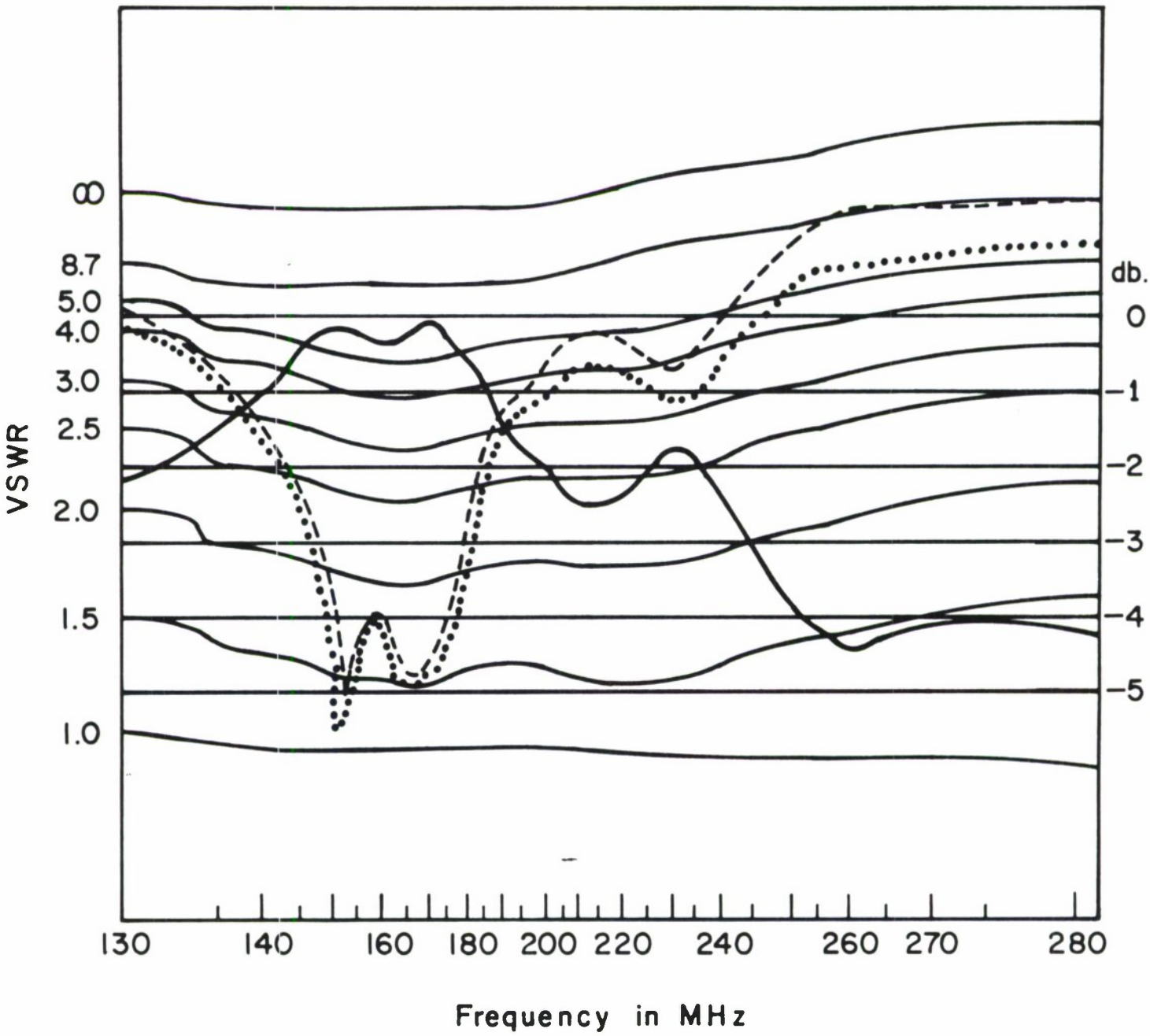

Figure 36. The transmission loss in db (solid curve) resulting from the power reflected by an antenna with the indicated VSWR (dashed curves). Use scale on the left and calibrated grid lines for VSWR. Use scale on right and parallel grid lines for transmission loss. The two VSWR curves are as defined in Figure 31.

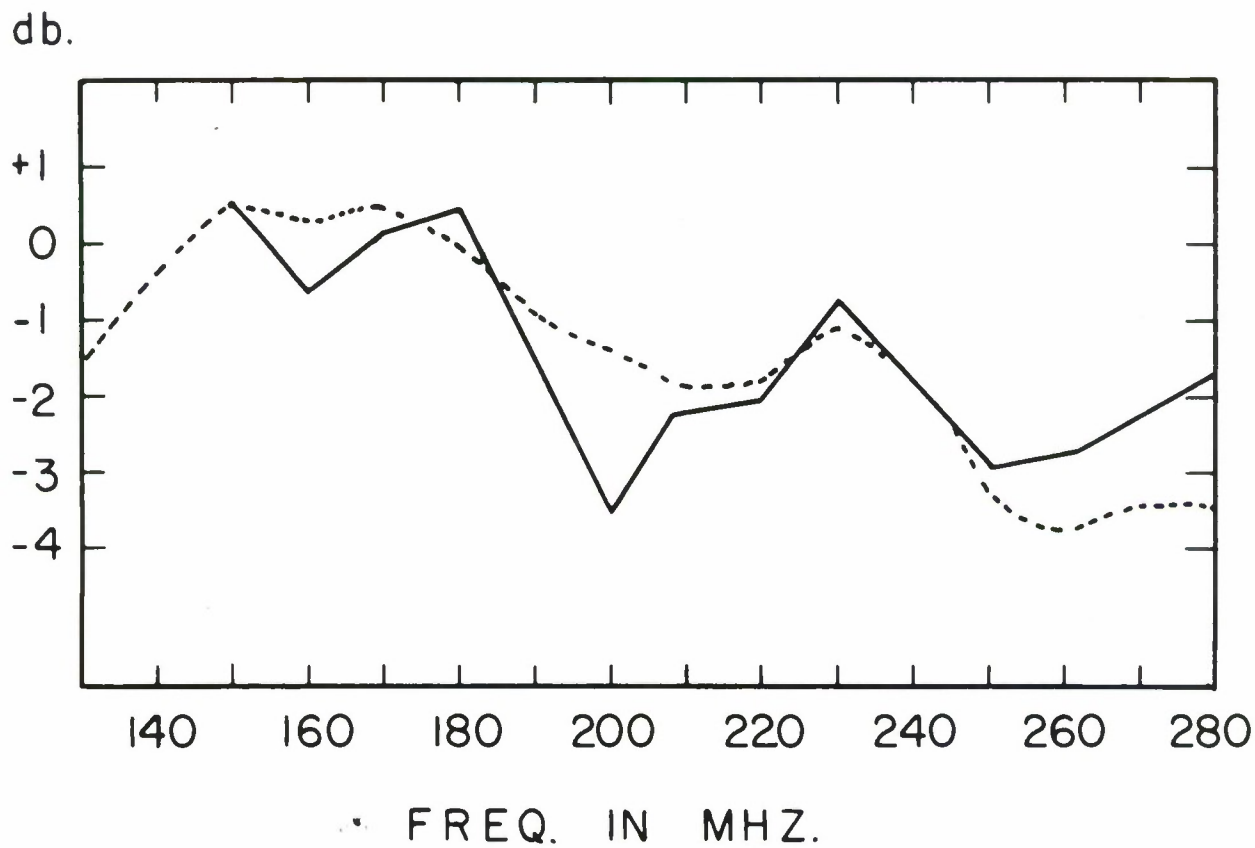

Figure 37. The measured maximum broadband power gain (solid curve) compared to the transmission loss curve (dashed curve) after the transmission loss curve has been normalized to the value of the gain curve at 150 MHz.

VIII. MEASUREMENTS ON A CUSP ANTENNA WITH DIFFERENT PARAMETERS

With the above information on the performance of the original Philco-Ford (P-F) CUSP antenna available, it was considered desirable to construct another CUSP antenna using a different set of parameters. Accordingly, a two arm balanced antenna with approximately the same base diameter, that was on hand*, was truncated to the same overall length as the P-F CUSP antenna. This conical antenna, with parameters shown in Figure No. 38b, will be identified as the 10° CUSP antenna. The metal inner cone from the P-F antenna was inserted inside and shorted to one arm as shown in Figure 39, and the antenna was excited by feed cable along the arms. Figure 40 is a photograph showing the Philco CUSP on the left, the 10° CUSP antenna in the center, and a 12° balanced antenna on the right. This latter antenna will be discussed in a later section.

It will be noted that for a fixed base size and height, the smaller cone angle of the new CUSP antenna (10° vs. 13.4°) results in a larger truncated tip. The 10° CUSP is also more loosely wrapped (α = 45° vs. α = 56°) and has narrower arms (δ 90° vs. δ = 147°). The relative gain of the two CUSP antennas is shown in Figure 41. We note that the 10° CUSP has a higher gain than the P-F CUSP from 220 to 280 MHz, then less gain in the transition region, and a gain comparable to that of the P-F CUSP in the 150 to 170 MHz region.

Swept "gain" measurements for the 10° CUSP are shown in Figures 42 and 43, at θ = 0° (end-on) and θ = 270° (broadside). The transition from predominantly end-fire to broadside radiation is again evident, although as shown in the radiation patterns (in appendix D hereto), the pattern remains essentially broadside up to higher frequencies than those for the P-F CUSP.

* This was the "40 inch" antenna used for comparison in reference 1.

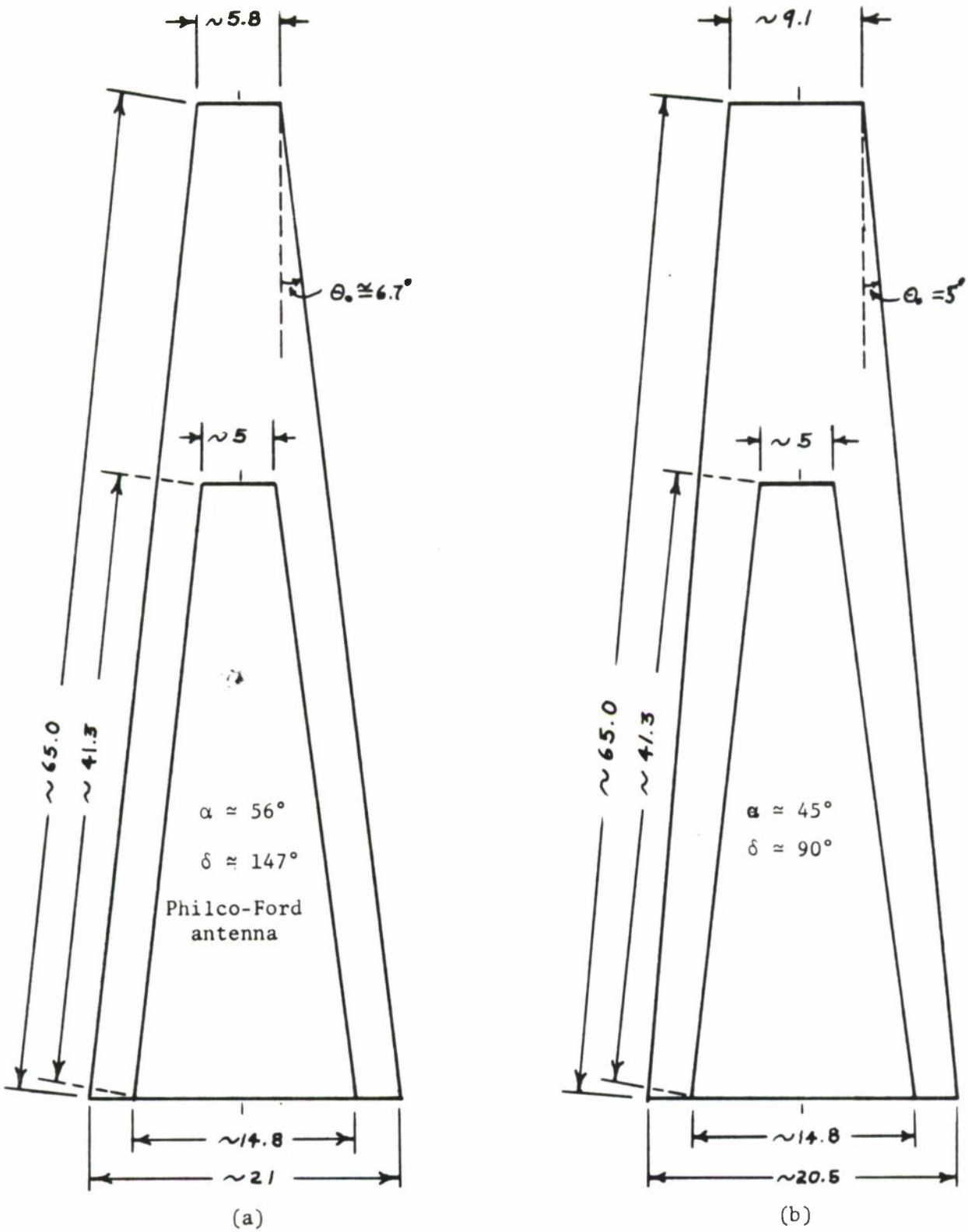

Figure 38 Measured parameters of the 2 unbalanced antennas. Measured values are all approximate with dimensions in cm. The cross section drawings are approximately to scale.

Figure 39. Photograph of the base end of the 10° CUSP antenna showing construction, and the placement of the inner metal cone.

Figure 40. Photograph of the Philco-Ford CUSP on the left, the 10° CUSP in the center, and a balanced antenna, with parameters approximately those of the P-F antenna, on the right.

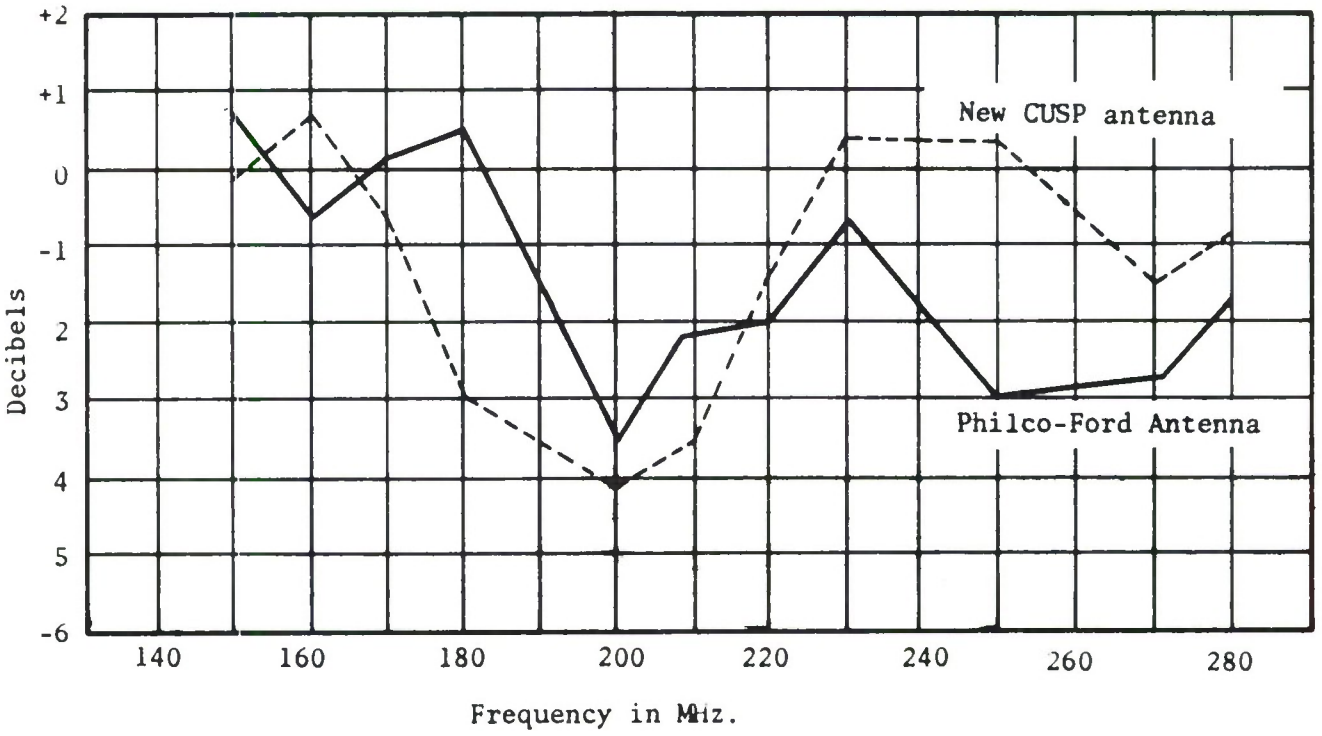

Figure 41. The measured maximum "Broadband Power Gain" of the Philco-Ford CUSP antenna and another CUSP antenna constructed with parameters shown in Figure 38b.

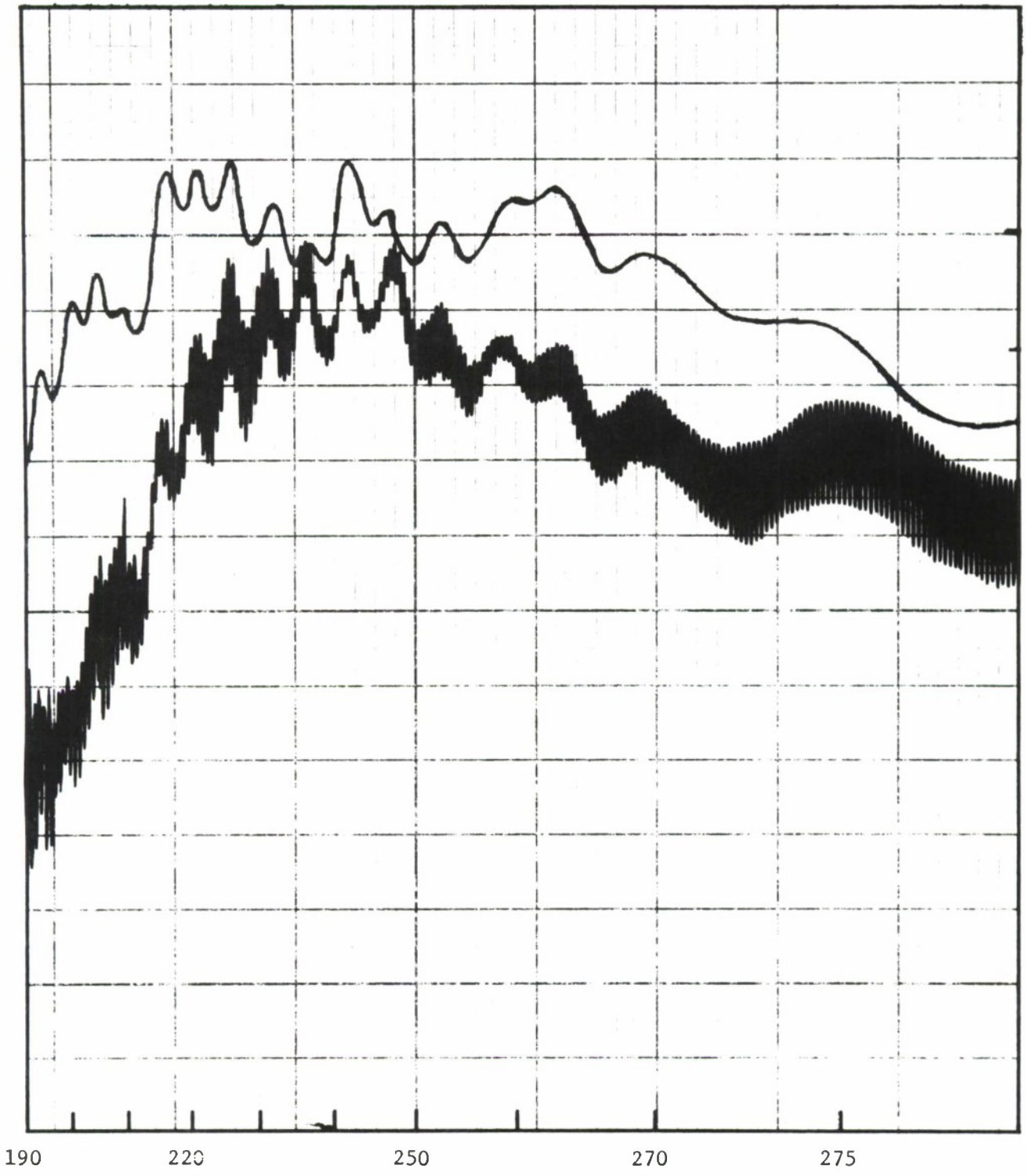

Figure 42 . Relative radiated power of 10° CUSP antenna at $\theta = 0°$ recorded with a rotating linearly polarized receiving antenna. For reference an approximate level that would have been radiated by a matched isotropic antenna is shown.

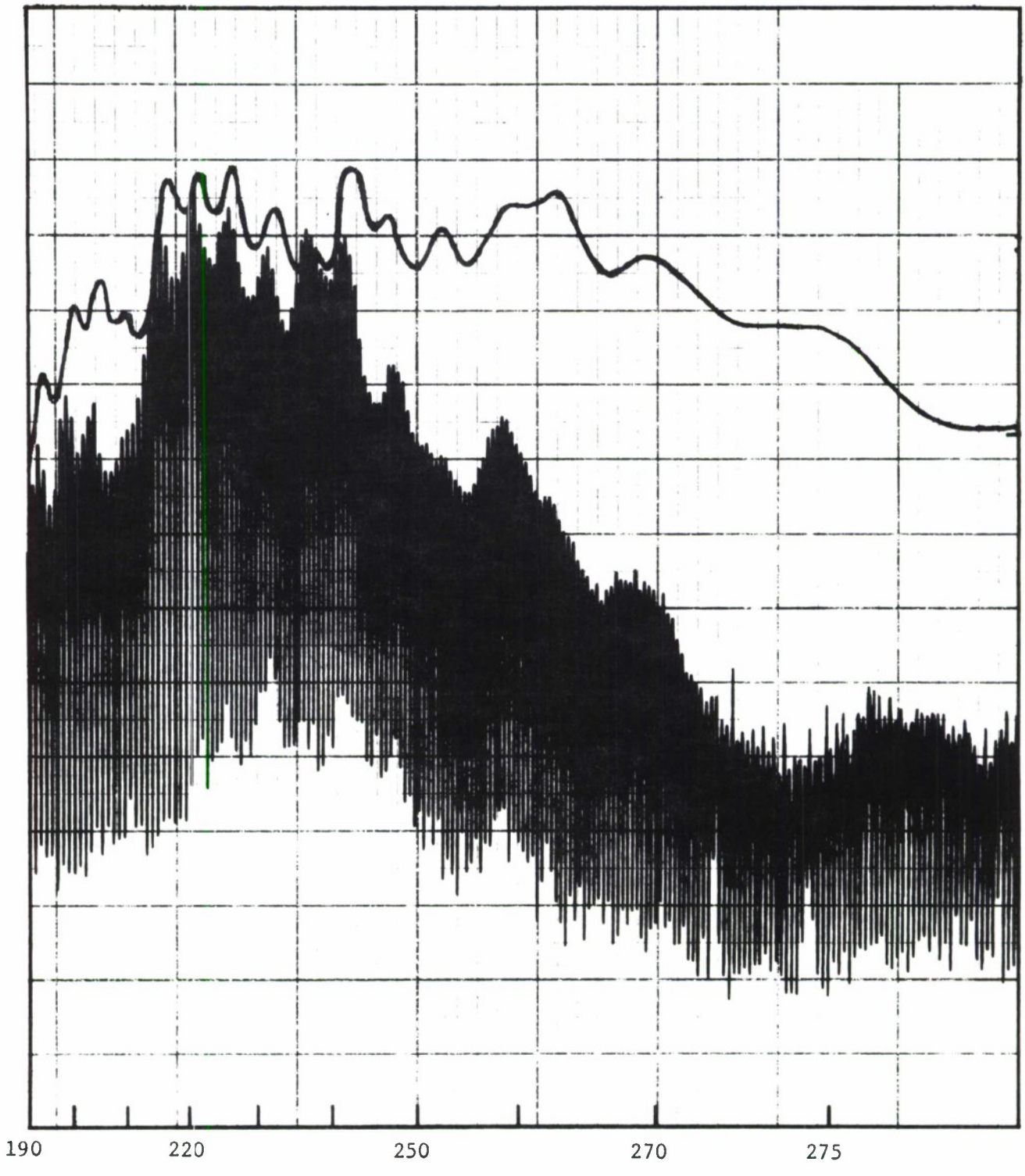

Figure 43 . Relative radiated power of 10° CUSP antenna at $\theta = 270°$ recorded with a rotating linearly polarized receiving antenna. For reference an approximate level that would have been radiated by a matched isotropic antenna is shown.

The higher gain at the upper frequencies, apparently is due to a lower input reflection coefficient. The measured input VSWR of the 10° CUSP is shown in Figure 44. This should be compared with that for the P-F CUSP in Figure 34. The relationship between the VSWR and gain of each antenna, and the inverse relationship between the VSWR and gains of the two antennas, makes a quite convincing point that the gain is primarily controlled by the amount of reflected energy. Dissipative losses have a secondary effect. The physical structures of the antenna would suggest as much.

There is an interesting similarity between the two VSWR curves, with the apparent "resonance" of the 10° CUSP, which occurs around 238 MHz, appearing in only residual form in the P-F CUSP.

There is some evidence of a greater dissipative loss in the P-F CUSP. It was constructed on a dielectric form approximately 3/16 inch in thickness, while the 10° CUSP was constructed from 0.10 inch thick dielectric*, clad with 1 oz. copper, (see Figures 2 and 39). At 160 MHz the VSWR of the two antennas is quite comparable, with that for the P-F CUSP being slightly lower than that for the 10° CUSP. However, at this frequency, the gain of the 10° CUSP measured approximately 1 db higher.

* Budd "Di-clad" 108-T.

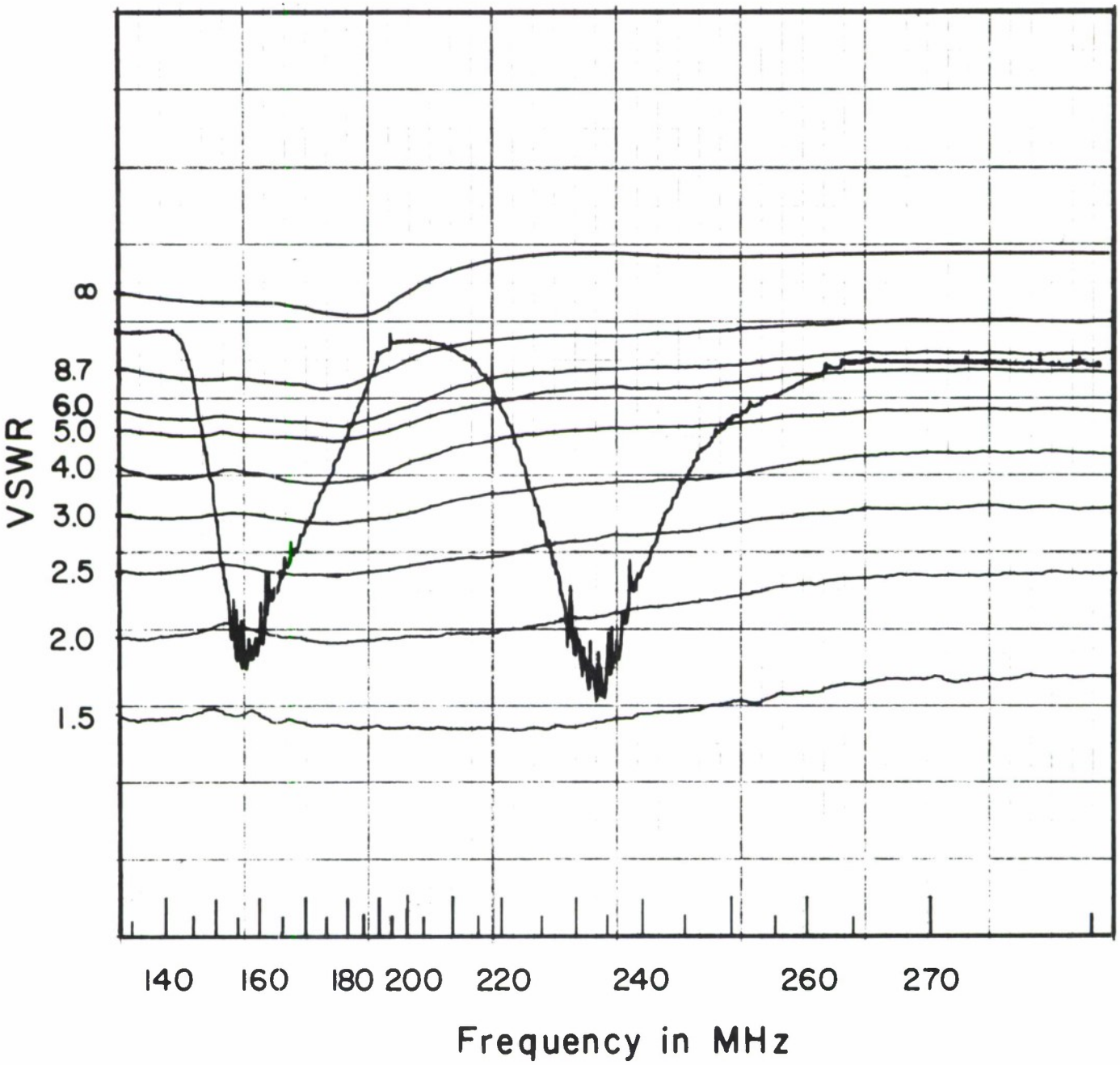

Figure 44 Measured VSWR, referred to 50 ohm line, of 10° CUSP Antenna constructed at University of Illinois.

IX. MEASUREMENTS ON RELATED BALANCED ANTENNAS

To compare the P-F CUSP antenna to a balanced antenna with the same parameters, the P-F CUSP was modified. The shorting strap between the inner cone and the arm was removed. The infinite balun feed was disconnected at the tip, and the antenna was excited with a coaxial 180° hybrid placed inside the metal cone. A balanced shielded line (two coaxial cables) carried energy from this hybrid along the cone axis from the tip of the inner metal cone to the tip of the antenna.*

The measured gain of this P-F balanced antenna, on-axis, is shown in Figure 45. It is compared with the on-axis gain of the P-F CUSP. These curves are quite comparable. The gain of this balanced antenna and the gain of the 10° CUSP, when converted to a balanced antenna in a manner similar to that described above, is shown in Figure 46. In this figure, the gain of a different balanced antenna, that shown on the right in Figure 40, is also shown. This latter antenna had a base diameter of 18.5 cm, a 12° cone angle, rate of wrap (α) of 57° and arm width (δ) of 150°. These parameters are comparable to those of the P-F CUSP (and balanced structure) and the measured gains are comparable.

The 10° antenna is definitely a higher gain antenna over the range of frequencies investigated. This shows up as increased gain when it is converted to a CUSP antenna, as long as the end-fire radiation predominates.

It is significant to compare the slope of all five curves (including both balanced and unbalanced antennas) in Figure 46 for frequencies from 200 to 230 MHz. At 200 MHz, when these antennas have a base diameter of

---

* This antenna has since been restored to its original condition.

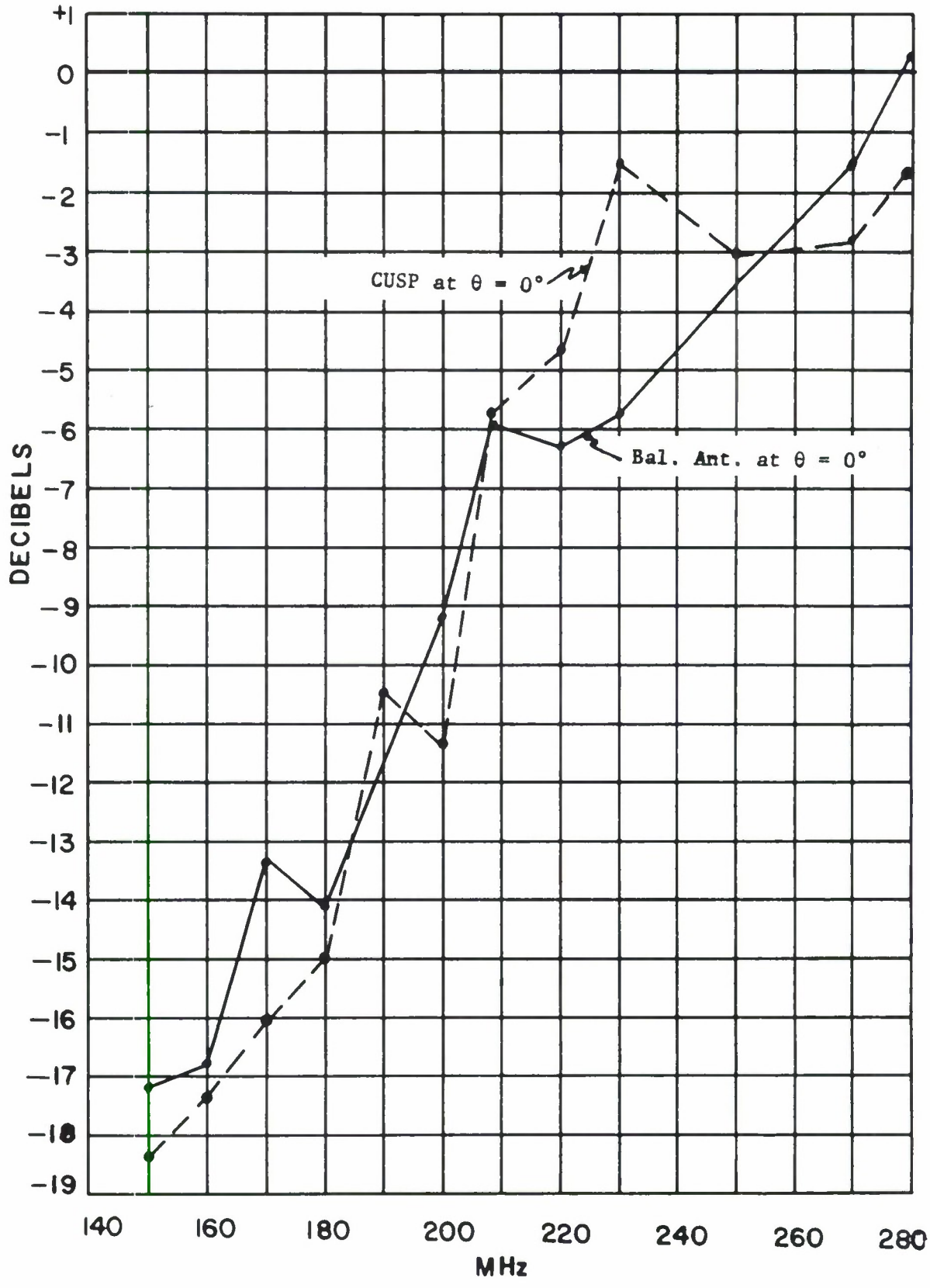

Figure 45. The measured "broadband power gain" of the P-F CUSP (on axis) and this antenna operated as a balanced structure.

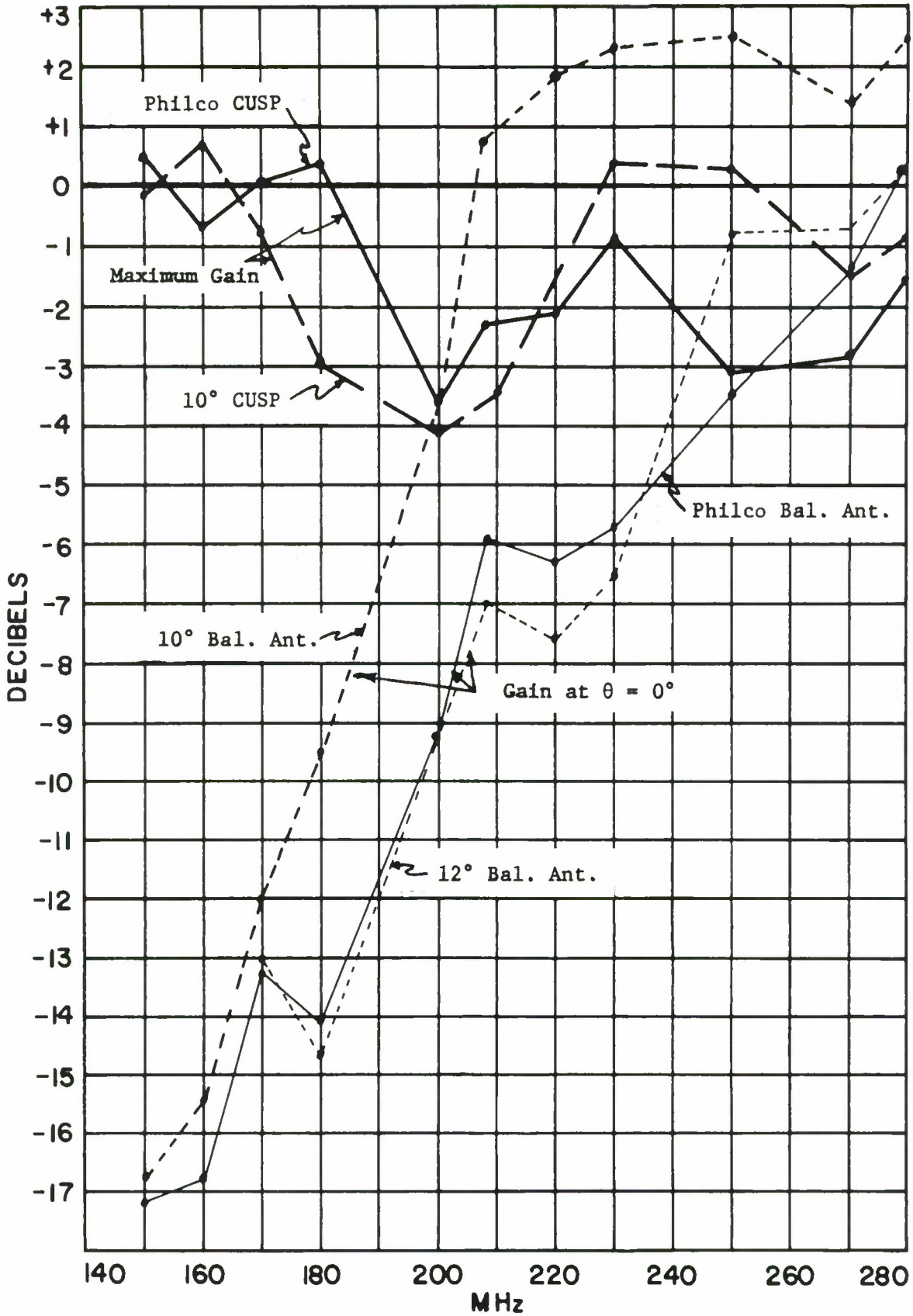

Figure 46. Measured "broadband power gain" of the P-F CUSP and 10° CUSP and the same antennas when converted to balanced excitation. The gain of another balanced antenna, with parameters comparable to those of the Philco antenna, is also shown.

approximately 0.14 wavelengths and a height of approximately 0.43 wavelengths, a transition takes place and a markedly different mode of radiation predominates. As this "broadside" mode develops, it brings the gain back up toward the isotropic level. This mode of operation will be discussed later.

Swept measurements for the three balanced antennas are shown in Figures 47, 48 and 49. The increased gain of the 10° antenna is clearly evident.

Two additional swept gain measurements are presented in Figures 50 and 51. These are not strictly comparable to those previously shown, but are of interest. Figure 50 shows the gain for the same 10° balanced antenna of Figure 46 and 47 except the metal cone (with the electronic package) was not inserted inside the antenna. Note that the presence of the metal cone reduced the gain at the higher and lower frequencies, and increased the axial ratio at the higher frequencies.

In Figure 51 the gain of this same antenna (without a metal core) is shown when the antenna tip was extended so that the total length of the cone was approximately 40 inches. This is the antenna used in reference 1 for comparison with the P-F CUSP. It was pointed out at that time that this was not a fair comparison, and hence this comparison has not been used in this report. The higher gain of this longer antenna at the higher frequencies is clearly evident.

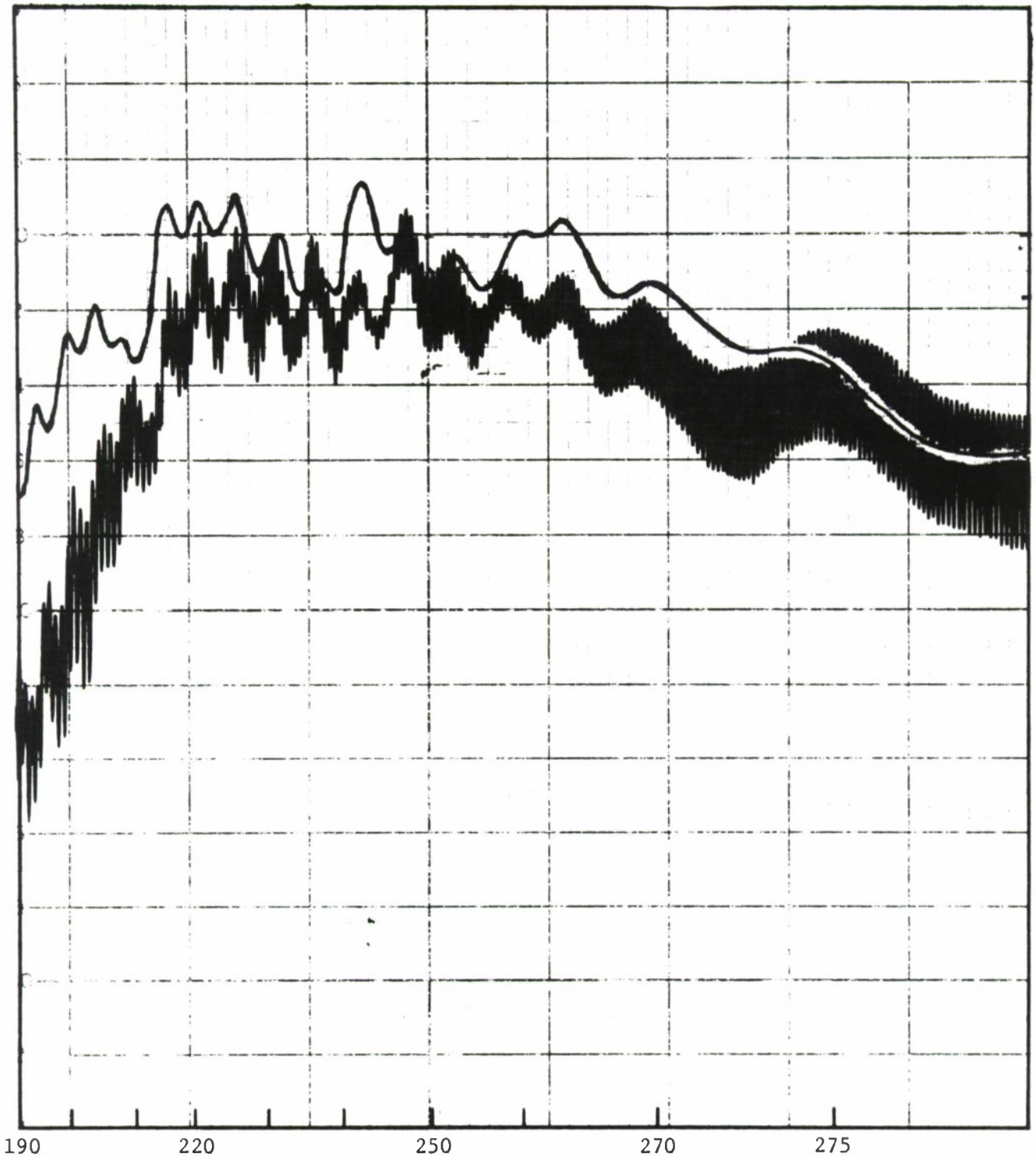

Figure 47. Relative radiated power of Truncated 10° Balanced Spiral antenna with metal core, at $\theta = 0°$ recorded with a rotating linearly polarized receiving antenna. For reference an approximate level that would have been radiated by a matched isotropic antenna is shown.

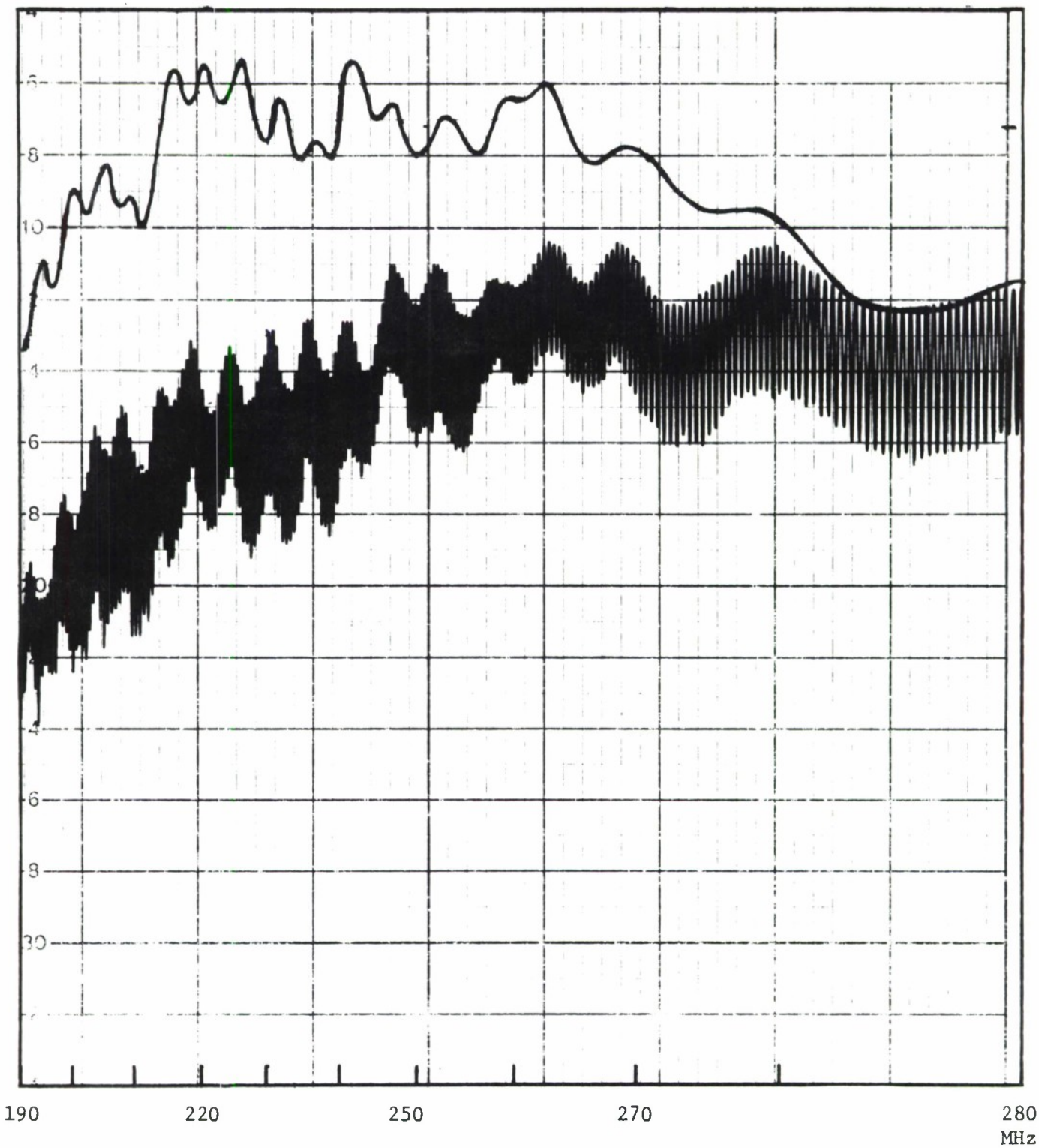

Figure 48 . Relative radiated power of Philco Balanced Spiral antenna at $\theta = 0°$ recorded with a rotating linearly polarized receiving antenna. For reference an approximate level that would have been radiated by a matched isotropic antenna is shown.

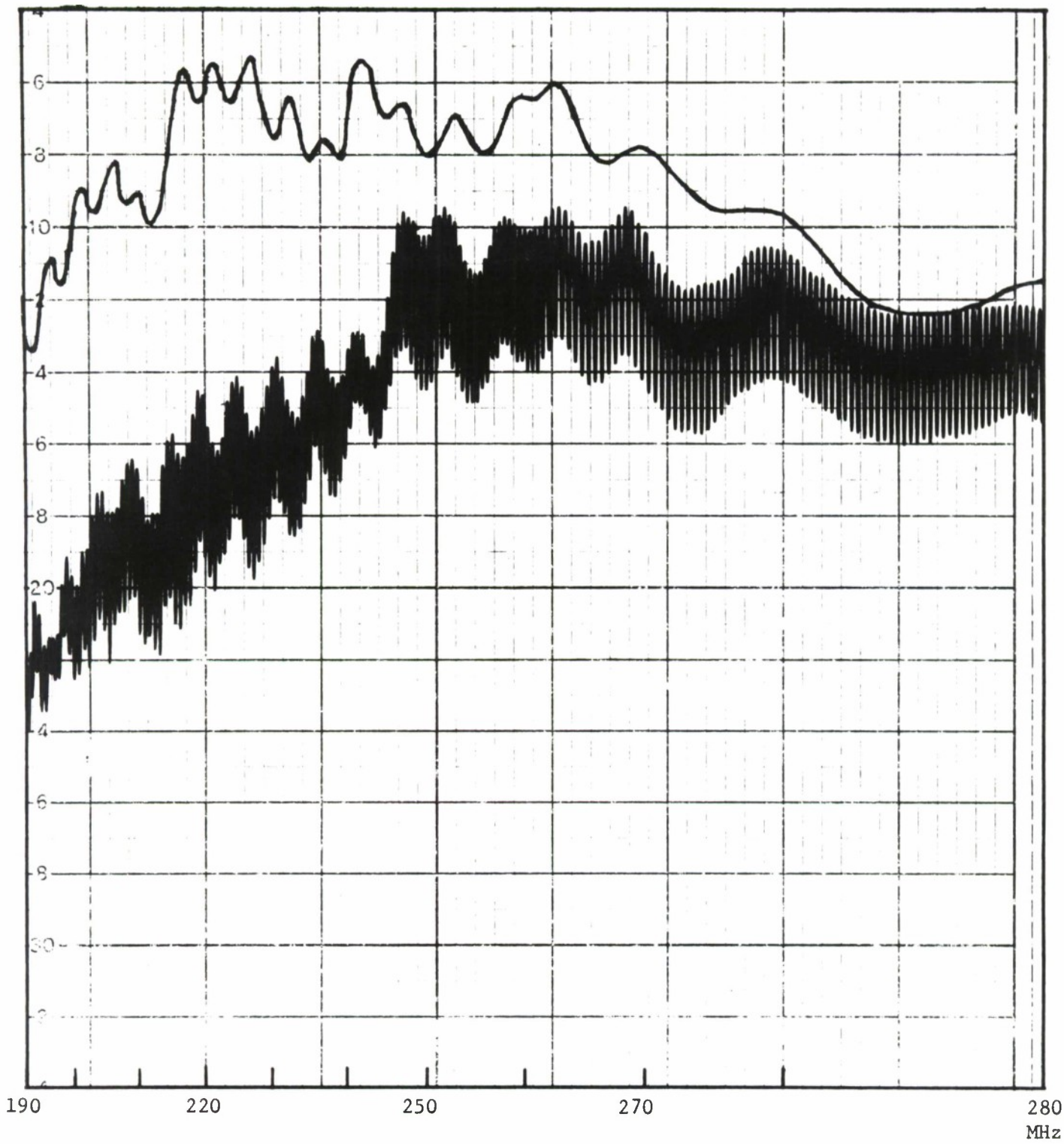

Figure 49 . Relative radiated power of 12° Balanced Spiral antenna at $\theta = 0°$ recorded with a rotating linearly polarized receiving antenna. For reference an approximate level that would have been radiated by a matched isotropic antenna is shown.

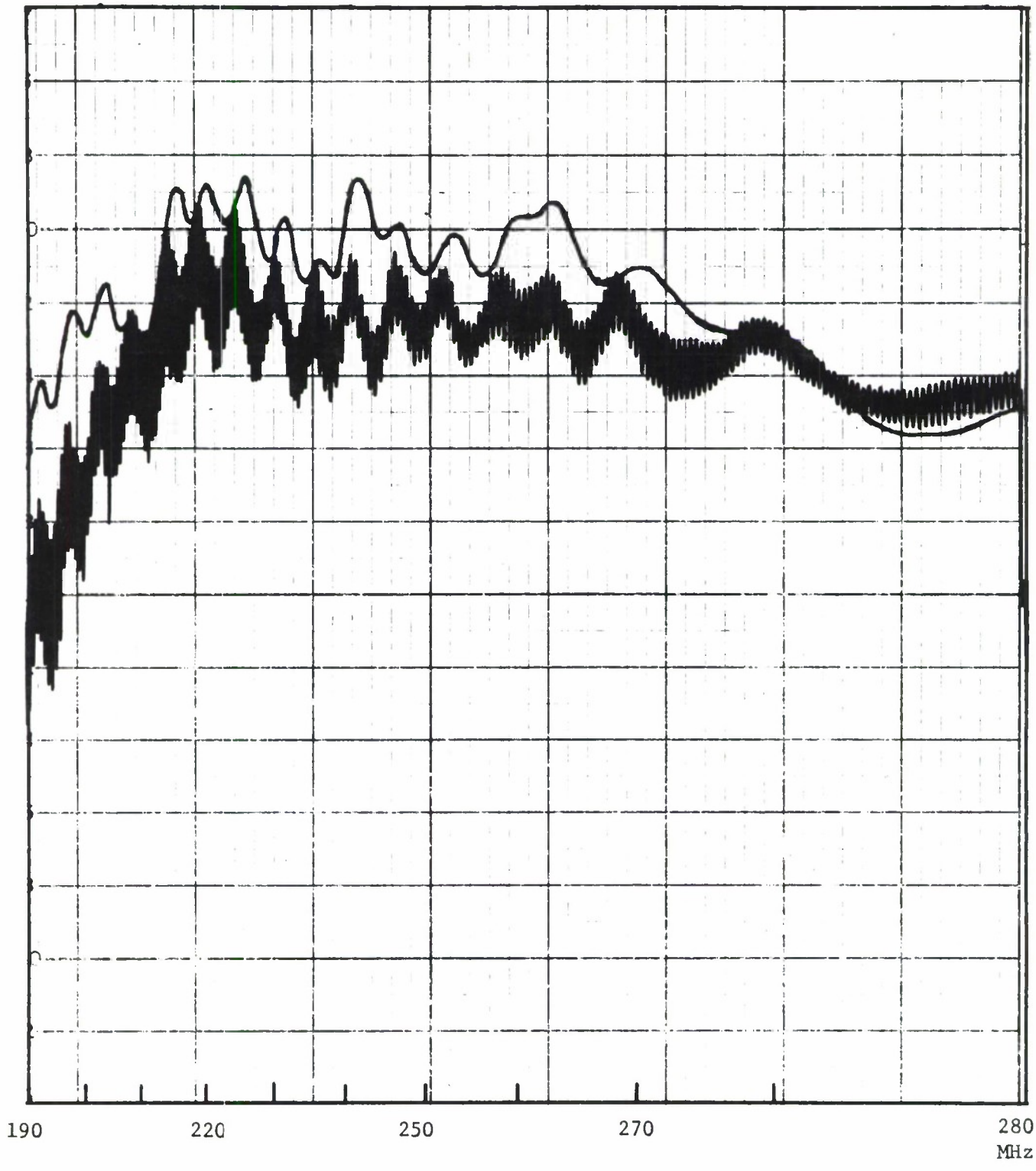

Figure 50. Relative radiated power of Truncated 10° Balanced Spiral antenna at $\theta = 0°$ recorded with a rotating linearly polarized receiving antenna. For reference an approximate level that would have been radiated by a matched isotropic antenna is shown.

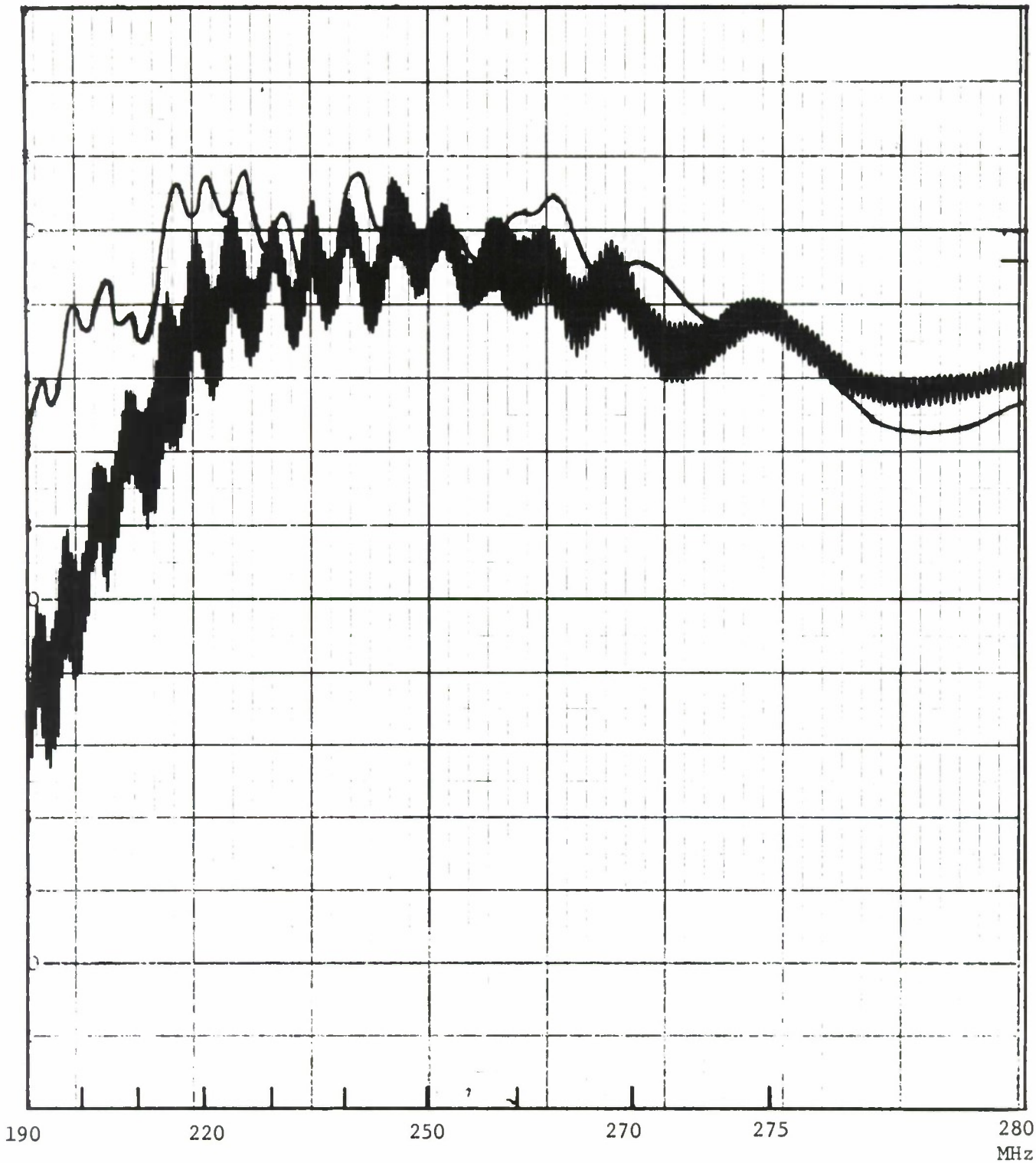

Figure 51 . Relative radiated power of 40 inch 10° Balanced Spiral antenna at $\theta = 0°$ recorded with a rotating linearly polarized receiving antenna. For reference an approximate level that would have been radiated by a matched isotropic antenna is shown.

X. AN INTERPRETATION OF THE PERFORMANCE OF THE SMALL UNBALANCED SPIRAL ANTENNA

A study of the documented characteristics of the small balanced and unbalanced conical spiral antennas, leads to an interpretation of the performance of these antennas in terms of incident and reflected current waves on the structure.

When the conical spiral antenna is excited at frequencies such that the diameter of the antenna at any region on the structure is small in wavelengths, this region behaves as a transmission line. The length of each turn of the arms is small in wavelengths, and hence the relative phase of the current on adjacent arms (because of the balanced excitation of the two arms) is approximately 180°. In normal operation of the balanced antenna this transmission line region is terminated in a region on the antenna such that the diameter, and the circumference, is large enough in wavelengths to establish a proper turn-to-turn phase progression that supports backward wave radiation. This region is identified as the active, i.e., the radiating region on the antenna. If there is no part of the antenna large enough in wavelengths to establish this backward-wave phase relationship, the antenna current on the two arms produces little radiation, and progressing to the base of the cone, is reflected back toward the apex region. This reflected current is carried back to the feed region, because the structure is again an inefficient radiator, and appears at the feed terminals, establishing a high input reflection coefficient, large VSWR on the feedline, and a low radiated power gain.

The unbalanced (CUSP) antenna, under study, is constructed from a balanced two arm conical spiral antenna by inserting a conducting inner conical core in this antenna, and then bonding the end of one of the two

spiral arms to this core at the base of the cone. The current progressing away from the apex feed region, on the two arms of the CUSP antenna, behaves in exactly the same manner as it does on the balanced structure until it reaches the base of the cone. This is pictorially indicated in Figure 52(A).

At the base of the cone, the antenna current on arm No. 1 is reflected back along the arm. The antenna current on arm No. 2 is fed over to the inner conducting core. Because of the symmetry of the structure, the incident currents which reach the base of the cone along the two arms are still equal in amplitude and 180° out of phase. The operation of the structure can now, to the first order, be interpreted in terms of these currents only. In these terms, the structure is a base fed monofilar antenna with the radiating arm (arm No. 1 in our example) fed against the center core. This is equivalent to the antenna of Figure 52(B).

It has been shown[9] that the spiral antenna arms can support transmission line type currents, flowing from the base toward the apex, that provide efficient radiation. These observations were made on multimode structures large enough in wavelengths to support the radiating modes in question.

On this base fed antenna, the turn length is small in wavelengths, and successive turns of the same arm are approximately in phase. This in-phase excitation of the turns of the radiating arm, causes the structure to radiate a maximum of energy broadside to the axis of these turns. Note that under this theory the other arm (arm No. 2) plays no part in this broadside radiation, and only acts as part of the transmission line extending from the apex to the base of the cone. If there is a smooth transition from this arm to the inner core, and if energy on this core is all radiated in the broadside mode, there will be little if any reflected

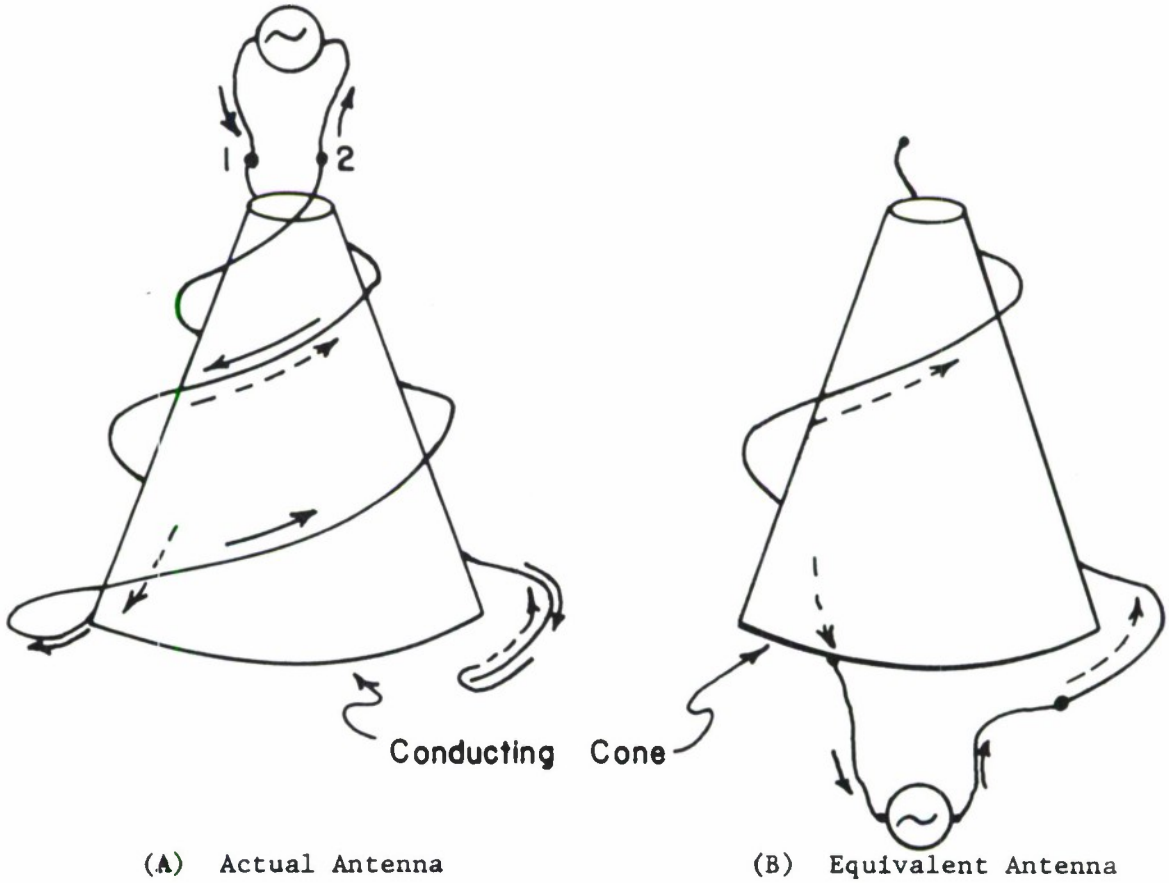

(A) Actual Antenna (B) Equivalent Antenna

Figure 52. Representation of the operation of the CUSP antenna. Solid arrows indicate transmission line currents, broken arrows indicate radiating currents.

current flowing on this arm back twoard the apex. Therefore its presence, in between the turns of the radiating arm, does not prevent broadside radiation.

If the structure is balanced, reflected currents flow on both arms. The currents on these interspersed arms are approximately 180° out of phase and broadside radiation is not possible.

Using the Philco-Ford CUSP antenna under study as an example, we note that at 150 MHz the base diameter of the antenna (21 cm) is approximately 0.105λ. The base circumference is approximately 0.33λ, the longest turn of each arm (on the center line of the arm) is approximately 0.31λ, and the largest pitch (or spacing between these turns) approximately 0.16λ.

It is known that many of the characteristics of localized regions on the conical spiral antenna can be interpreted in terms of the helix[3,10]. For this analogy to be most applicable we should consider the tape helix, however the literature that is available on the tape helix as a radiating antenna is not extensive. It is on the thin wire arm helix, and we can profit by considering such structures.

Using the dimensions referred to above, and considering the structure to be a base fed monofilar antenna, we can plot these parameters on a "spacing-circumference chart for helices" extracted from Kraus[11] as shown in Figure 53. Thus under the above assumptions, this antenna is well within the "normal mode" region at 150 MHz.

In using this chart, we should note that as the frequency is increased, our operating point moves along a line of constant spiral (or pitch) angle. However, Patton[10] has shown that we should not expect the region of operation for the axial mode of the balanced two arm conical spiral to coincide with that shown for the "beam" or axial mode of the one arm helix.

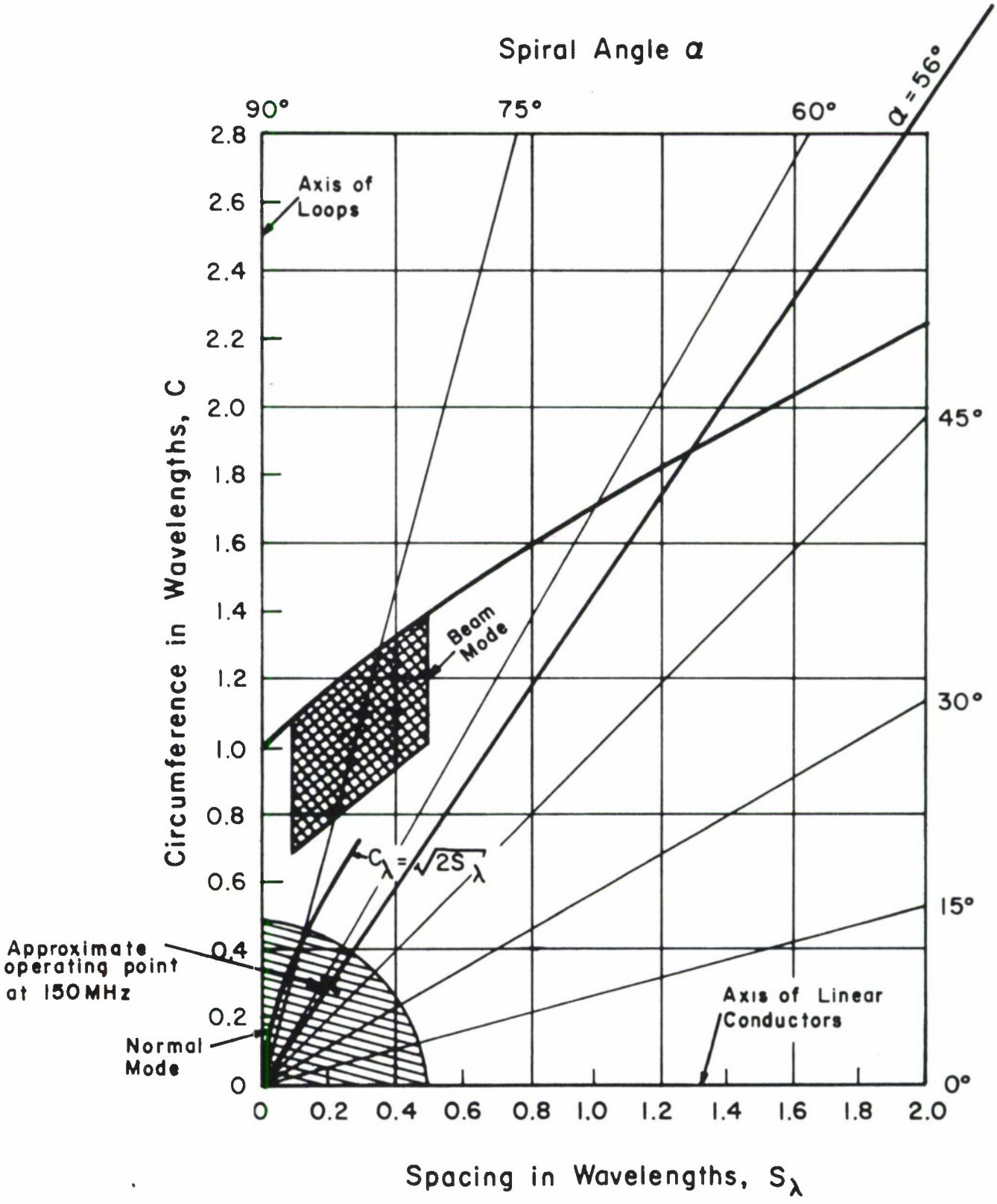

Figure 53. Approximate operating point for P-F CUSP antenna at 150 MHz when it is considered to be a base-fed monofilar helix and its average parameters are plotted on a "spacing-circumference chart for helices" (extracted from reference 11).

On this chart we note that the line $C_\lambda = \sqrt{2S_\lambda}$ indicates circular polarization. Our operating point is below that line, indicating elliptical polarization with a major component along the axis of the cone. We observed high ellipticity, and the field is so oriented.

The theory outlined above would appear to be a logical explanation for the transition in the characteristics of the CUSP antenna, as the antenna is operated at longer and longer wavelengths. However, to investigate this theory further, the 10° CUSP antenna which had been constructed at the University of Illinois (shown in Figures 39 and 40) was modified to be the single-arm antenna shown in Figure 52(B). That is to say, one complete arm, and the bond that was joining this arm to the inner core, was removed from the antenna. The remaining arm was excited against the inner conical metal core by bringing a 50 ohm coaxial cable through a small hole in the side of this core at the base of the cone, soldering the braid of this cable to the core, and connecting the center conductor of this cable to a short tapered metal tab connected to the base end of the arm. The resulting antenna was a single arm, conical, tape helix, fed against an inner metal core. No attempt was made to match the antenna to the 50 ohm cable.

The antenna, as modified, is shown in Figures 54 and 55. The single arm is clearly shown in Figure 54. The inactive coaxial cable, which had been placed upon this arm in the original CUSP configuration to make the geometry of the two arms identical, was left on the single arm of the helix. It plays no part in the excitation of the antenna. The method of exciting this single arm antenna is shown in Figure 55. The center conductor of the coaxial cable, which is visible inside the metal core, extends through the core and connects to the tapered tab leading to the broad end of the arm.

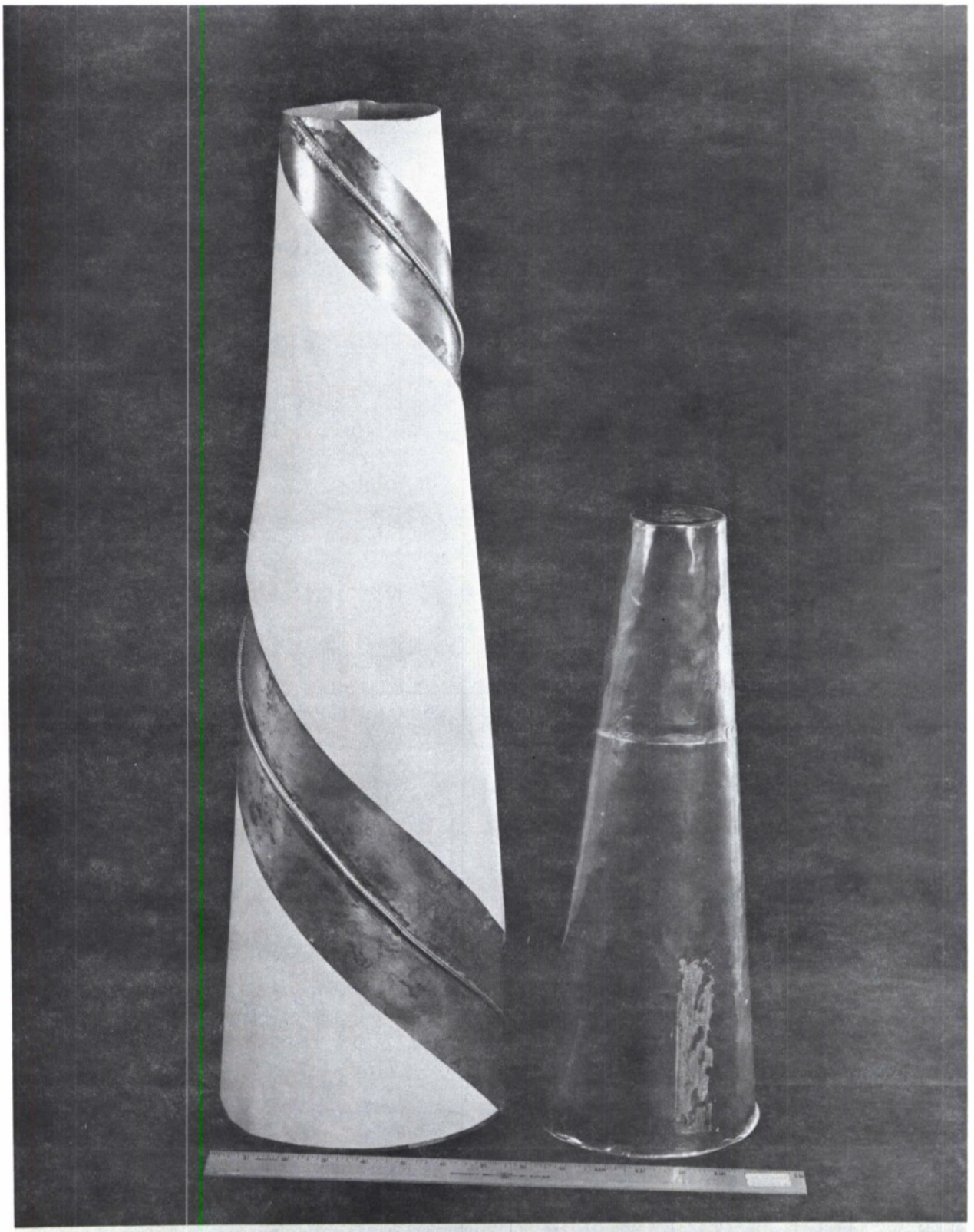

Figure 54. Photograph of the monofilar conical helix and metal core. Cone and core dimensions are given in Figure 38(b).

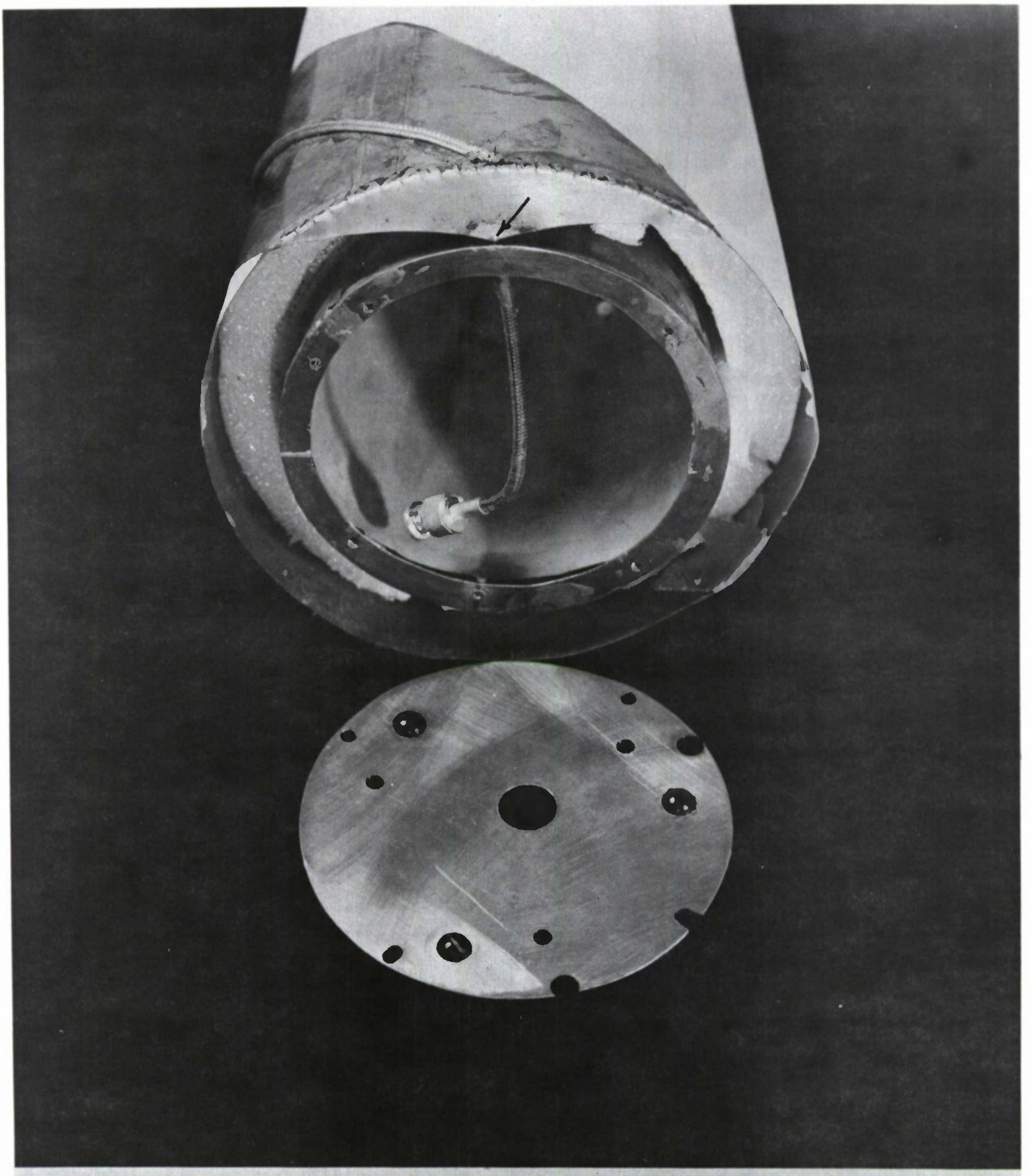

Figure 55. Base view of monofilar conical helix with core inserted. Arm is excited against the core (at point indicated by arrow) by the center conductor of the coaxial line which is visible inside the core.

The radiation pattern of this helical antenna at 150 MHz is shown in Figure 56. This is the same type of broadside radiation pattern recorded for this structure when it was a CUSP antenna. This pattern can be compared to the 150 MHz pattern for the Philco-Ford CUSP antenna in Figure 10. Additional radiation patterns for this helix, for frequencies up through 280 MHz, are shown in Appendix E hereto.

The measured maximum gain of this single arm helix is compared with that for this same structure when it was the 10° CUSP antenna, and that for the Philco-Ford CUSP antenna, in Figure 57. At the lower frequencies the gain of all three antennas is comparable. From 180 to 220 MHz the helix has the greater gain, undoubtedly due to the fact that on the CUSP antenna both the backfire axial and the broadside modes are radiating, reducing the gain in either mode. The conical tape helix with metal core is an efficient radiator with the maximum of radiation shifting slowly from broadside ($\theta = 90°$) to approximately $\theta = 122°$ at 270 MHz and then $\theta = 126°$ at 280 MHz.

The measured VSWR of this conical tape helix antenna is shown in Figure 58. This curve should be compared with Figures 44 and 32. The similarity is striking. The shift of the minima of the VSWR curve of the helix, to a higher frequency than it had been when the antenna was in the CUSP configuration is not surprising. The conical spiral arms, which carry energy from the apex to the base of the cone on the CUSP antenna, act as an impedance transformer of unknown characteristics. This transformation is not present on the base fed helix.

Normal-mode radiation from the narrow arm helix is considered to be a narrow band phenomenon. As the VSWR in Figure 58 and the radiation patterns in Appendix E indicate, the broad tapered arms, on the antenna under study, apparently increase this bandwidth substantially.

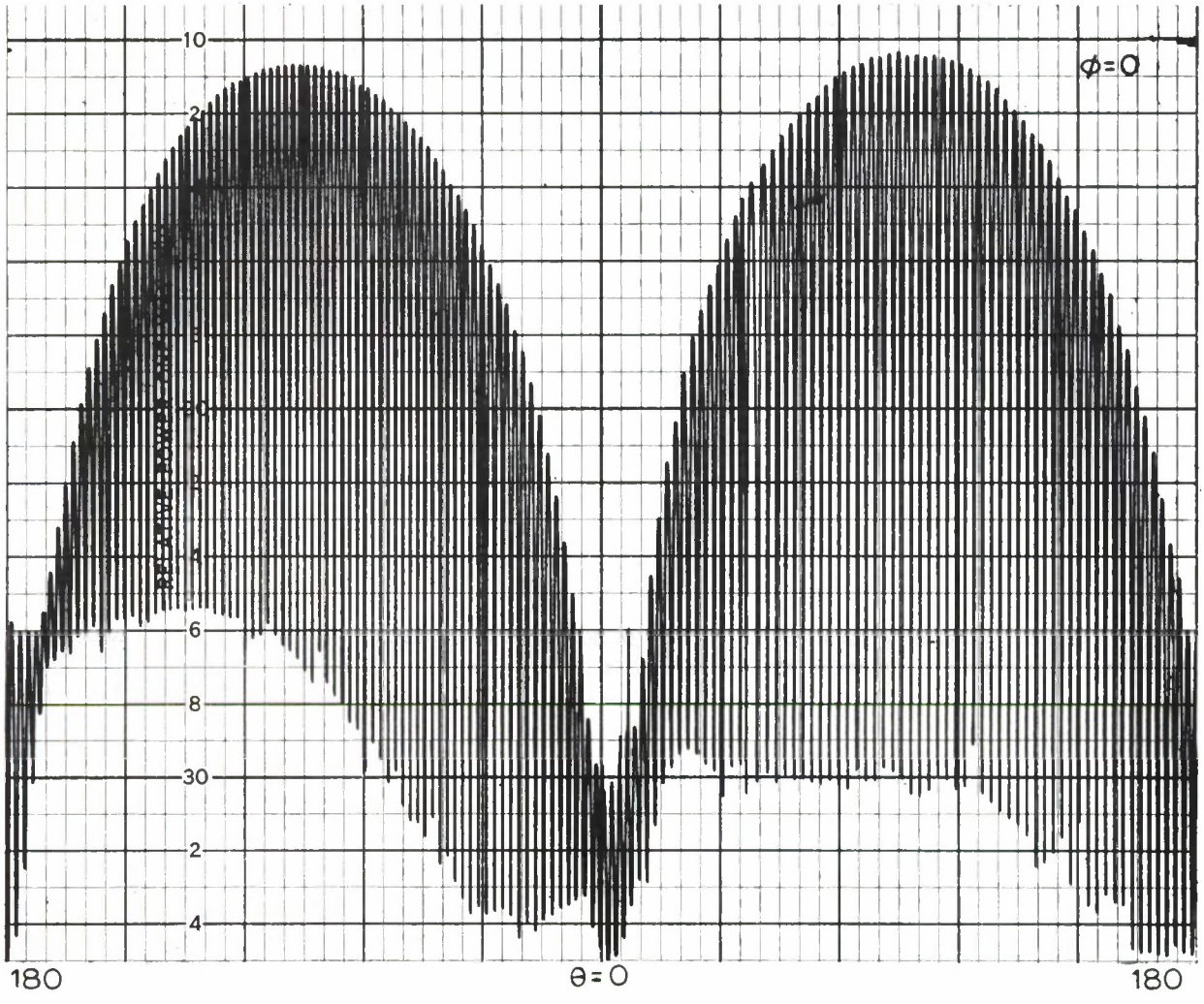

Figure 56. Radiation pattern of monofilar conical helix fed against an inner metal cone. Frequency 150 MHz 2π variation in θ, fixed ϕ. Vertical scale in db.

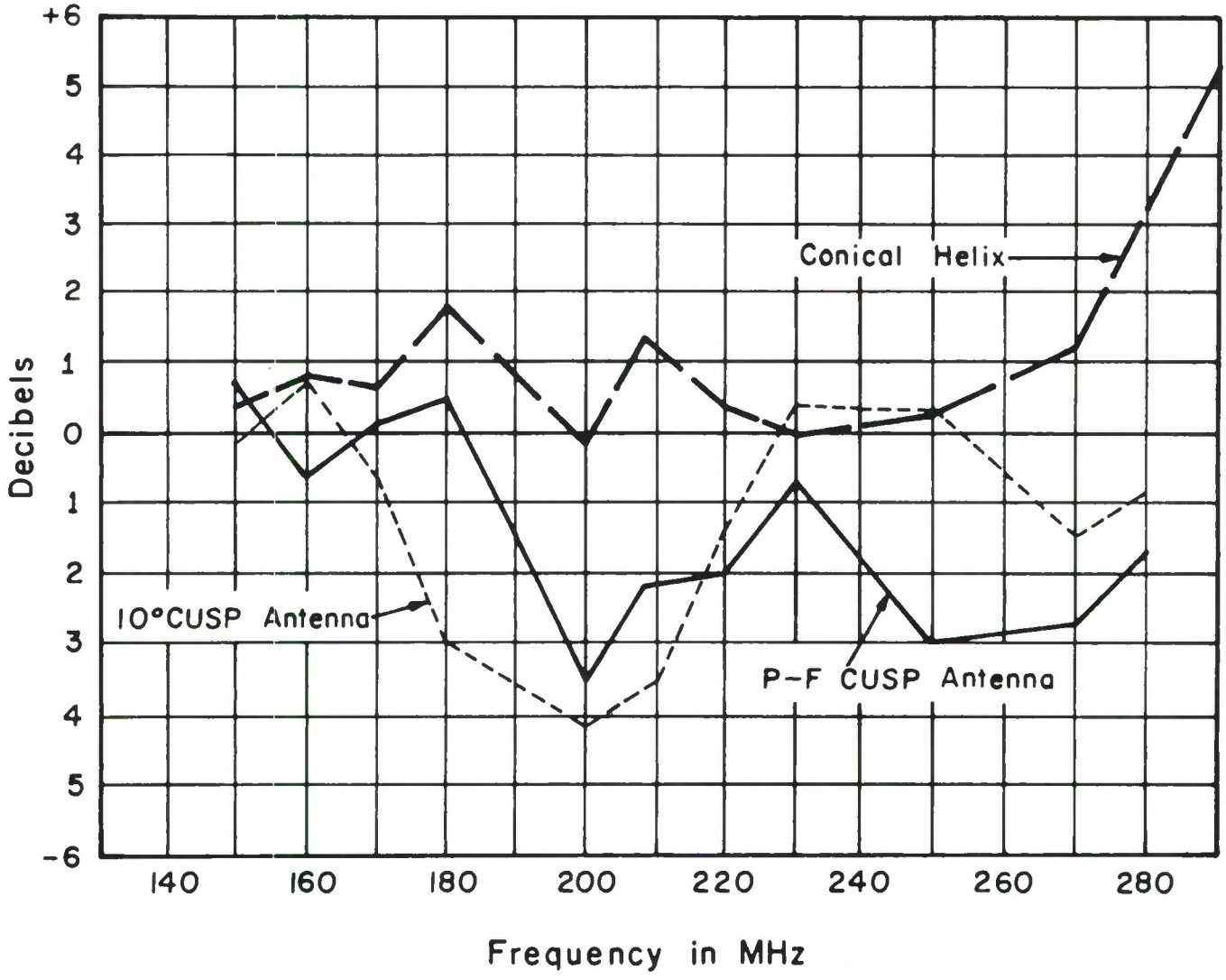

Figure 57. The measured "Broadband Power Gain" of the two CUSP antennas, and the monofilar conical helix constructed with parameters of the 10° CUSP antenna shown in Figure 38b.

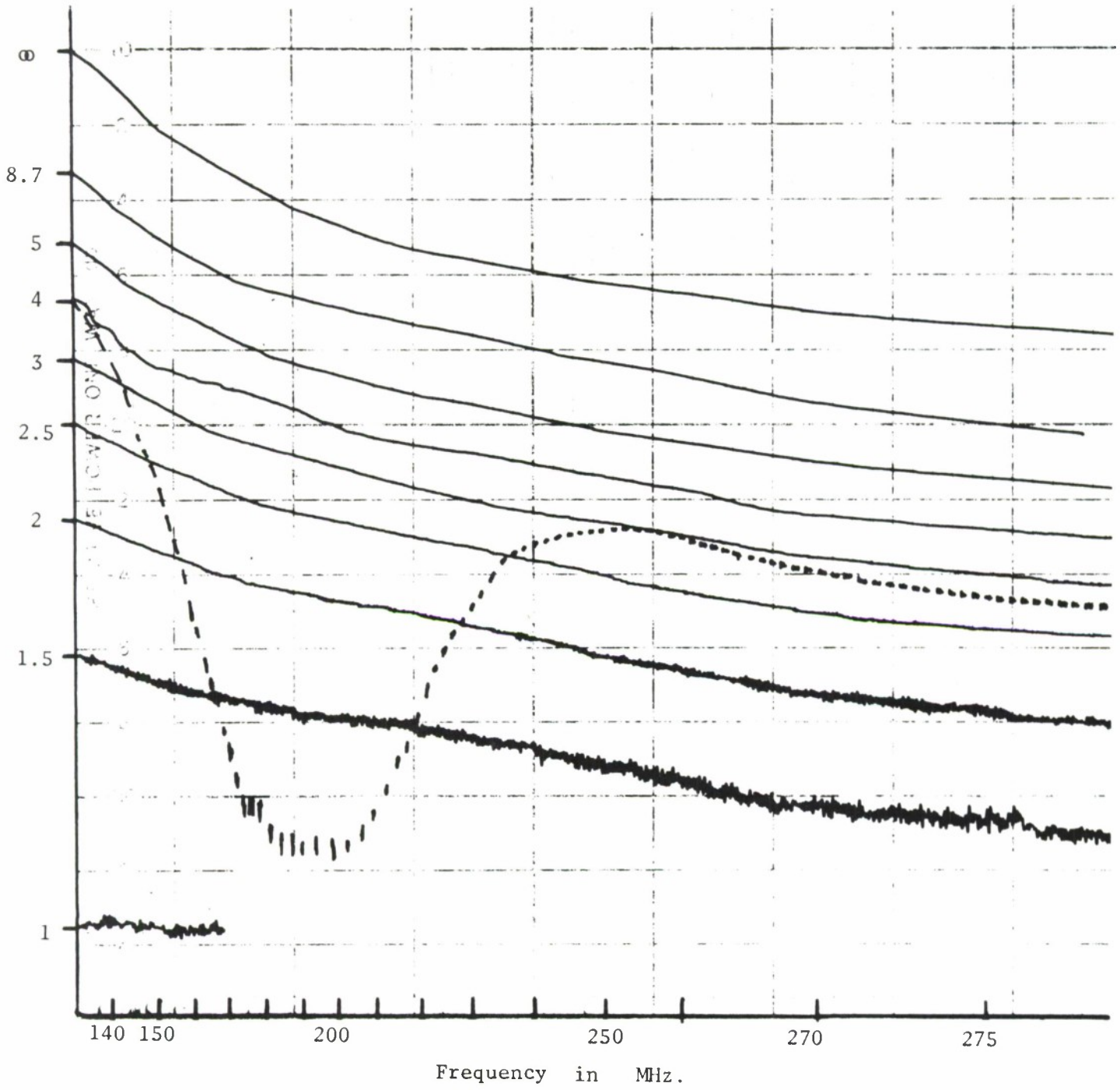

Figure 58 Measured VSWR, referred to 50 ohm line, of monofilar conical helix with inner conical core.

The agreement between the radiation patterns, measured power gain, and input VSWR curves of the CUSP antennas and the single arm conical tape helix antenna,leaves little doubt that the above theory of operation of the CUSP antenna is valid.

Figure 54 suggests that the chosen parameters for the original CUSP antenna and the length of the inner metal core may not have been optimum for operation at these very long wavelengths. When the CUSP antenna is operating as a base-fed helix, a tighter wrap and a different length core would be preferable.

XI. DISCUSSION OF MEASUREMENTS AND RESULTS

In an evaluation of the results of this investigation, it might be pointed out that considerable care was taken to make the measurements and resulting data as reliable and meaningful as possible. All measurements of relative gain and VSWR were repeated several times to eliminate any possibility of an anomalous result. No change in the antenna or the equipment settings was made unless a known condition with prior measured data could be returned to and repeated. All measurements of VSWR were referred to the same point in the system. All measurements of gain were made under as nearly identical physical conditions as possible, and all such measurements were made without change in the settings of the electronic instruments. Frequency readings during measurements were checked and monitored with the spectrum analyzer and crystal controlled markers.

It is recognized, however, that gain measurements are probably the least accurate of all antenna measurements, and accurate results require an extremely good antenna range. The University of Illinois range is far from ideal; however all reasonable precautions were taken to make the measurements meaningful.

A realistic estimate of the overall error in the fixed-frequency maximum gain measurements is probably 1 db. This author feels that such an error is probably realistic for most antenna gain measurements unless very specialized range conditions are established.

XII. CONCLUSIONS AND RECOMMENDATIONS

Balanced and unbalanced conical log-spiral antennas operated at wavelengths 2 to 3 times longer than would normally be considered using previously published design data, have been studied. The particular type of unbalanced antenna which was considered was constructed by inserting a metal conical core inside a balanced two arm antenna, and then bonding one arm of the antenna to this core at the base of the cone.

The performance of the spiral antennas, which are made to be unbalanced by modifying or loading the ends of one or both arms, can be interpreted in terms of the reflected current waves on the structure. On the small structure the two arms act as a transmission line,carrying energy from the feed terminals at the apex,down to the base of the antenna. At this base,the current flowing on the arms will be reflected back toward the apex or feed region. The reflected currents on the arms can be decomposed into balanced and unbalanced components,with only the unbalanced component becoming the source of radiation.

The unbalanced antenna considered here, is equivalent to a normal-mode monofilar conical tape helix fed against a conducting conical core. The efficiency of radiation is related to the degree of unbalance in the reflected current on the antenna arms.

It seems clear that, as now constructed, these CUSP antennas will always radiate broadside when the diameter of the cone is small in wavelengths. Thus the maximum of radiation from this antenna, when operated over a very wide bandwidth, will move from an axial to broadside direction. For many applications this behavior could become a serious limitation.

With knowledge of the phenomena causing radiation from these antennas, one can now suggest how the radiation might be controlled to obtain an axial beam. When viewed as a base-fed traveling wave antenna, it becomes clear that the turn-to-turn phasing on the antenna must be such as to set up the axial beam (end-fire) mode of the helix. One approach would be to make both arms slow wave structures, to insure maintaining the balanced transmission line from the apex to the base of the cone. One arm can then be terminated,by connecting it to a center core as at present. The slow wave geometry would have to be designed to accumulate enough delay per turn, so that the reflected wave on the one radiating arm would provide end-fire radiation in the helical beam mode. Whether such delays can be achieved in practice, and the effect of this large delay on the normal back-fire radiation of the spiral when the antenna is operated at shorter wavelengths, would have to be investigated.

In the above type antenna,the termination of the one arm, i.e., the inner metal cone, becomes part of the radiating structure, the arm itself does not. Radiation from structures that have an added delay on one arm might be controlled by again making both arms with a slow wave geometry, then adding sufficient delay on one arm to make the reflected waves on the two slow wave arms have the desired turn-to-turn phase relationship. This would be equivalent to a base-fed bifilar helix.

Although these large phase delays on the slow wave arms may prove to be difficult to achieve, some control over the radiation from these unbalanced conical spiral (CUSP) antennas now seems realizable.

REFERENCES

1. Dyson, J. D., "The Radiation Characteristics of one Unbalanced Conical Log-Spiral Antenna," Report No. 71-4, Antenna Laboratory, University of Illinois, Urbana. (Report No. 4, Sub-Contract CC-401, Prime Contract F19628-70-C-0230, MIT Lincoln Laboratory) April 7, 1971.

2. Dyson, J. D. and M. D. Johnson, "The Radiation Characteristics of a Pyramidal Unbalanced Spiral Antenna," Report No. UIAL-71-13, Antenna Laboratory, University of Illinois, Urbana. (Report No. 5, Sub-Contract CC-401, Prime Contract F19628-70-C-0230, MIT Lincoln Laboratory), September 15, 1971.

3. Dyson, John D., "The Characteristics and Design of the Conical Log-Spiral Antenna," IEEE Transactions, AP-13, No. 4, July 1965, pp. 488-499.

4. Peters, Leon Jr., "Use of High-Resistance Audio Cable for Pattern Measurements," Ohio State University, Antenna Laboratory, Contract AF18(600)-160, Proj. 481, DDC No. AD-24625, 15 September 1953.

5. Dyson, John D., "Antenna Near Field Measurements," Electromagnetics and Antenna (Ed. P. E. Mayes), College of Engineering, University of Illinois, Urbana, Illinois, February 1967, pp. 57-114.

6. Greene, Frank M., "NBS Field-Strength Standards and Measurements," Proc. of IEEE, Vol. 55, No. 6, June 1967, pp. 970-981.

7. _____, "Test Procedure for Antennas," IEEE Standard No. 149, January 1965.

8. Dyson, John D., "An Investigation of a Conical Log-Spiral Antenna Operated Such that the Base is Very Small in Wavelengths," Report No. 70-12, Antenna Laboratory, University of Illinois, Urbana. (Report No. 3, Sub-contract CC-401, Prime Contract AF 19(628)-5167), July 1970.

9. Kim, O. K. and J. D. Dyson, "A Log-Spiral Antenna with Selectable Polarization," IEEE Transactions, AP-19, No. 5, September 1971, pp. 675-6.

10. Patton, W. T., "The Backfire Bifilar Helical Antenna," Tech. Rept. No. 61, Contract AF 33(657)8460, Antenna Laboratory, University of Illinois, Urbana, (DDC No. AD-289084) September 1962.

11. Kraus, J. D., Antennas, McGraw-Hill Book Company, 1950, p. 176.

Appendices A, B, C, D, E follow.

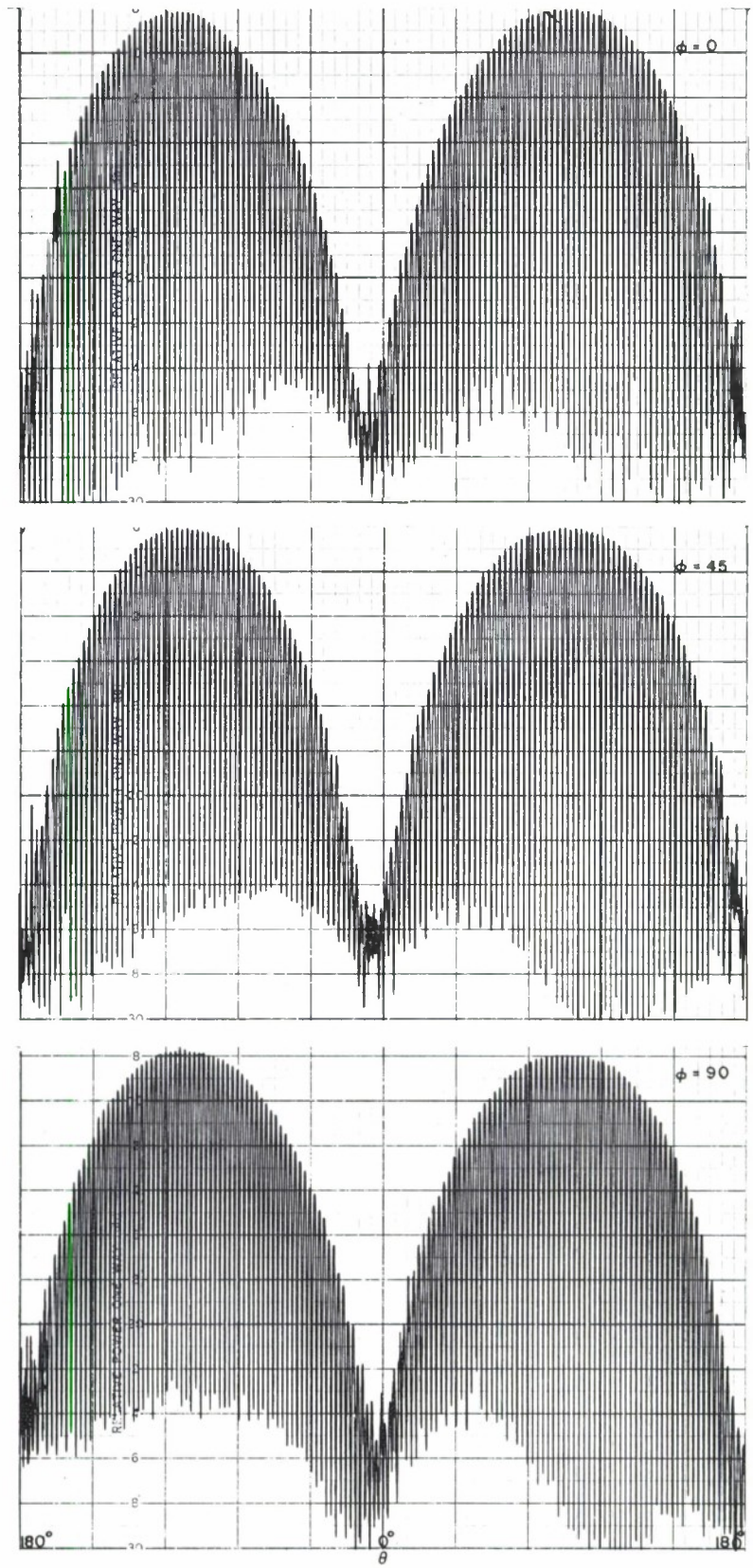

Figure A-1 Radiation Pattern of Unbalanced Conical Antenna. 2π variation in θ, ϕ = 0, 45 and 90. Frequency 150 MHz.

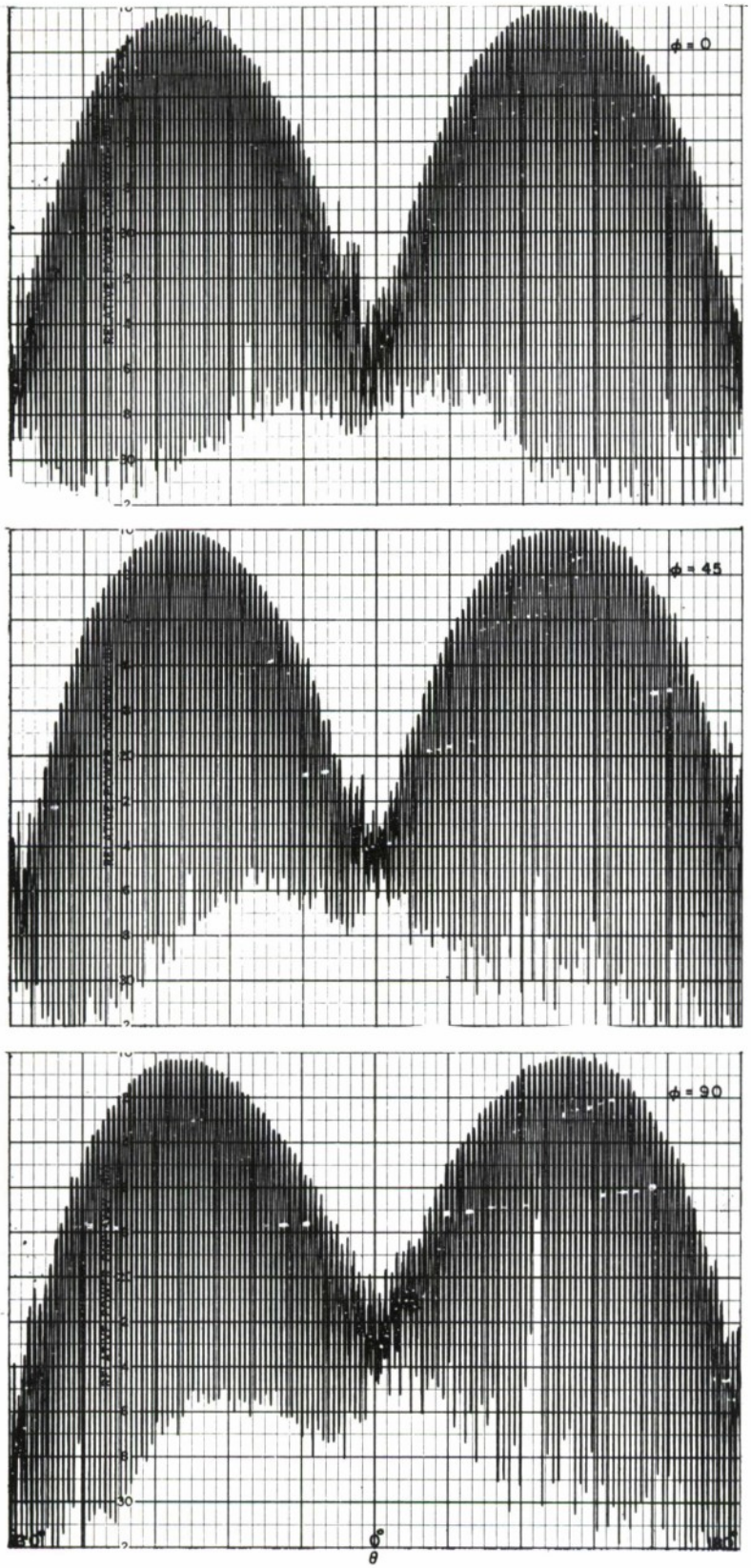

Figure A-2 Radiation Pattern of Unbalanced Conical Antenna. 2π variation in θ, ϕ = 0, 45 and 90. Fraquency 160 MHz.

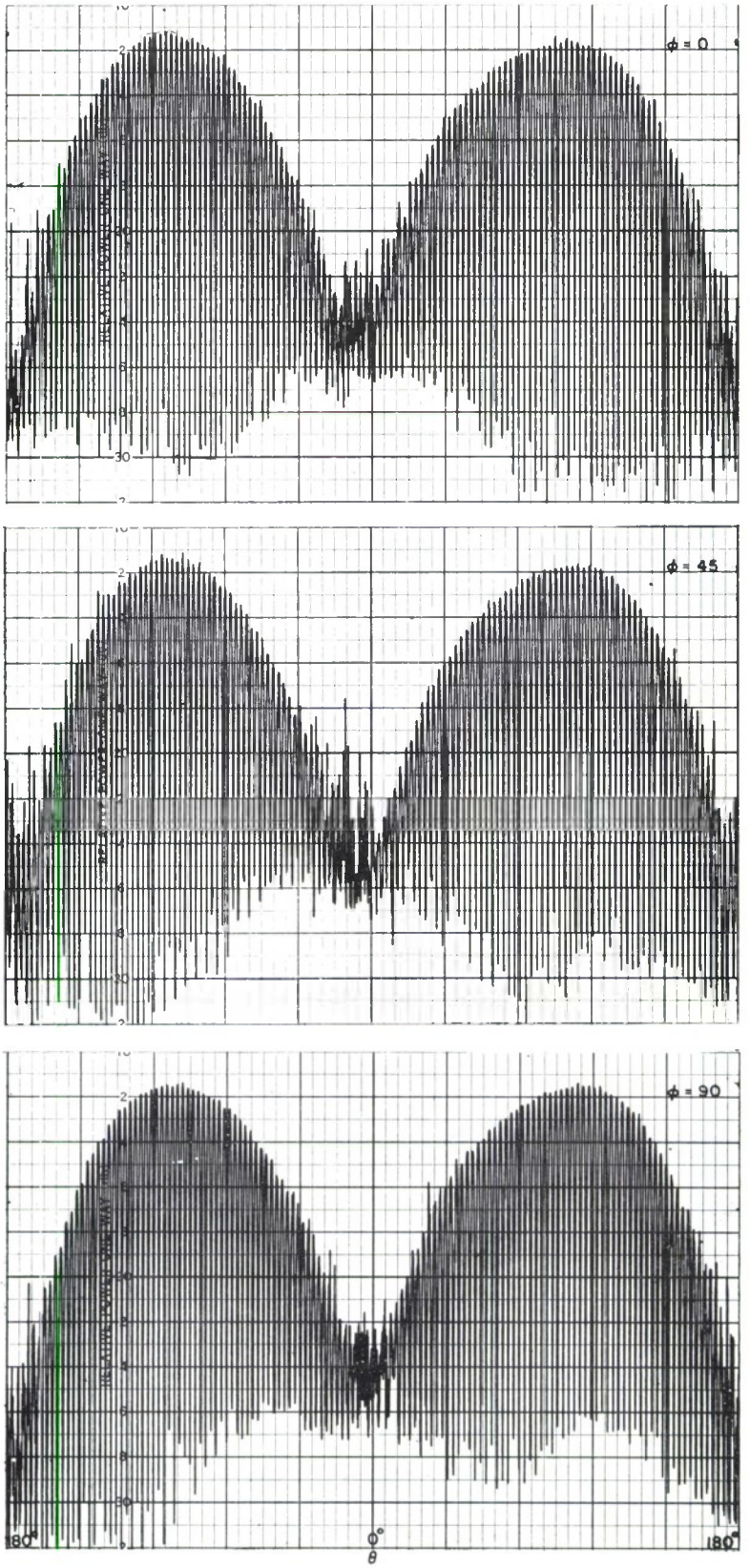

Figure A-3 Radiation Pattern of Unbalanced Conical Antenna. 2π variation in θ, ϕ = 0, 45 and 90. Frequency 170 MHz.

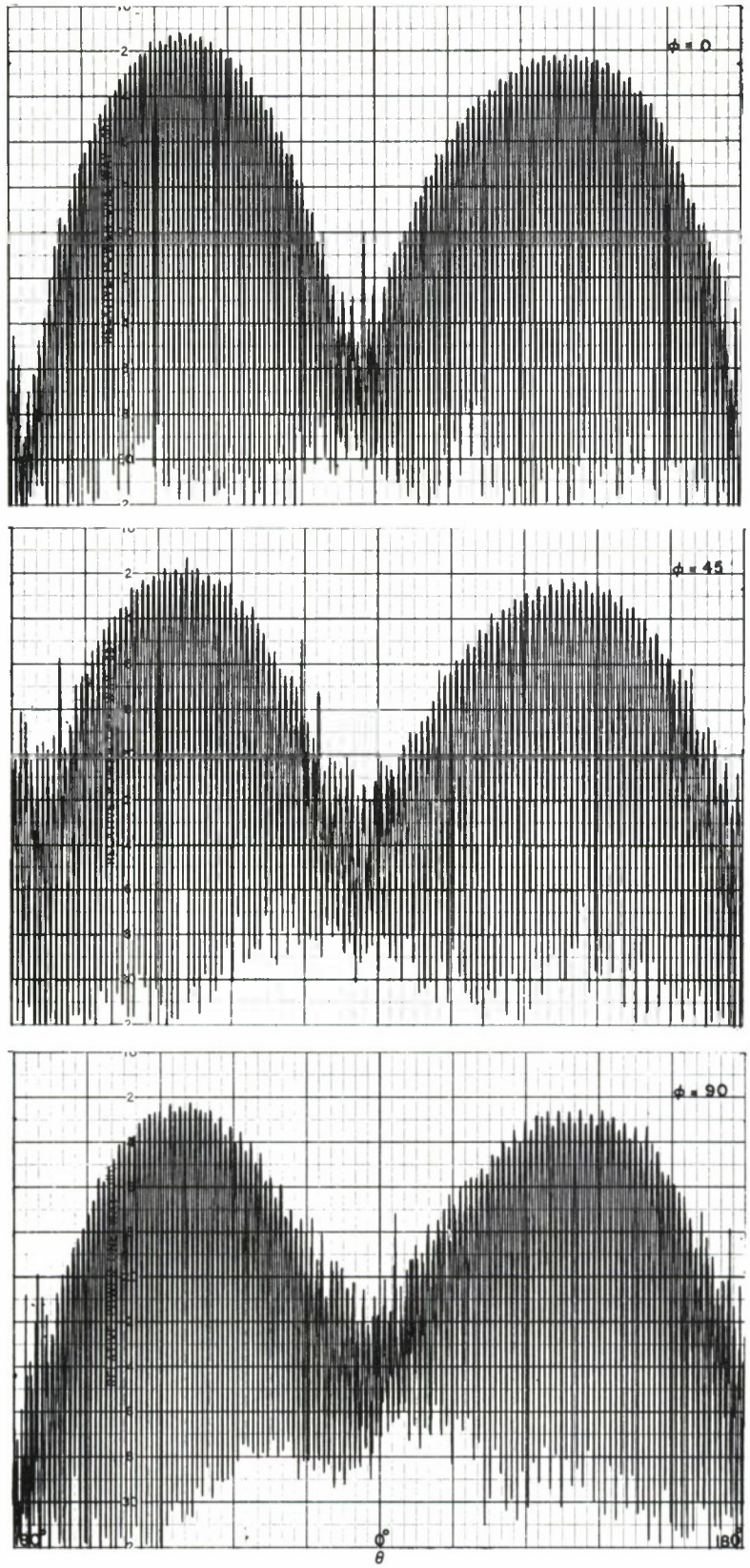

Figure A-4 Radiation Pattern of Unbalanced Conical Antenna. 2π variation in θ, ϕ = 0, 45 and 90. Frequency 180 MHz.

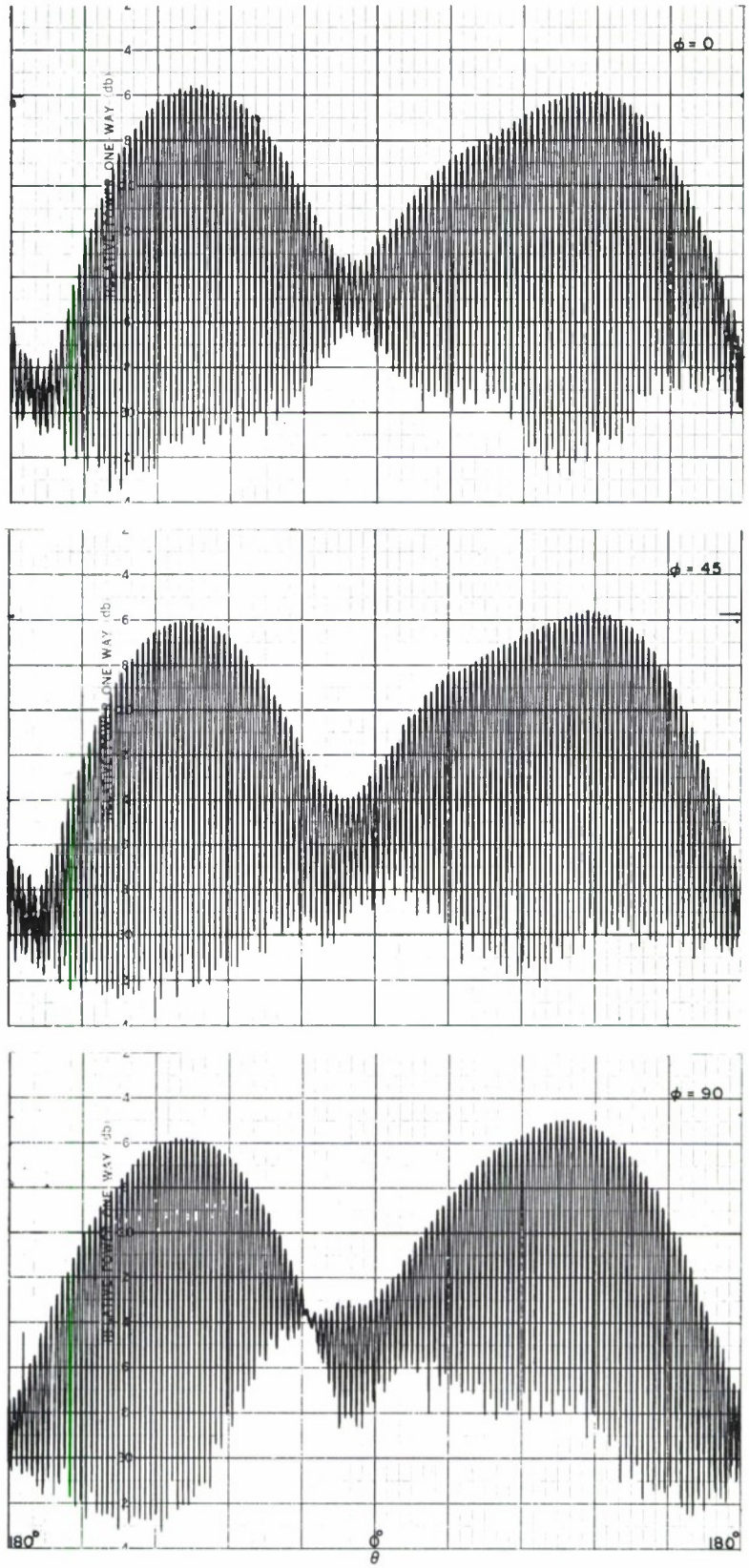

Figure A-5 Radiation Pattern of Unbalanced Conical Antenna. 2π variation in θ, ϕ = 0, 45 and 90. Frequency 200 MHz.

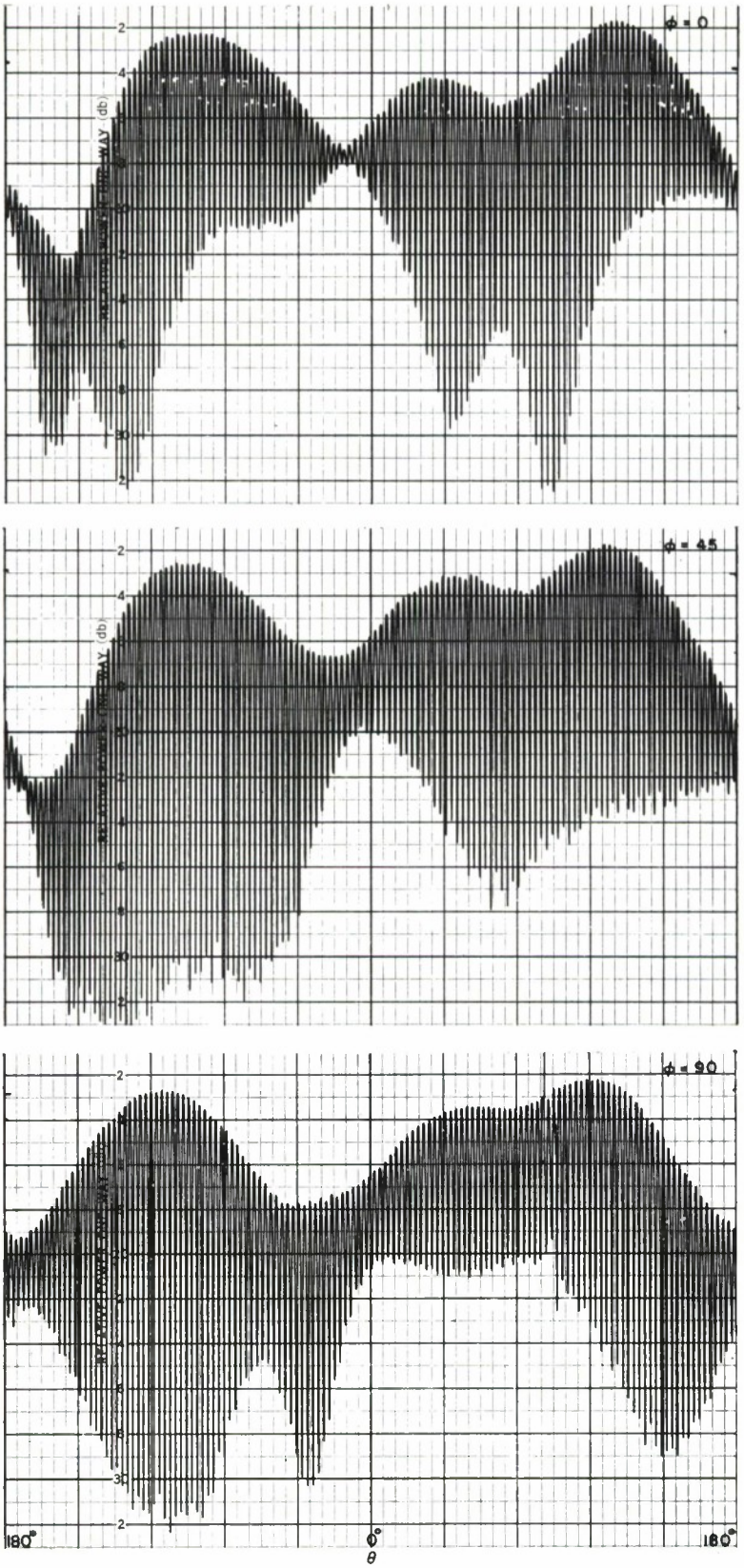

Figure A-6 Radiation Pattern of Unbalanced Conical Antenna. 2π variation in θ, ϕ = 0, 45 and 90. Frequency 220 MHz.

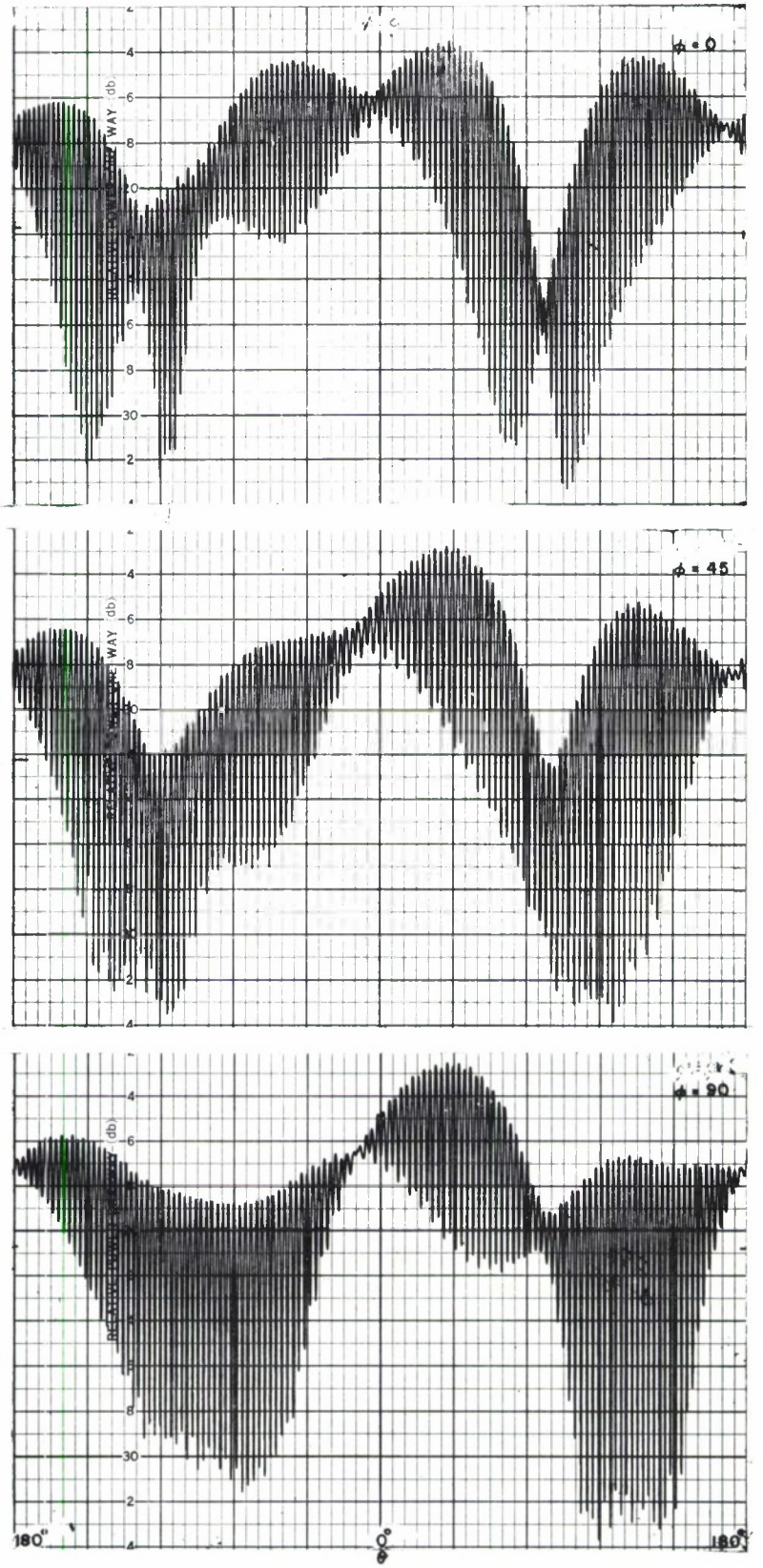

Figure A-7 Radiation Pattern of Unbalanced Conical Antenna. 2π variation in θ, φ = 0, 45 and 90. Frequency 270 MHz.

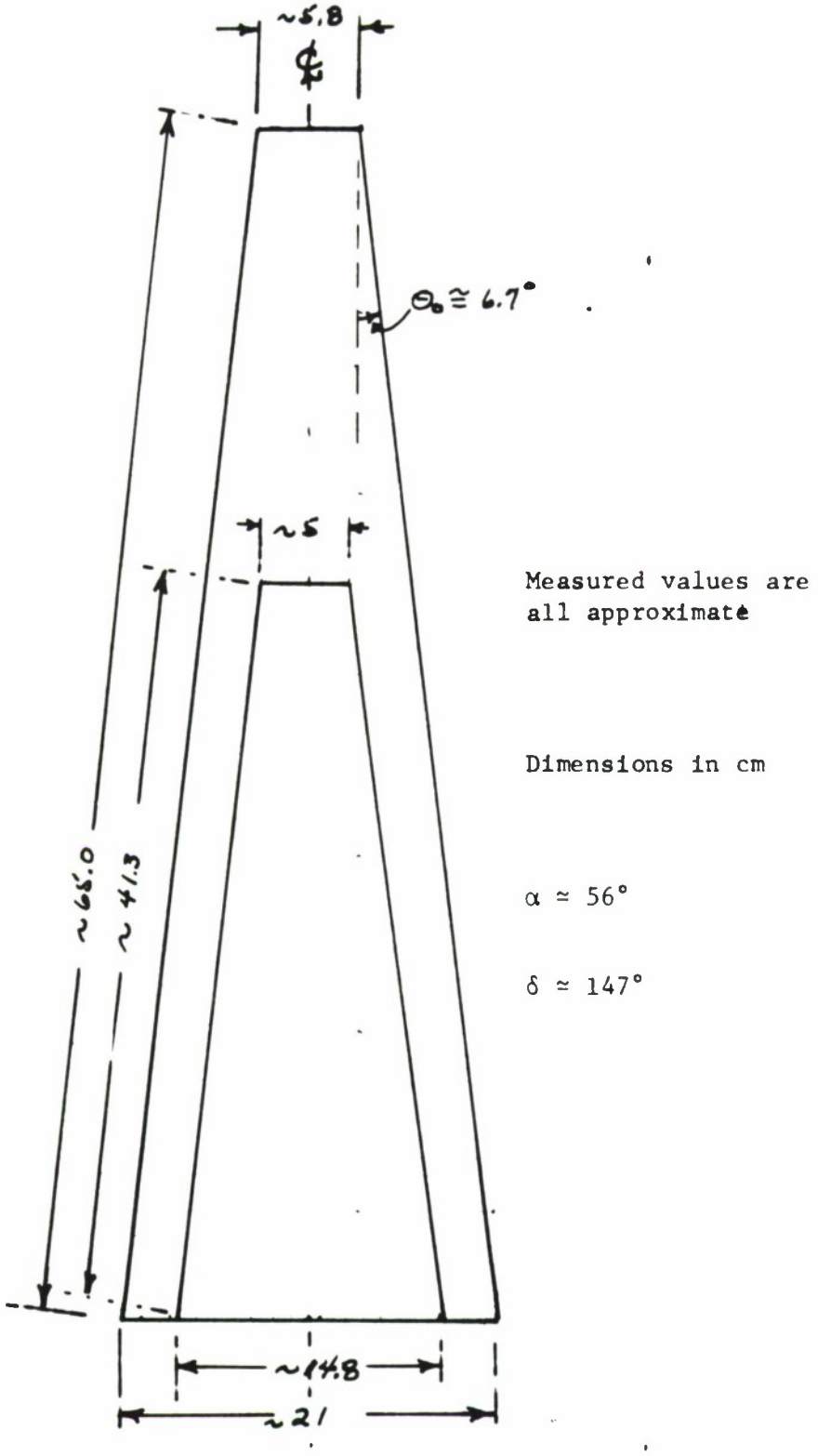

Figure B-1. Measured parameters of the unbalanced antenna. The cross section drawing is approximately to scale.

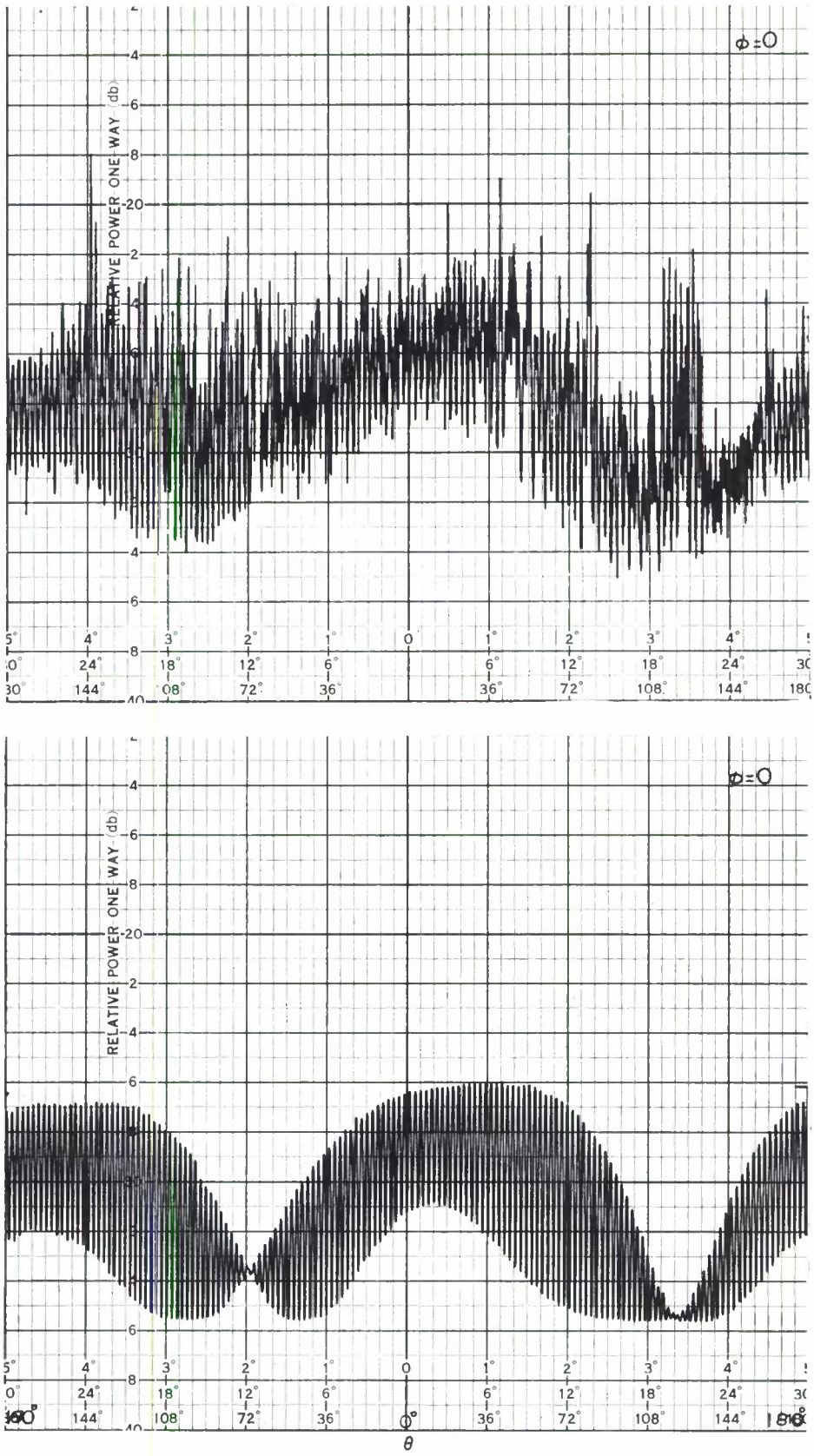

Figure C-1: Radiation Patterns indicating the improved signal to noise ratio achieved with the cavity used as a filter. f = 180MHz. Philco-Ford antenna with shorting strap removed and with balanced feed on axis.

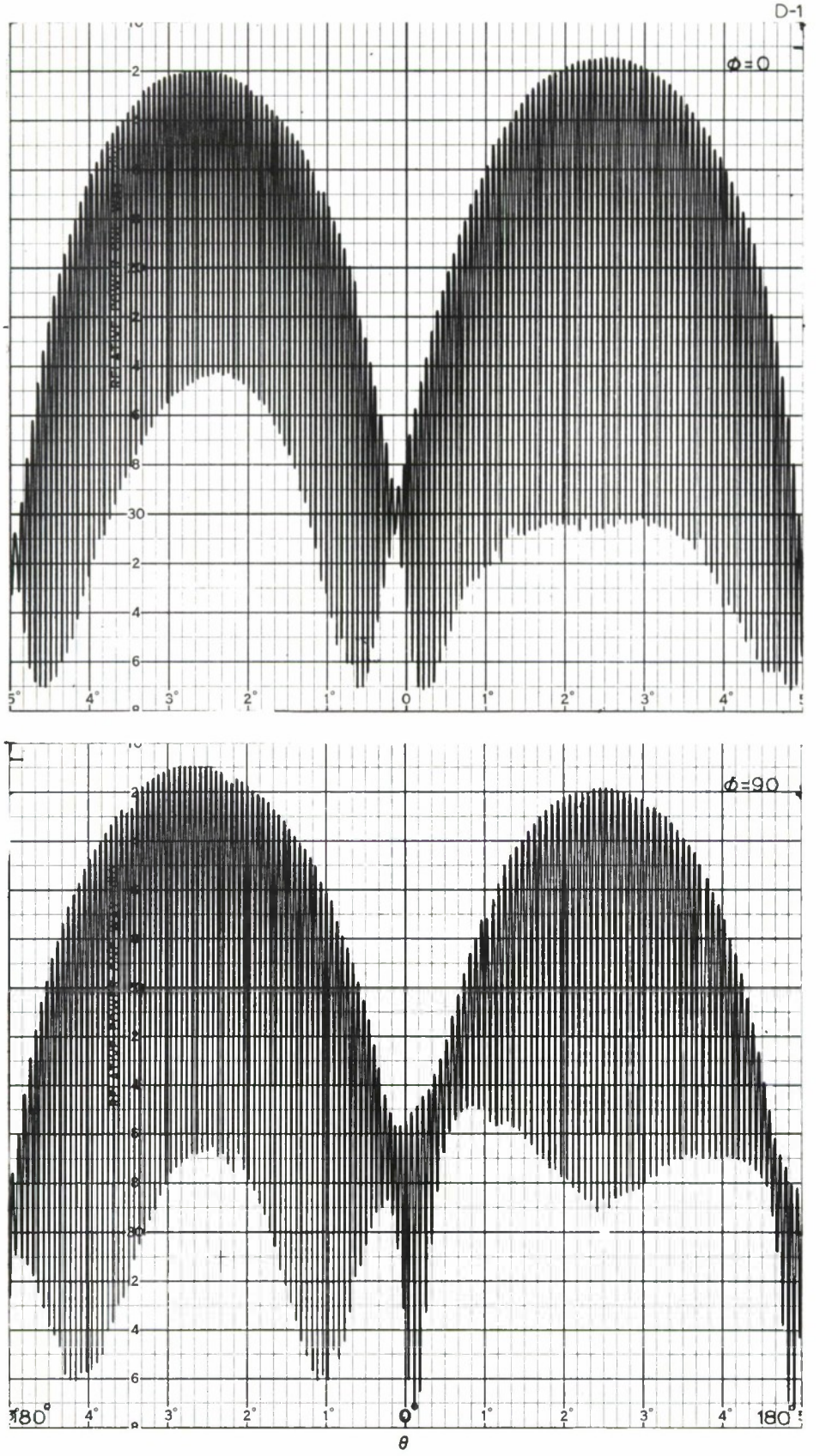

Figure D-1: Radiation Pattern 10° C.U.S.P. Antenna. 2¢ variation in θ, Φ = 0 and 90. Frequency 150 MH_z

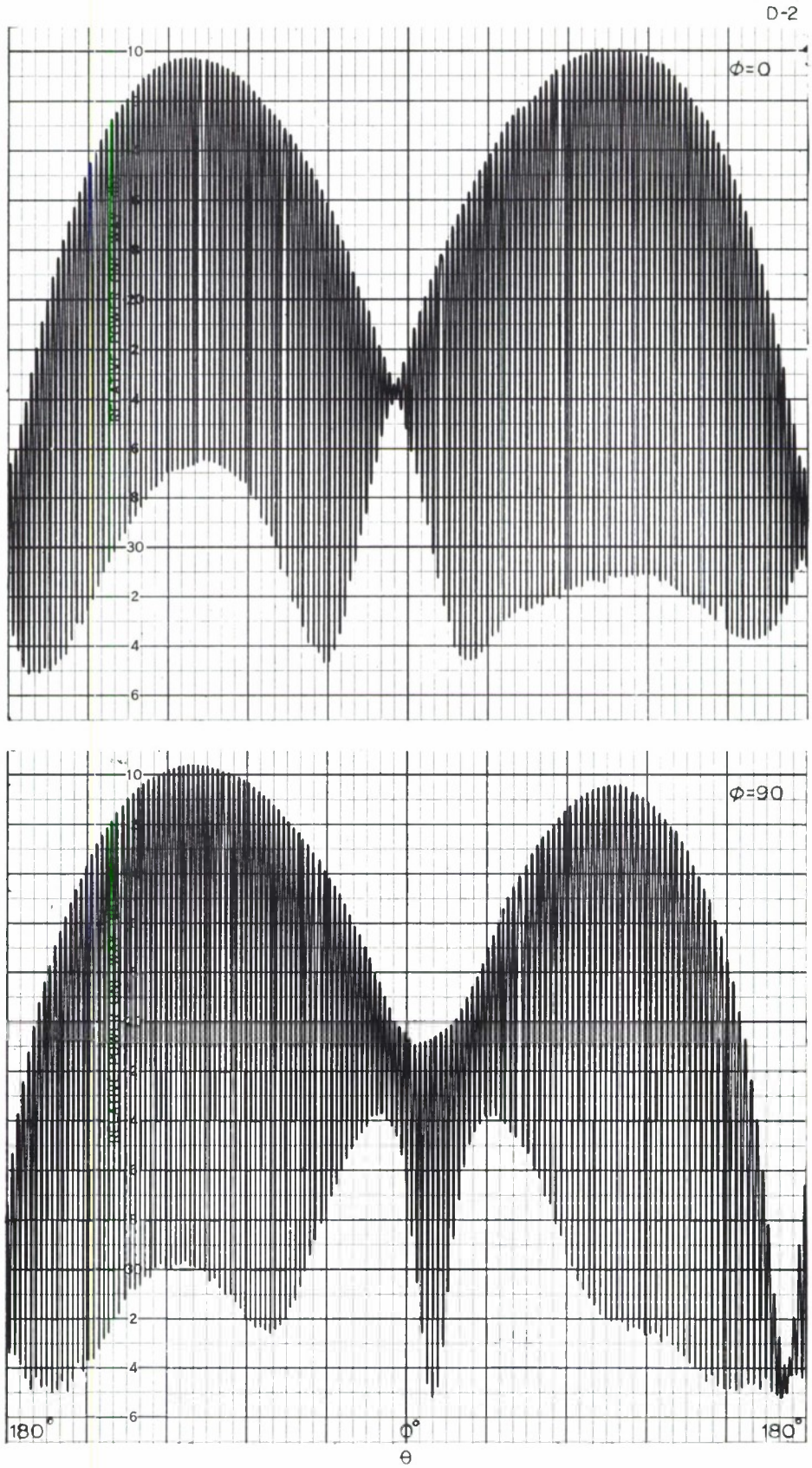

Figure D-2 Radiation Pattern 10° C.U.S.P. Antenna: 2π variation in θ, Φ = 0 and 90. Frequency 160 MH_z

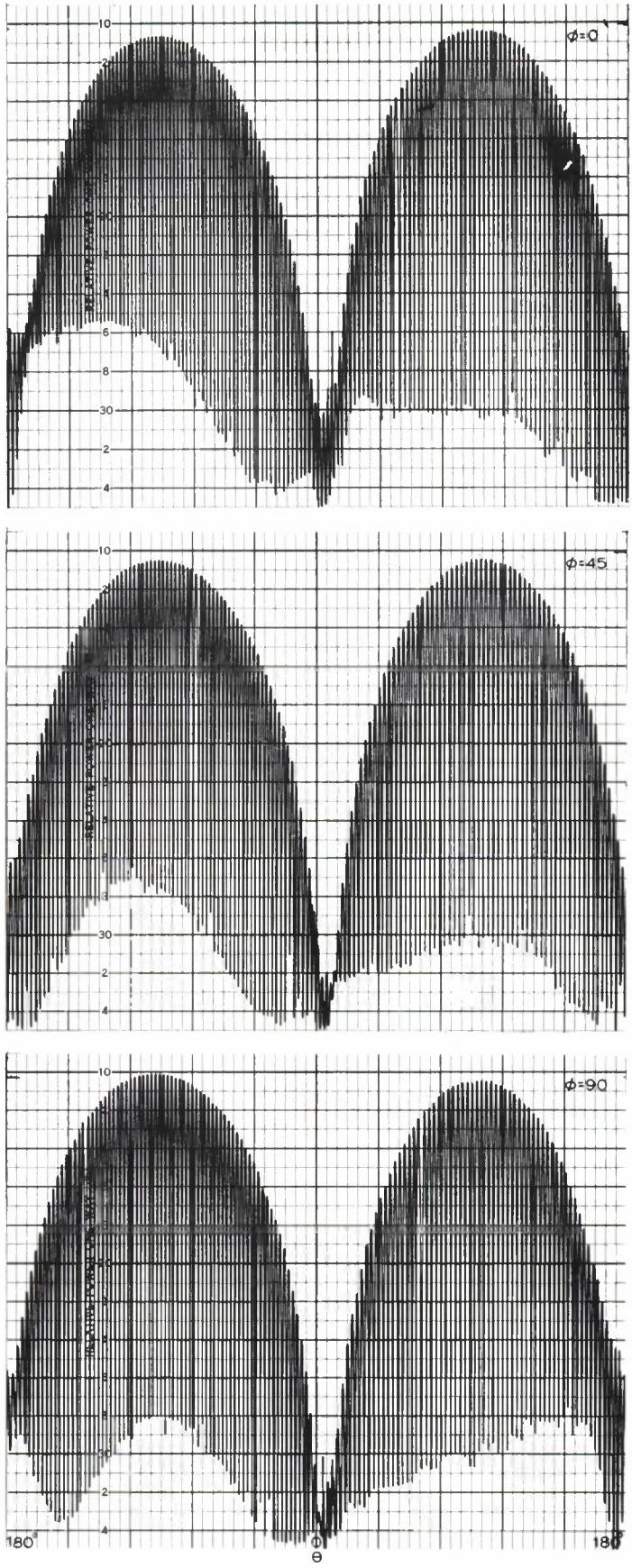

Figure E1. Radiation patterns of monofilar conical helix fad againat an inner metal cone. Frequency 150 MHz 2π variation in θ.

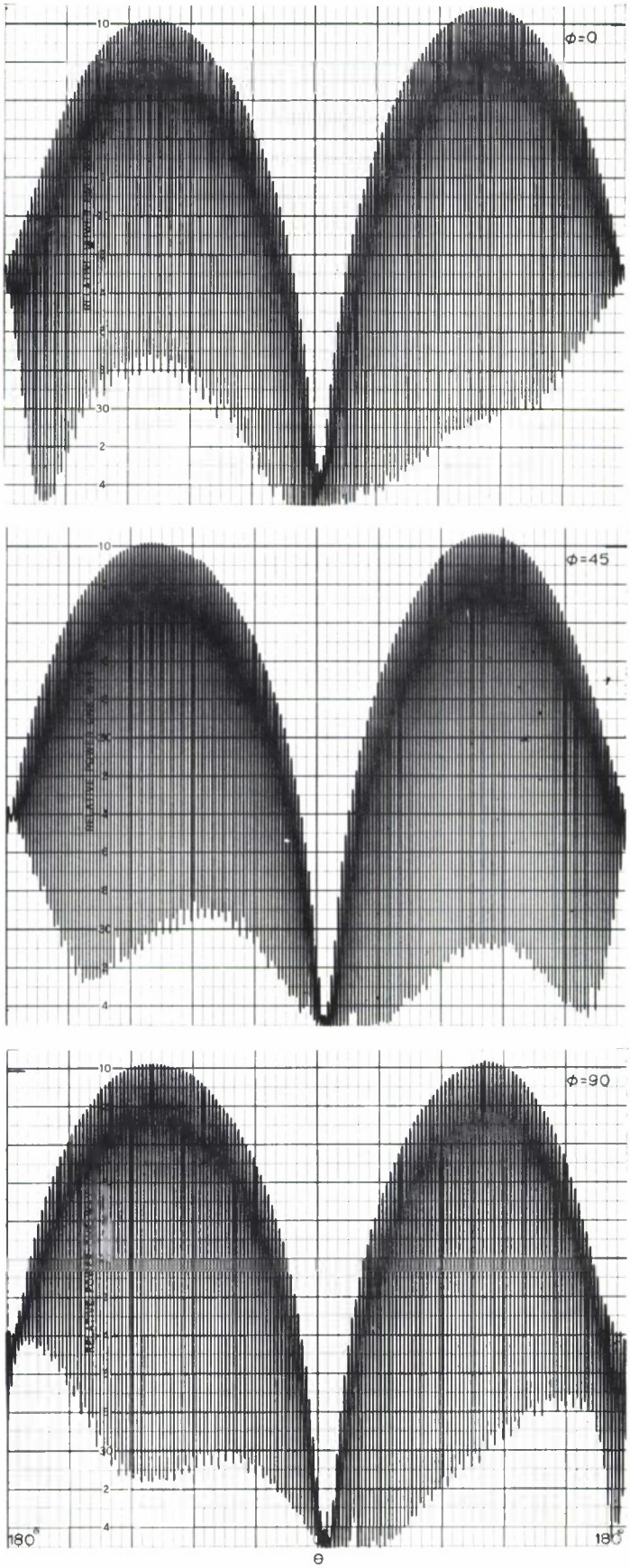

Figure E2. Radiation patterns of monofilar conical helix fad against an inner metal cone. Frequency 180 MHz 2π variation in θ.

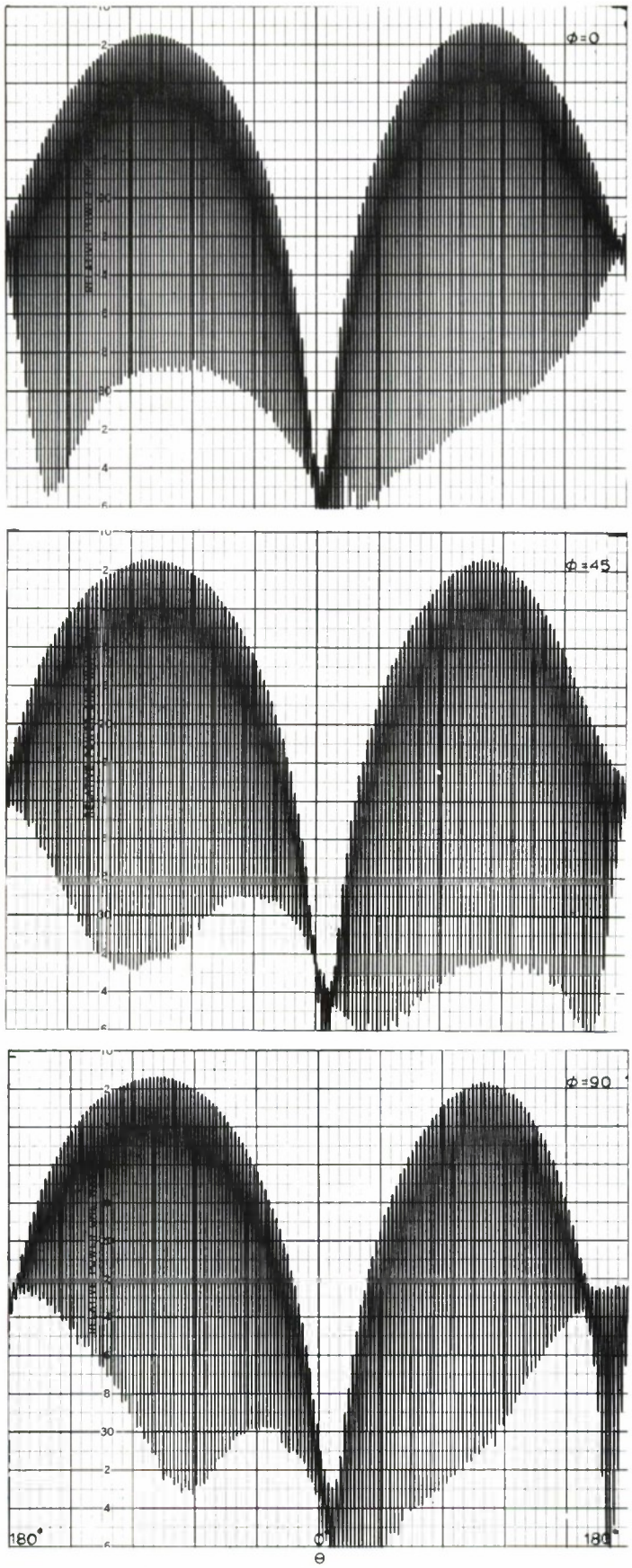

Figure K3. Radiation patterns of monofilar conical helix fad againet an inner metal cone. Frequency 200 MHz 2π variation in θ.

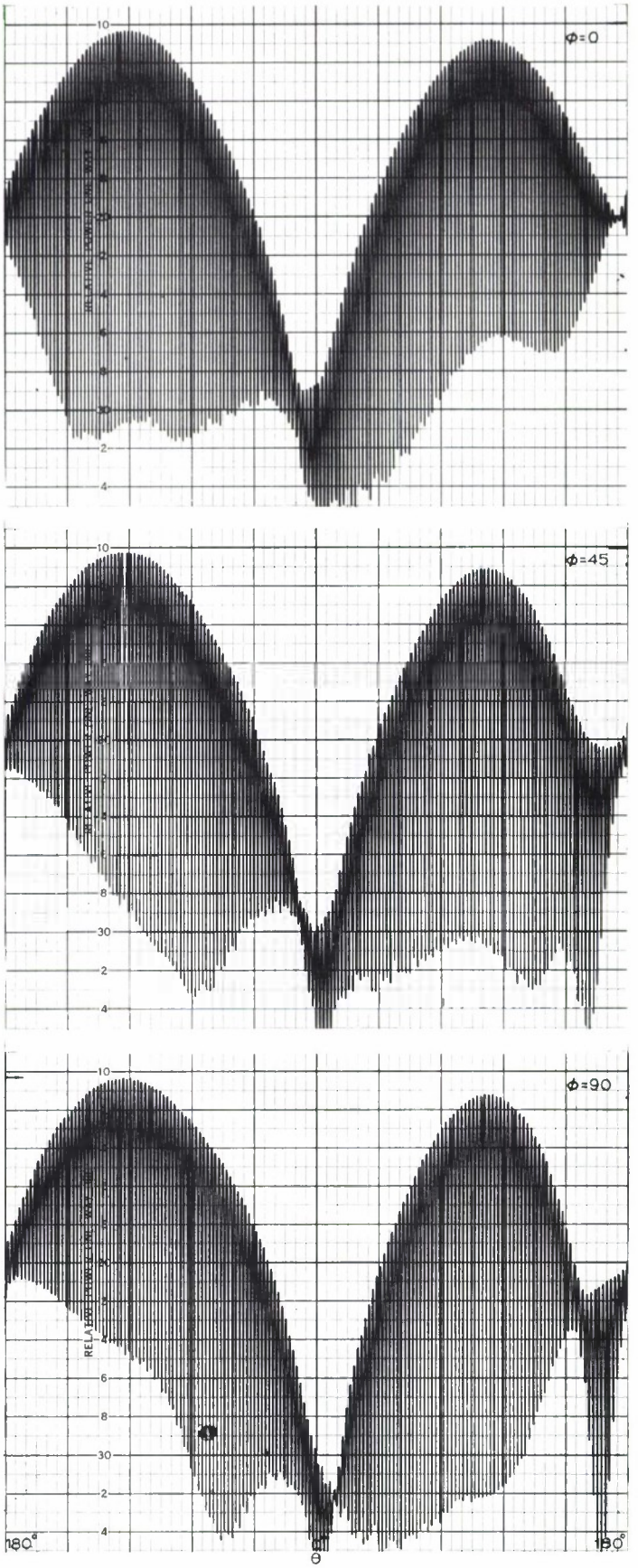

Figure E4. Radiation patterns of monofilar conical helix fed against an inner metal cone. Frequency 220 MHz 2π variation in θ.

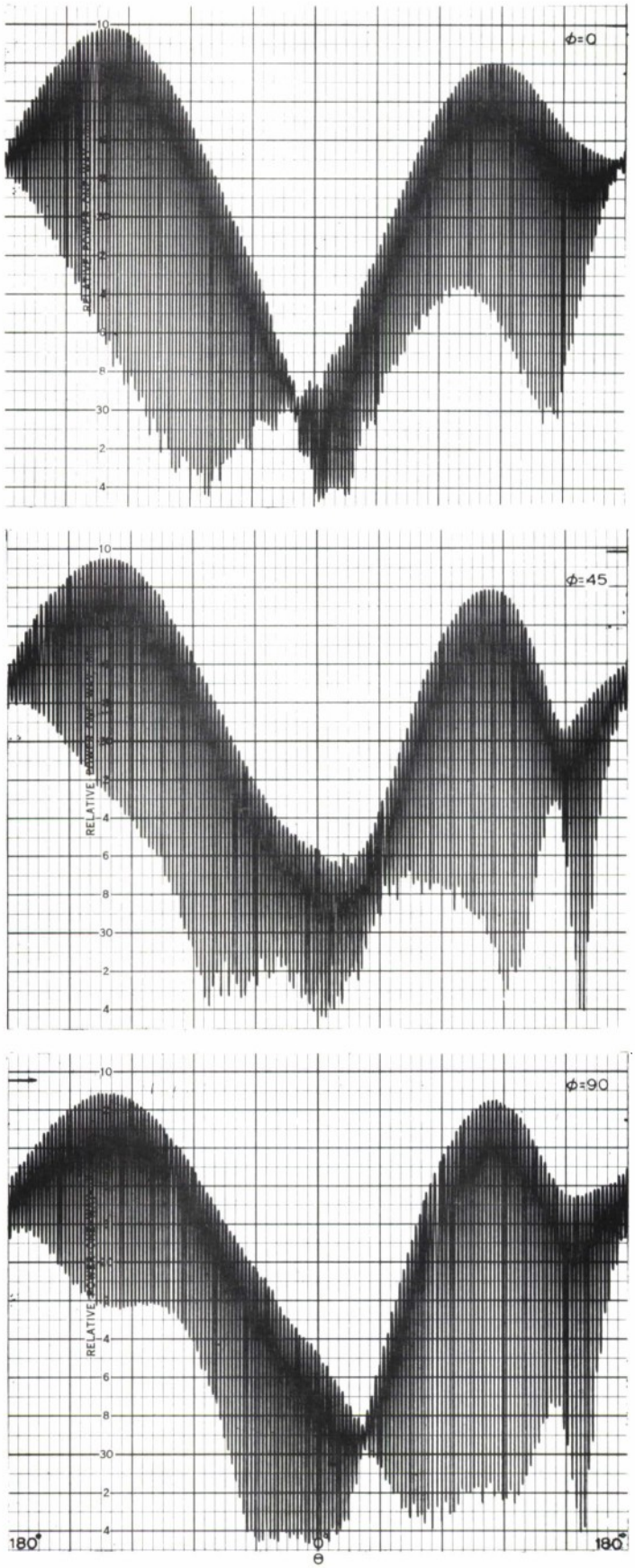

Figure 53. Radiation patterns of monofilar conical helix fed against an inner metal cone. Frequency 250 MHz 2π variation in θ.

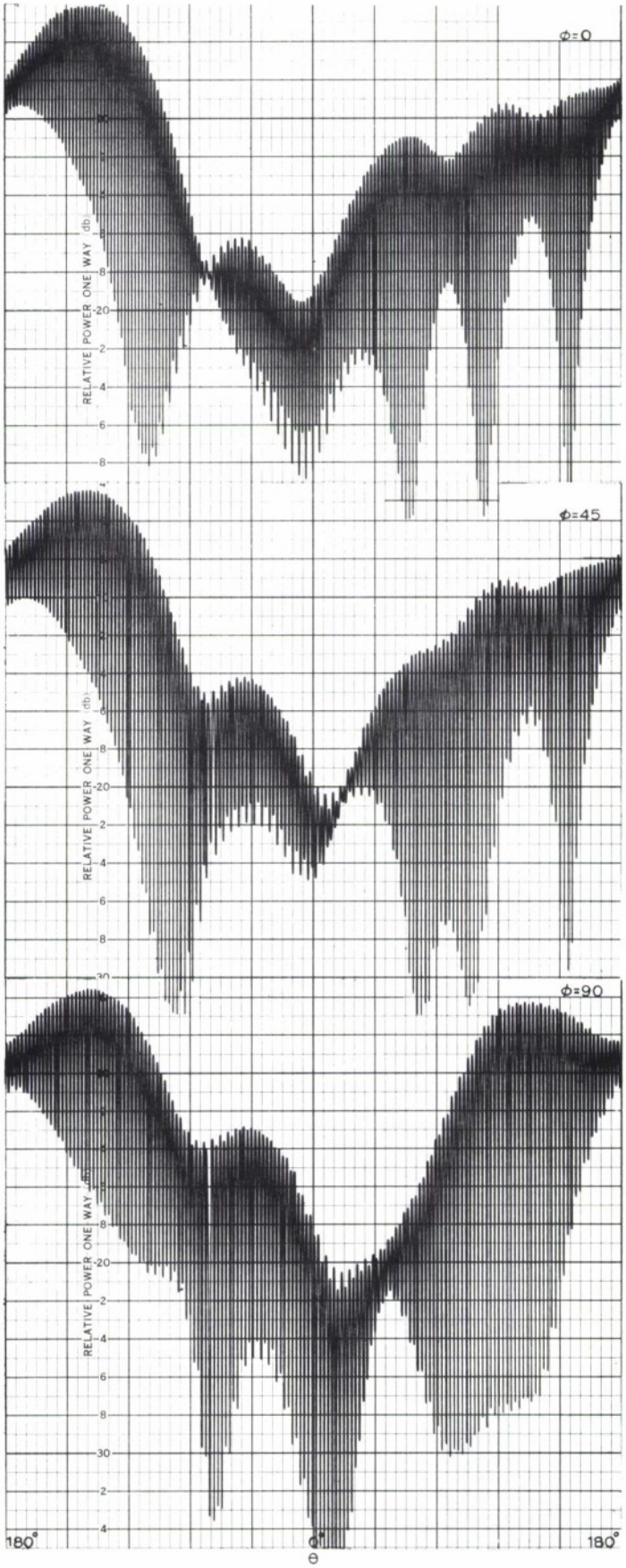

Figure E6. Radiation patterns of monofilar conical helix fed against an inner metal cone. Frequency 300 MHz 2π variation in θ.

Unclassified
Security Classification

DOCUMENT CONTROL DATA - R&D

(Security classification of title, body of abstract and indexing annotation must be entered when the overall report is classified)

1. ORIGINATING ACTIVITY *(Corporate author)* University of Illinois, Antenna Laboratory under Purchase Order CC-401 to M.I.T. Lincoln Lab.	2a. REPORT SECURITY CLASSIFICATION Unclassified 2b. GROUP None

3. REPORT TITLE

Investigation of Some Electrically Small Conical Log-Spiral Antennas

4. DESCRIPTIVE NOTES *(Type of report and inclusive dates)*

Annual Report for period 1 October 1970 through 31 August 1971

5. AUTHOR(S) *(Last name, first name, initial)*

Dyson, J. D.

6. REPORT DATE	7a. TOTAL NO. OF PAGES	7b. NO. OF REFS
30 September 1971	115	11

8a. CONTRACT OR GRANT NO.	9a. ORIGINATOR'S REPORT NUMBER(S)
F19628-70-C-0230 b. PROJECT AND TASK NO. 627A c. Purchase Order CC-401 d.	UIAL-71-14 9b. OTHER REPORT NO(S) *(Any other numbers that may be assigned this report)* ESD-TR-71-297

10. AVAILABILITY/LIMITATION NOTICES

Approved for public release; distribution unlimited.

11. SUPPLEMENTARY NOTES	12. SPONSORING MILITARY ACTIVITY
None	Air Force Systems Command, USAF

13. ABSTRACT

This report is concerned with an evaluation and an experimental study of the radiation patterns, power gain, and voltage standing wave ratio of balanced and unbalanced spiral antennas when operated at wavelengths much longer than would be considered normal for this size structure. The unbalanced antenna which was studied was a bifilar logarithmic spiral constructed on a dielectric cone with an inner metal core to house electronic equipment. At the base, one arm is bonded to the core. At these long wavelengths a transition from the normal back-fire axial radiation occurs, and the antenna raidates a maximum of energy broadside to the cone axis. This radiation is due to the unbalanced component of the reflected energy on the antenna arms.

DD FORM 1 JAN 64 1473

Unclassified
Security Classification

Unclassified

Security Classification

14. KEY WORDS	LINK A		LINK B		LINK C	
	ROLE	WT	ROLE	WT	ROLE	WT
Spiral Antenna						
Antenna Gain						
Unbalanced Spiral Antenna						

INSTRUCTIONS

1. ORIGINATING ACTIVITY: Enter the name and address of the contractor, subcontractor, grantee, Department of Defense activity or other organization *(corporate author)* issuing the report.

2a. REPORT SECURITY CLASSIFICATION: Enter the overall security classification of the report. Indicate whether "Restricted Data" is included. Marking is to be in accordance with appropriate security regulations.

2b. GROUP: Automatic downgrading is specified in DoD Directive 5200.10 and Armed Forces Industrial Manual. Enter the group number. Also, when applicable, show that optional markings have been used for Group 3 and Group 4 as authorized.

3. REPORT TITLE: Enter the complete report title in all capital letters. Titles in all cases should be unclassified. If a meaningful title cannot be selected without classification, show title classification in all capitals in parenthesis immediately following the title.

4. DESCRIPTIVE NOTES: If appropriate, enter the type of report, e.g., interim, progress, summary, annual, or final. Give the inclusive dates when a specific reporting period is covered.

5. AUTHOR(S): Enter the name(s) of author(s) as shown on or in the report. Enter last name, first name, middle initial. If military, show rank and branch of service. The name of the principal author is an absolute minimum requirement.

6. REPORT DATE: Enter the date of the report as day, month, year, or month, year. If more than one date appears on the report, use date of publication.

7a. TOTAL NUMBER OF PAGES: The total page count should follow normal pagination procedures, i.e., enter the number of pages containing information.

7b. NUMBER OF REFERENCES: Enter the total number of references cited in the report.

8a. CONTRACT OR GRANT NUMBER: If appropriate, enter the applicable number of the contract or grant under which the report was written.

8b, 8c, & 8d. PROJECT NUMBER: Enter the appropriate military department identification, such as project number, subproject number, system numbers, task number, etc.

9a. ORIGINATOR'S REPORT NUMBER(S): Enter the official report number by which the document will be identified and controlled by the originating activity. This number must be unique to this report.

9b. OTHER REPORT NUMBER(S): If the report has been assigned any other report numbers *(either by the originator or by the sponsor)*, also enter this number(s).

10. AVAILABILITY/LIMITATION NOTICES: Enter any limitations on further dissemination of the report, other than those imposed by security classification, using standard statements such as:

(1) "Qualified requesters may obtain copies of this report from DDC."

(2) "Foreign announcement and dissemination of this report by DDC is not authorized."

(3) "U. S. Government agencies may obtain copies of this report directly from DDC. Other qualified DDC users shall request through _____."

(4) "U. S. military agencies may obtain copies of this report directly from DDC. Other qualified users shall request through _____."

(5) "All distribution of this report is controlled. Qualified DDC users shall request through _____."

If the report has been furnished to the Office of Technical Services, Department of Commerce, for sale to the public, indicate this fact and enter the price, if known.

11. SUPPLEMENTARY NOTES: Use for additional explanatory notes.

12. SPONSORING MILITARY ACTIVITY: Enter the name of the departmental project office or laboratory sponsoring *(paying for)* the research and development. Include address.

13. ABSTRACT: Enter an abstract giving a brief and factual summary of the document indicative of the report, even though it may also appear elsewhere in the body of the technical report. If additional space is required, a continuation sheet shall be attached.

It is highly desirable that the abstract of classified reports be unclassified. Each paragraph of the abstract shall end with an indication of the military security classification of the information in the paragraph, represented as *(TS), (S), (C), or (U).*

There is no limitation on the length of the abstract. However, the suggested length is from 150 to 225 words.

14. KEY WORDS: Key words are technically meaningful terms or short phrases that characterize a report and may be used as index entries for cataloging the report. Key words must be selected so that no security classification is required. Identifiers, such as equipment model designation, trade name, military project code name, geographic location, may be used as key words but will be followed by an indication of technical context. The assignment of links, rules, and weights is optional.

Unclassified

Security Classification